Muography
how - why- who/where/how

Cristina Cârloganu
LPC/IN2P3/ CNRS

Two useful interactions

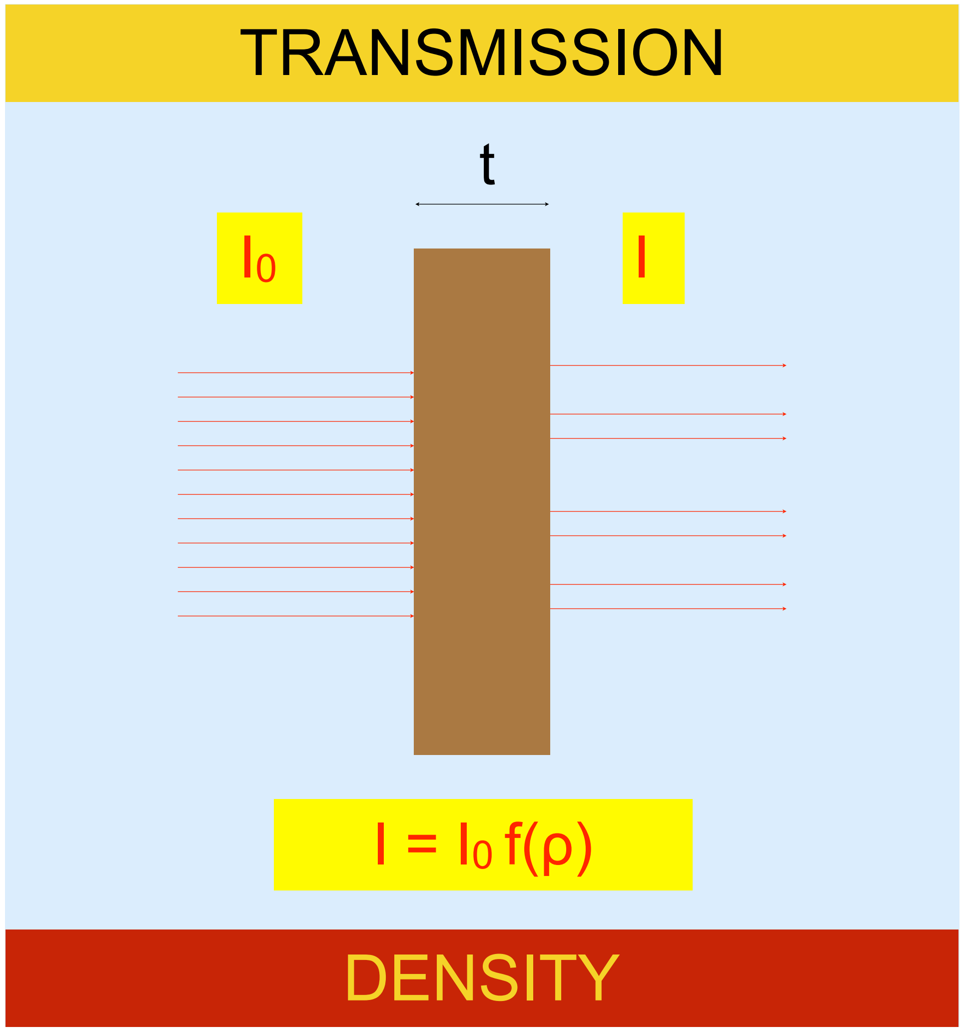

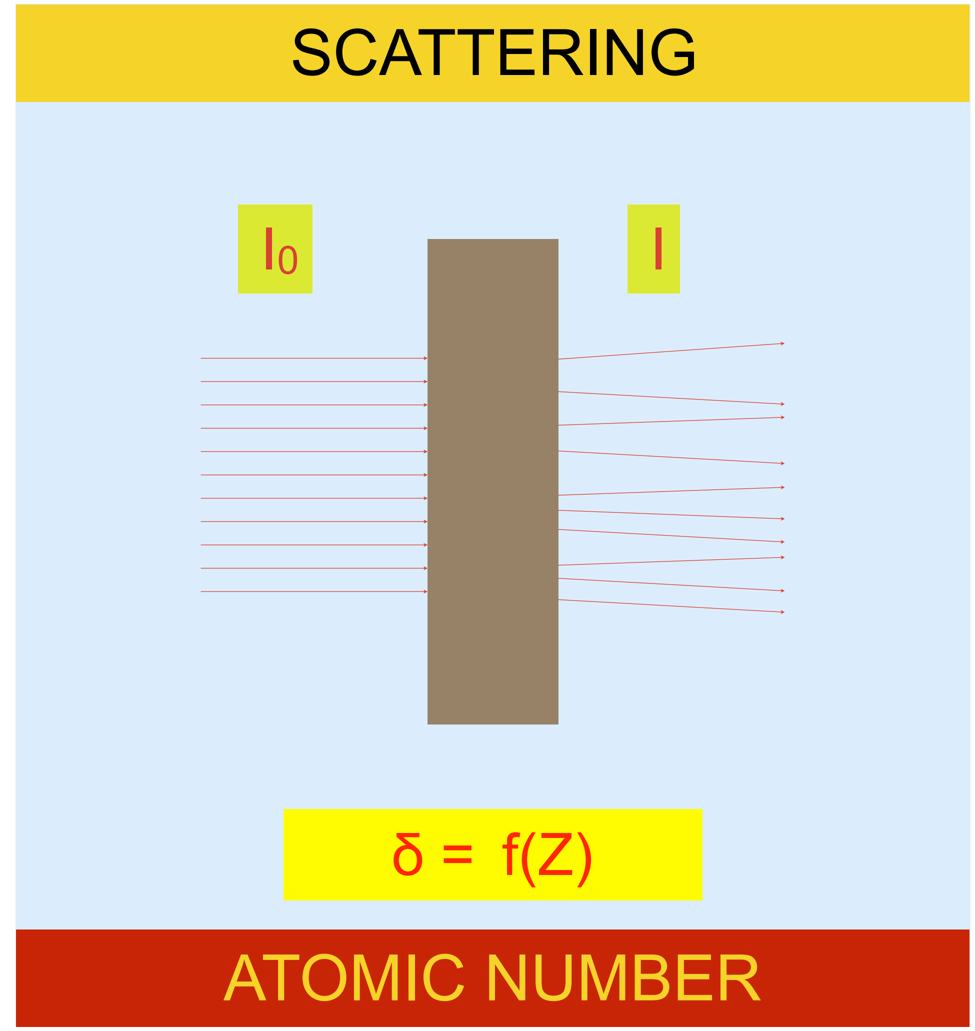

- 2D image
- relies on incident flux knowledge
- applicable to very large targets

- 3D image
- necessary to measure each individual track before and after the target
- high position resolution, large area detectors
- small to medium targets

Transmission muography in a nutshell ...

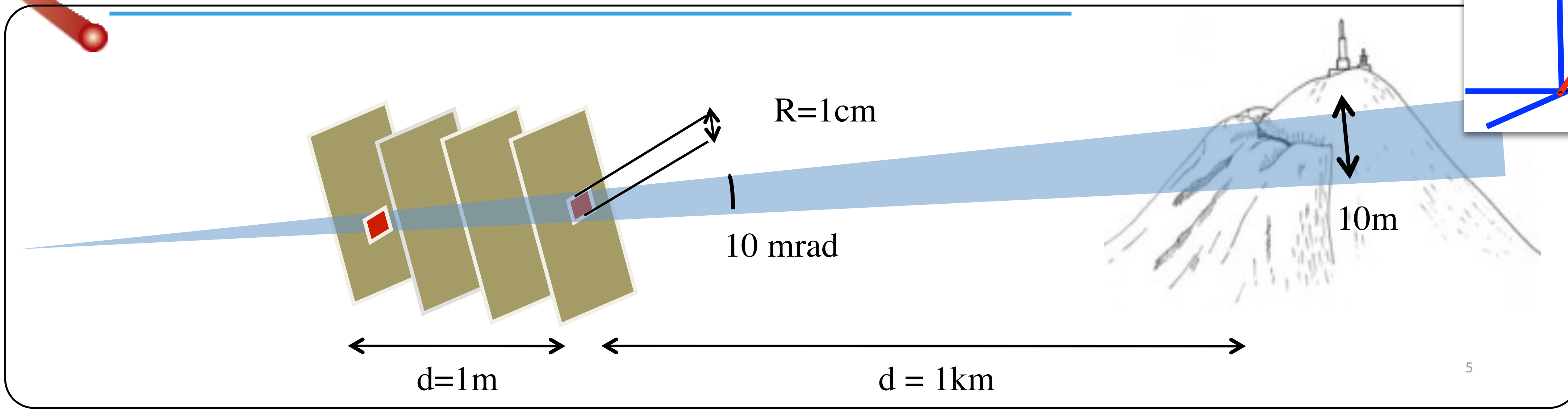

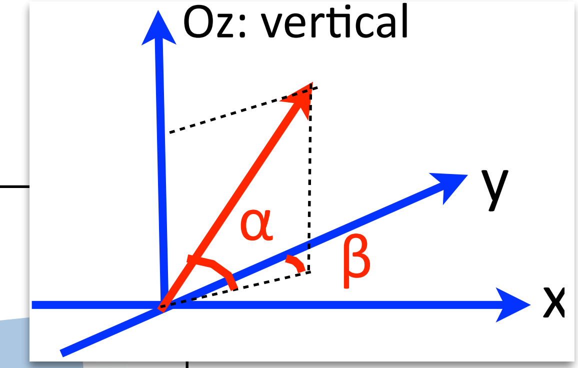

$$\mathcal{T}_\rho(\alpha, r(\alpha,\beta)) = \frac{\Phi(\alpha, r(\alpha,\beta))}{\Phi_0(\alpha)}$$

$$\boxed{\int \rho(\alpha,\beta)dr = \mathcal{F}(\mathcal{T}(\alpha,\beta))}$$

$$\Phi(\alpha,\beta) = \frac{N(\alpha,\beta)}{Seff(\alpha,\beta)\Delta T \Delta\Omega}$$

$$S_{eff} = S_{det}\varepsilon_{det}A_{geom}\varepsilon_{illum}$$

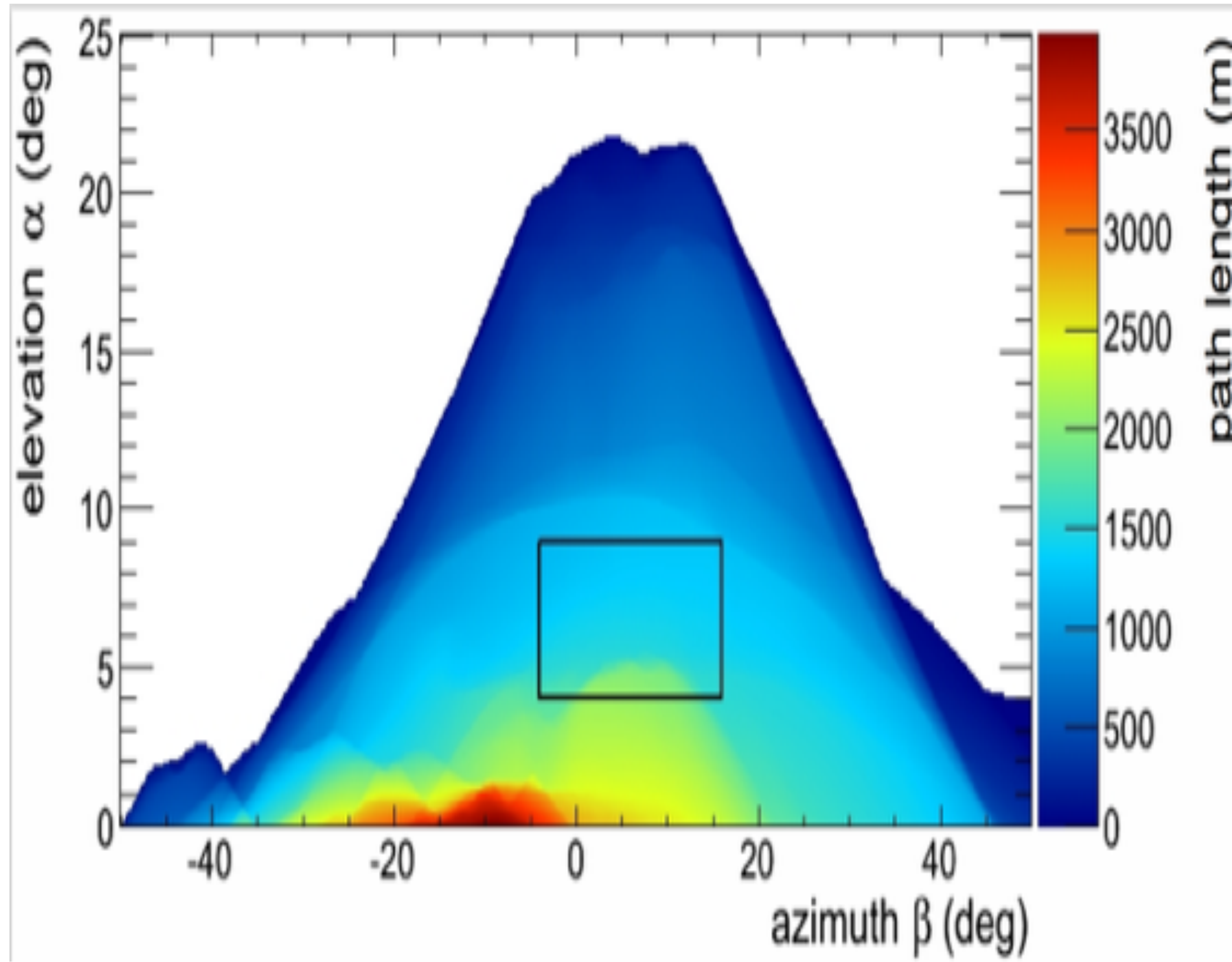

Effective surface

$$\mathcal{N}(\alpha,\beta) = \Delta T \cdot \int_{p_{\text{th}}}^{\infty} S_{\text{eff}}(\alpha,\beta,p)\cdot \Phi(\alpha,\beta,p)\,\mathrm{d}p$$

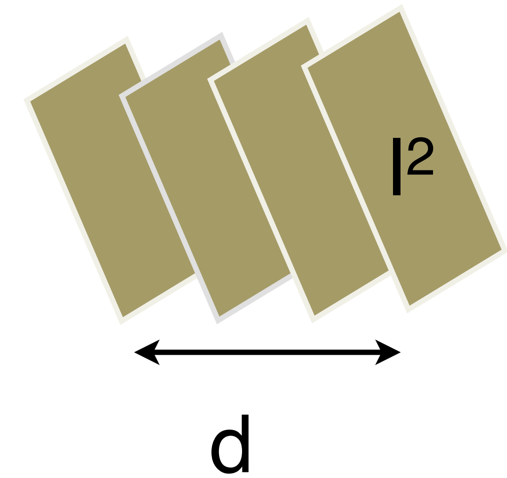

$$\mathcal{A}(\alpha,\beta) = \cos\alpha\cdot\cos\beta\cdot\sup\left(0, 1-\frac{d\cdot\text{abs}(\tan\beta)}{l}\right)\cdot\sup\left(0, 1-\frac{d\cdot\text{abs}(\tan\alpha)}{l\cos\beta}\right)$$

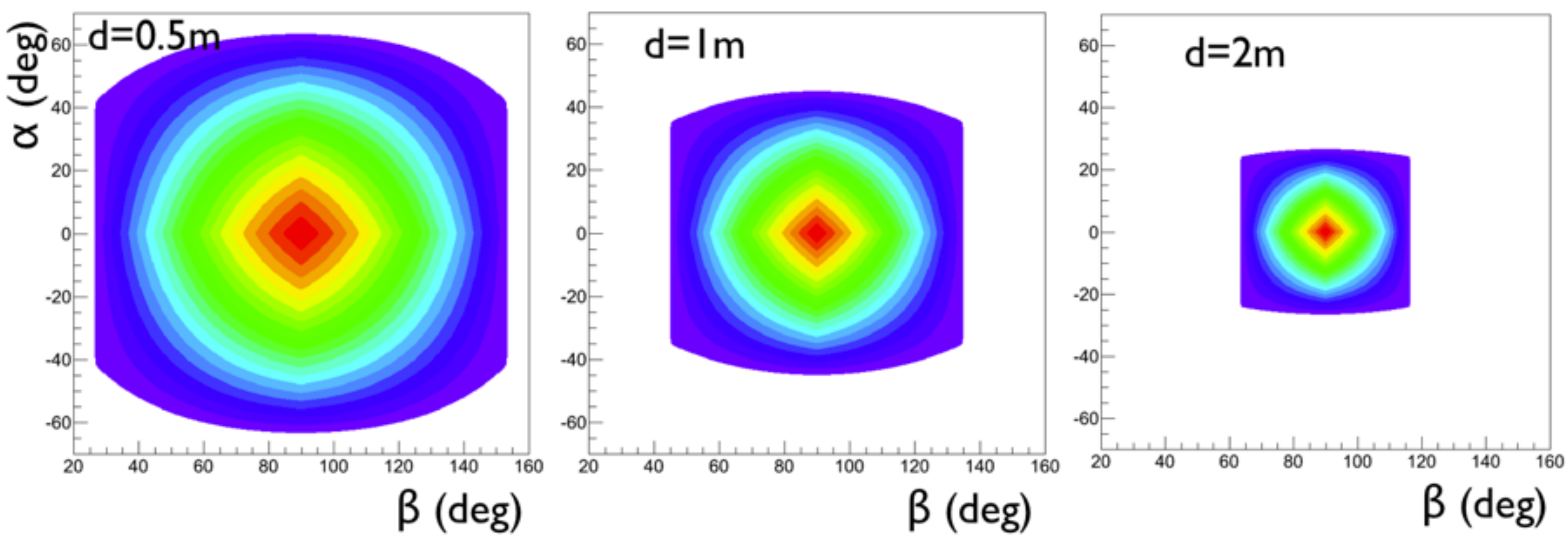

... and the real life complexity

$N/N_0(\alpha,\beta)$ ⟹ $\int\rho(r,\alpha,\beta)\,dr / \int dr$

$\mathcal{T}_\rho$ is calculated from an measured number of muons in a given direction

Measurement = Signal + **Background**

Only known after measurements and detailed Monte Carlo simulations

Can be calculated beforehand analytically

Table 1. Transmitted Flux of Ballistic Atmospheric-Muons Behind Different Rock Thicknesses and the Inverted Density Through a Muographic Measurement Affected by a Background Flux of 1.94 $m^{-2}\ d^{-1}\ deg^{-2}$ (the Quadratic Mean of the MU-RAY and TOMUVOL Measurements Given in Equations (4) and (5))

Integrated Density (True, mwe)	Elevation Angle (deg)	Transmitted Flux ($m^{-2}\ d^{-1}\ deg^{-2}$)	Integrated Density (measured, mwe)	Bias (%)
500	18	3.18	389.7	−22
1000	11	0.83	539.6	−46
2000	3	0.19	498.3	−75

J. Geophys. Res. Solid Earth, 120, doi:10.1002/2015JB011969

Background sources

Cecchini & Spurio

http://www.geosci-instrum-method-data-syst.net/1/185/2012/gi-1-185-2012.pdf

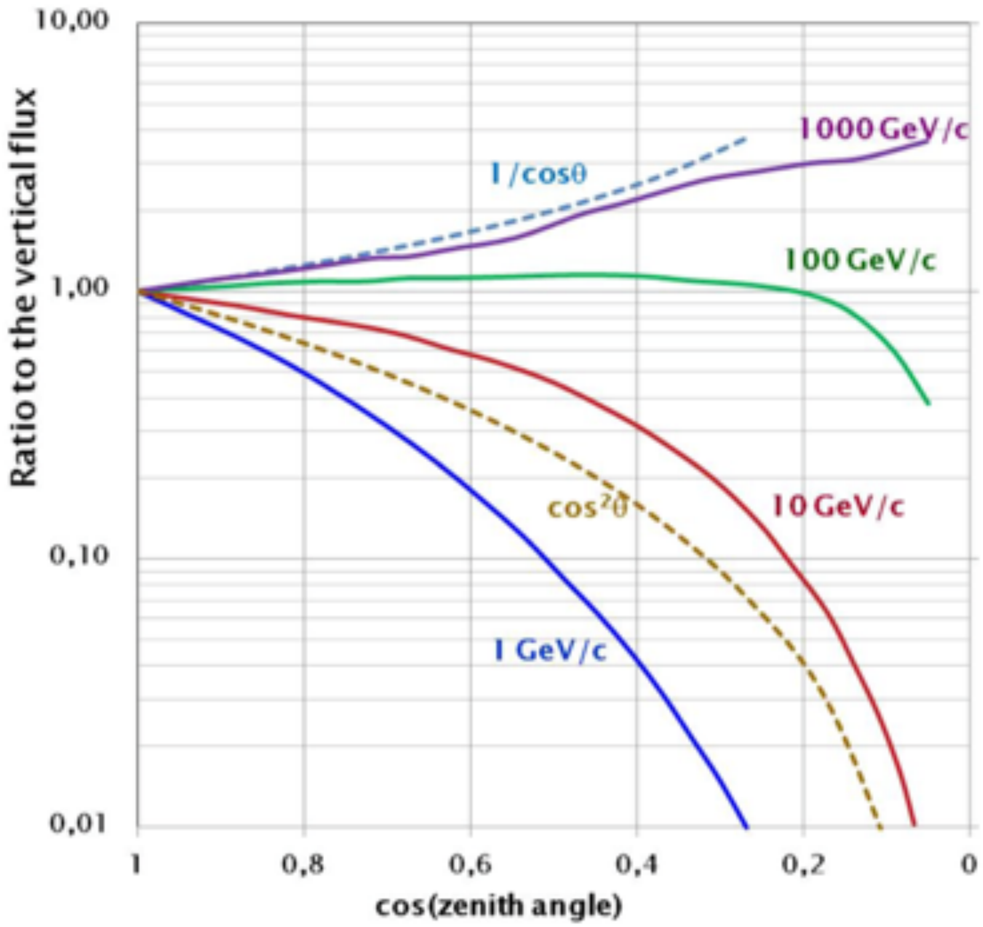

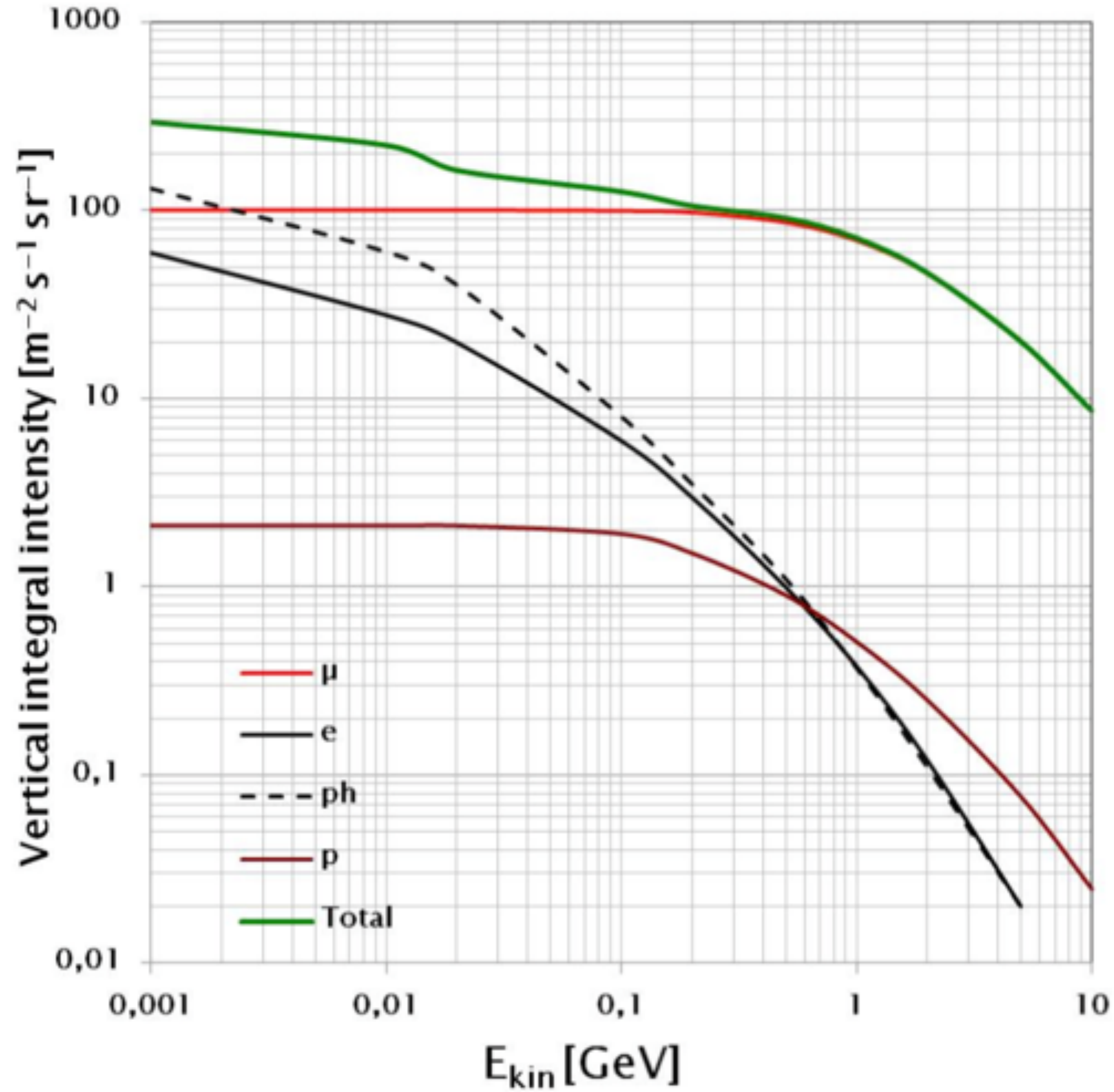

Fig. 1. Integral fluxes averaged over the 11-yr solar cycle of μ, e, p and photons (ph) arriving at geomagnetic latitudes $\sim 40°$ vs. their kinetic energy.

Background study

Geophysical Journal International Advance Access published May 19, 2016

Monte Carlo simulation for background study of geophysical inspection with cosmic-ray muons

Ryuichi Nishiyama[1,2]

Akimichi Taketa[1]

Seigo Miyamoto[1]

Katsuaki Kasahara[3]

[1] *Earthquake Research Institute, The University of Tokyo, Japan*

[2] *Albert Einstein Center for Fundamental Physics, Laboratory for High-Energy Physics, University of Bern, Switzerland*

[3] *Research Institute for Science and Engineering, Waseda University, Japan*

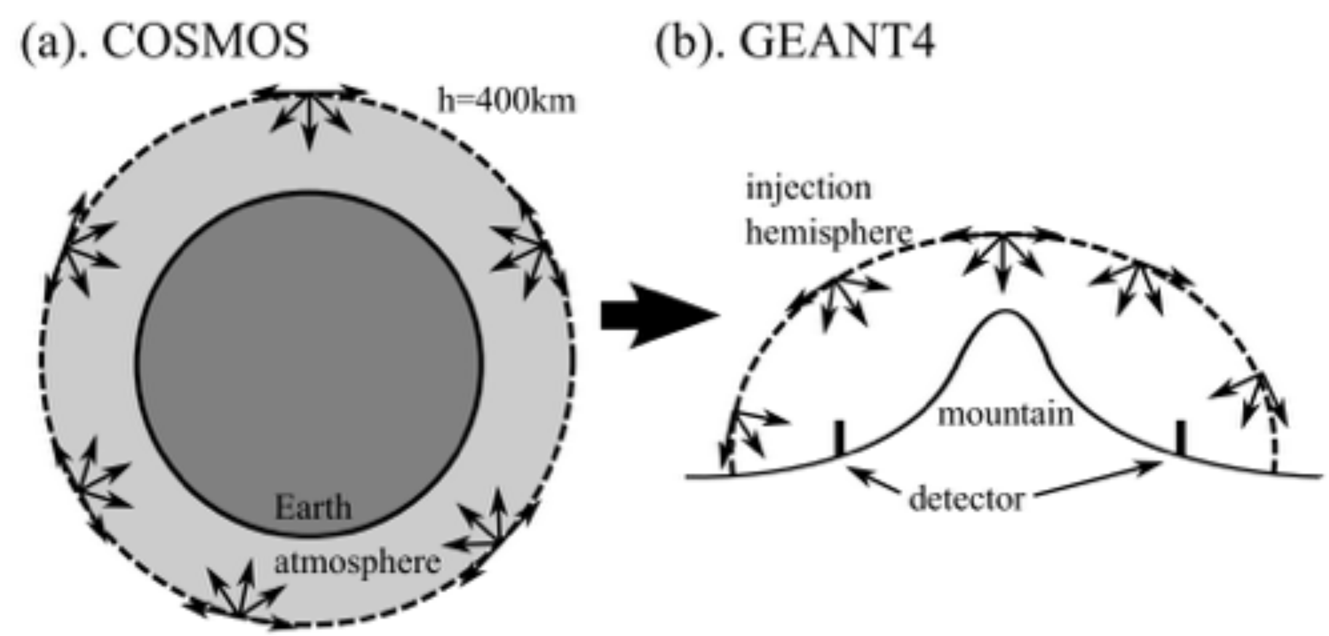

(a).

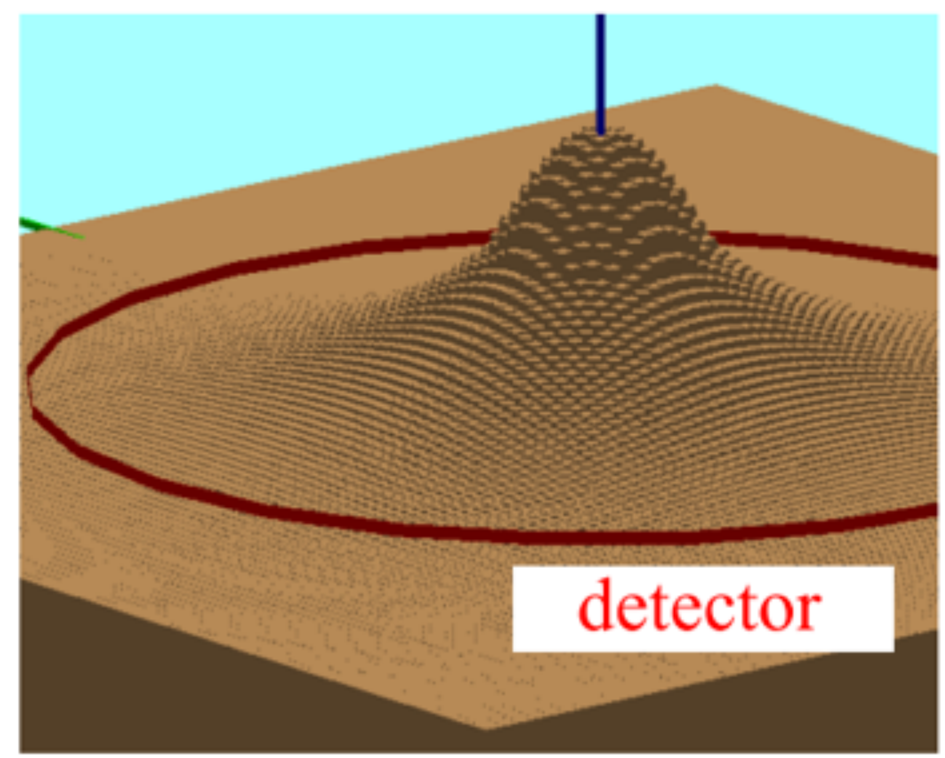

Background study

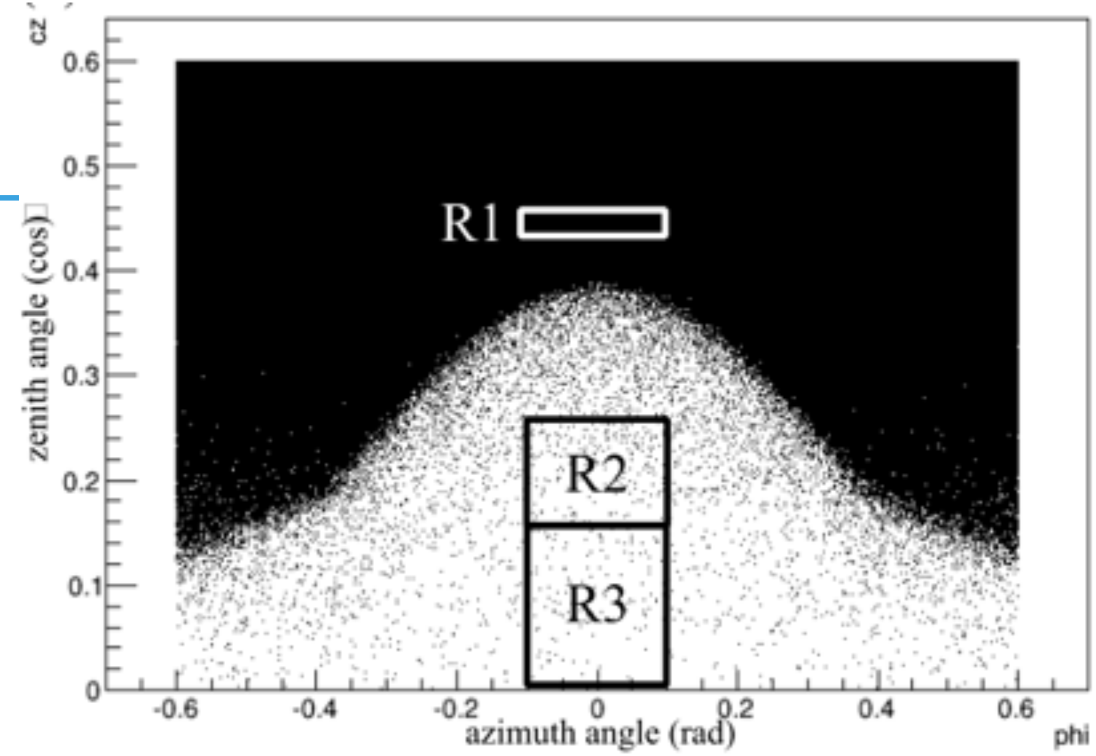

(c).

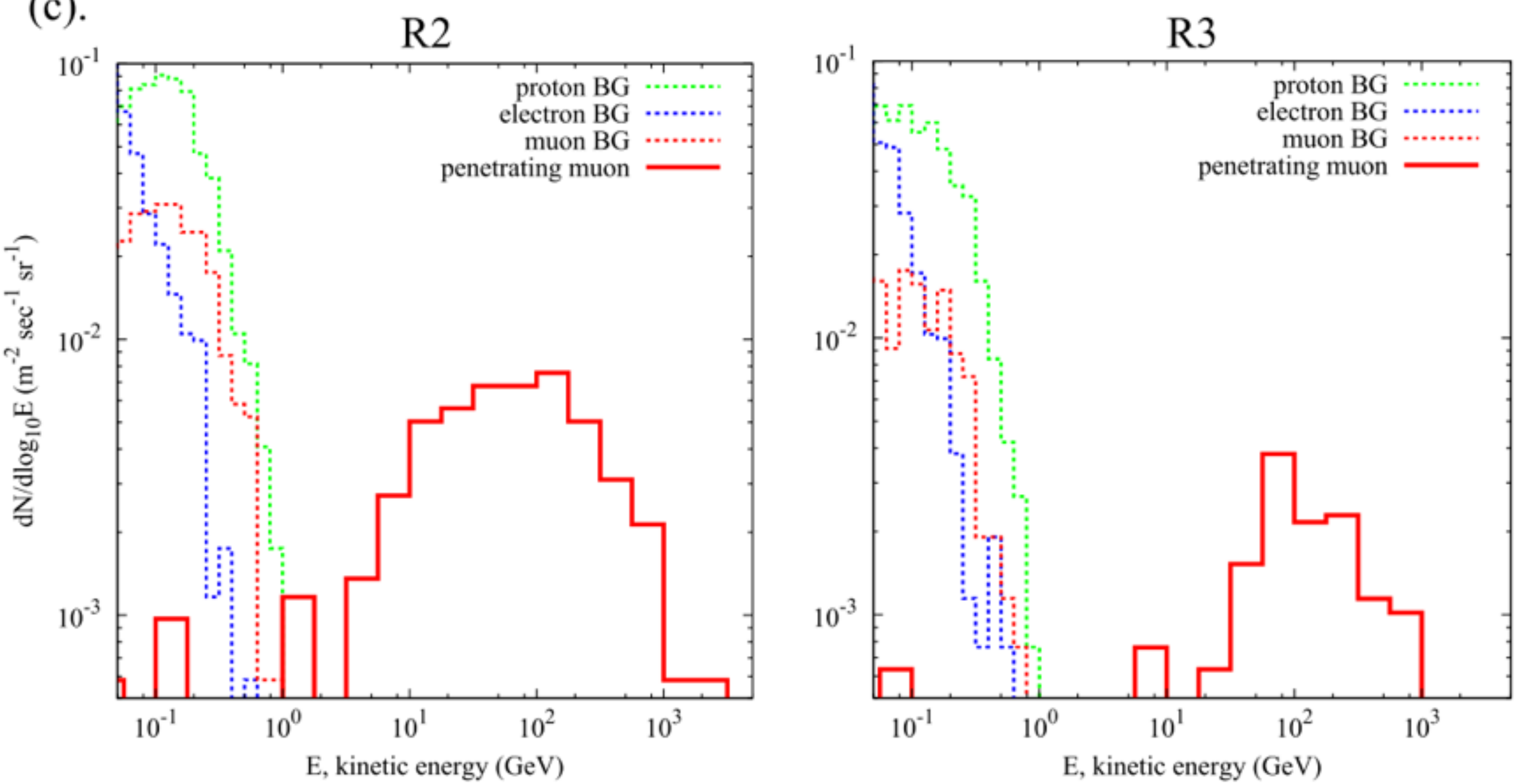

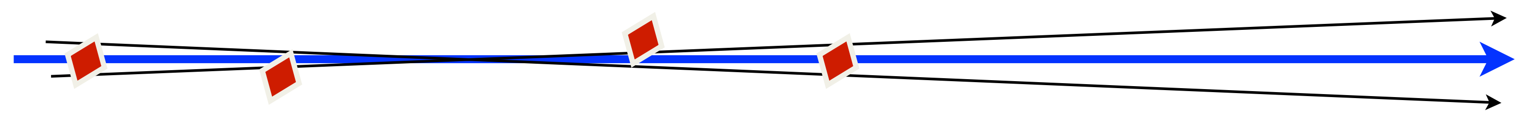

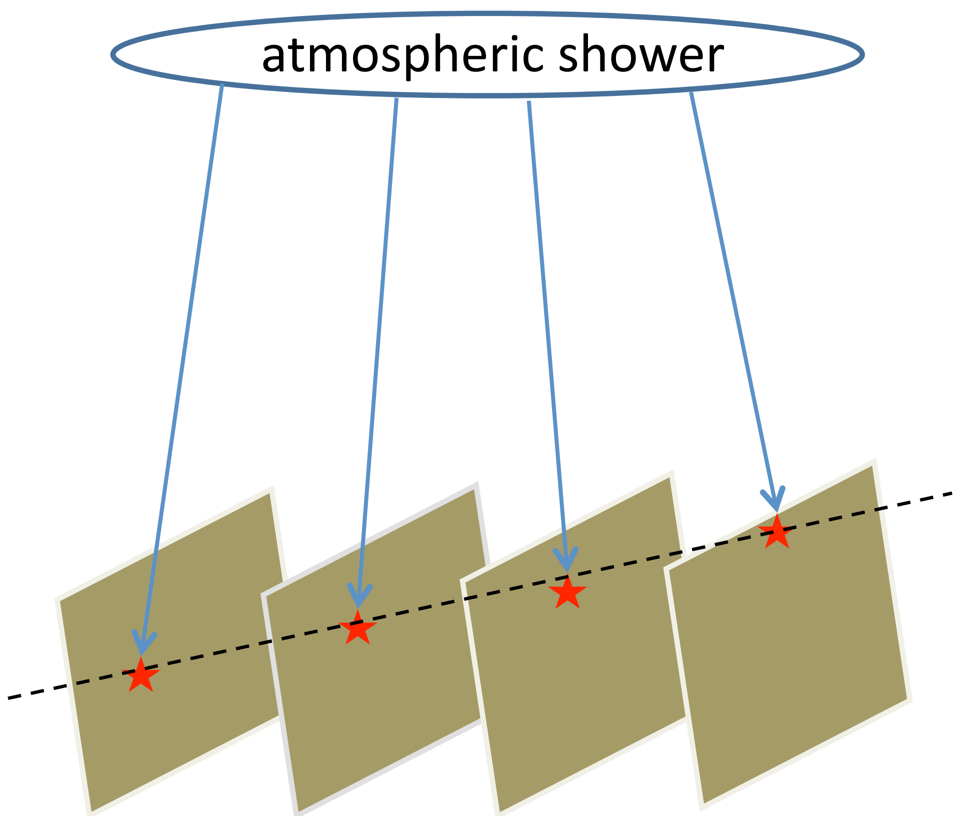

Tanaka et al. 2012

Geosci. Instrum. Method. Data Syst., 3, 29–39, 2014
www.geosci-instrum-method-data-syst.net/3/29/2014/
doi:10.5194/gi-3-29-2014

Geoscientific Instrumentation Methods and Data Systems
Open Access

Experimental study of source of background noise in muon radiography using emulsion film detectors

R. Nishiyama[1], S. Miyamoto[1], and N. Naganawa[2]
rsity of Tokyo, Tokyo, Japan
of Science

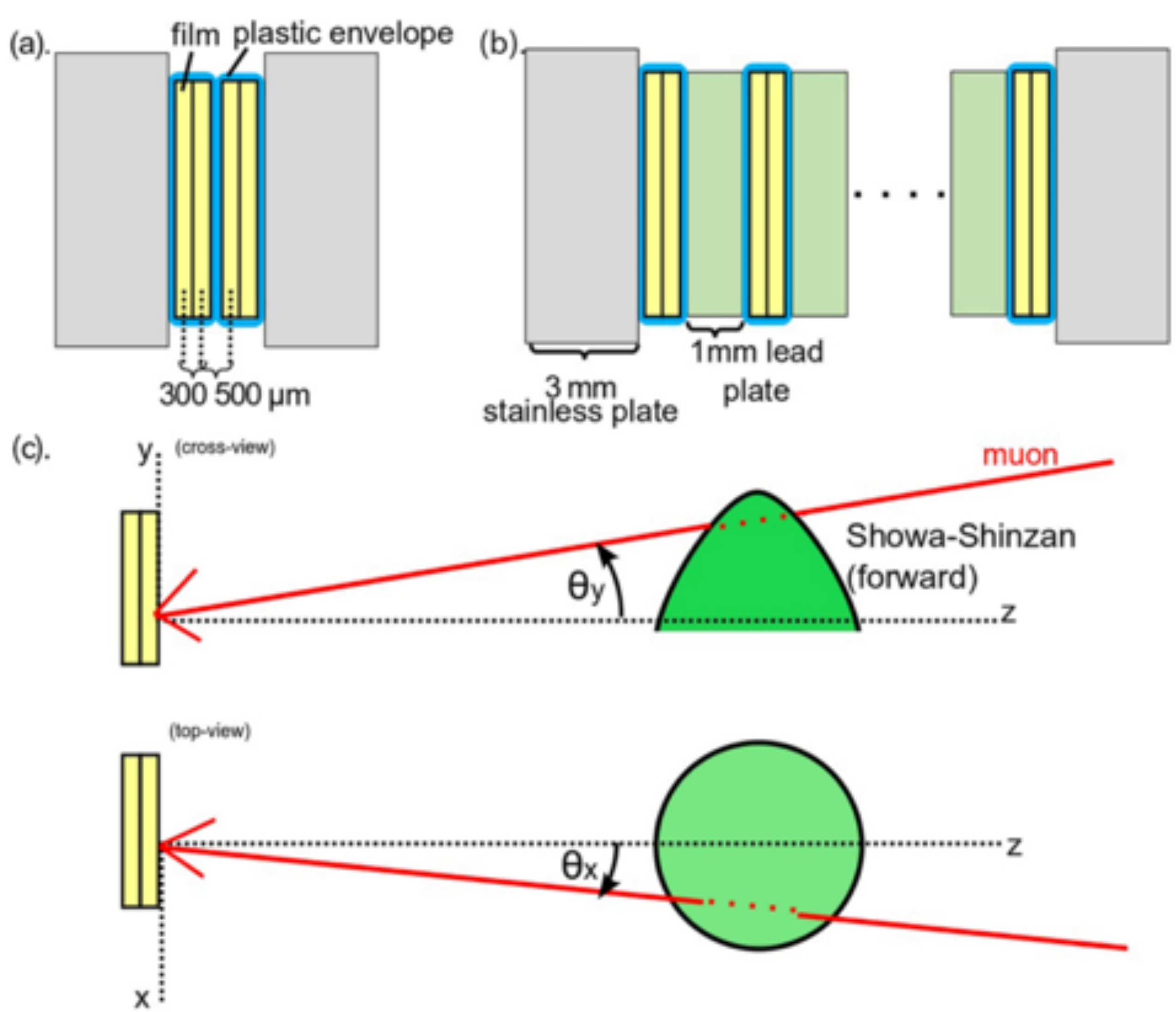

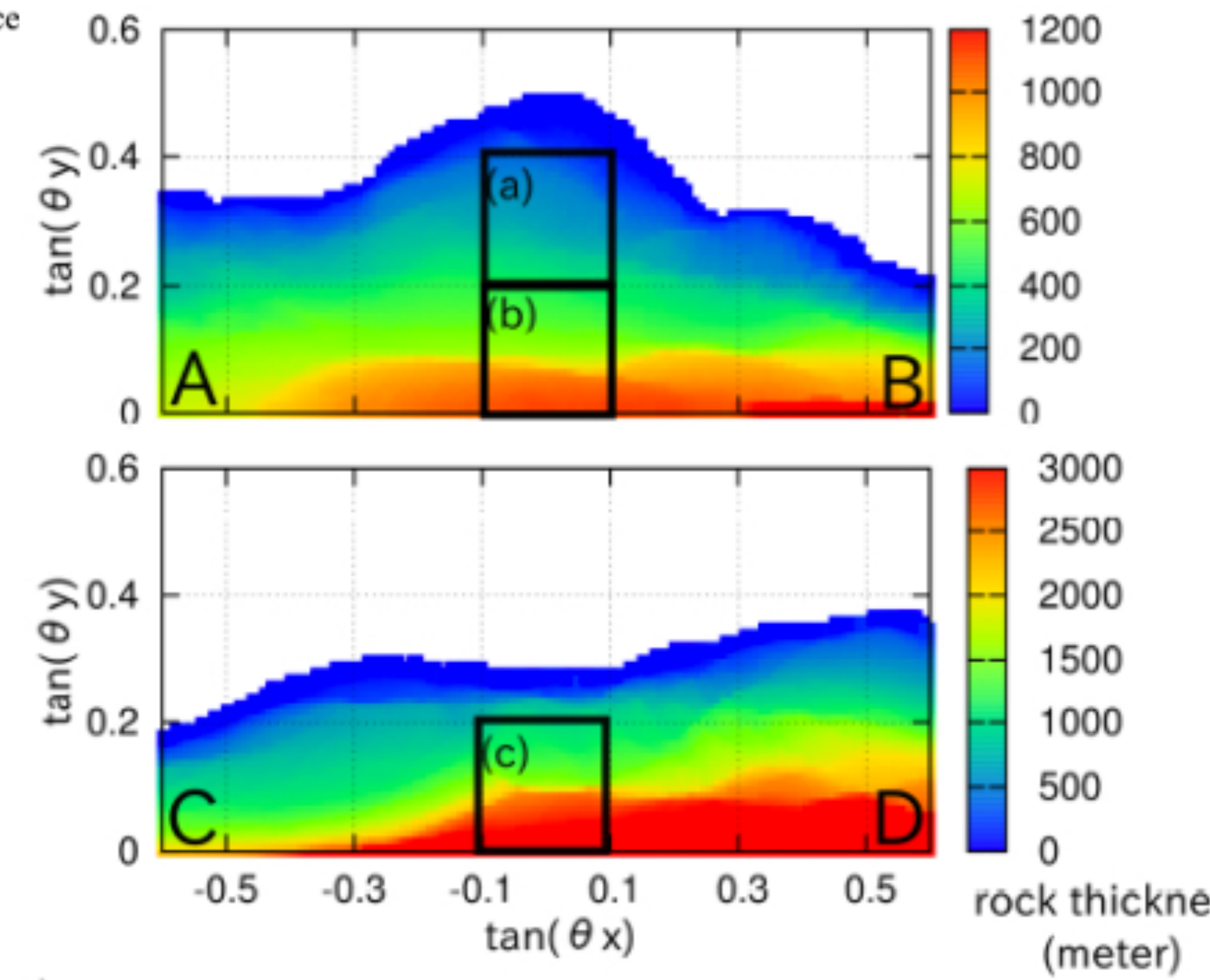

g)

Table 1. The number of the selected tracks for the three angular domains (a), (b), and (c) for the quartet detector (top) and EC (bottom). The last rows show the particle fluxes with efficiency compensation using ϵ_{tot} values for each inclination range.

Quartet detector: $S = 27\,cm^2$, $T = 1.45 \times 10^7$ s				
inclination range: θ^Q	domain (a)	domain (b)	domain (c)	efficiency (%)
0–0.126	151	71	–	91.5 ±
0.126–0.200	168	34	–	90.2 ±
0.200–0.262	1	3	27	72.4 ±
0.262–0.317	–	–	20	62.0 ±
0.317–0.368	–	–	28	54.5 ±
0.368–0.416	–	–	27	50.3 ±
0.416–0.461	–	–	2	45.4 ±
total statistics	320	108	104	
flux: $F^Q(cm^{-2}\,sr^{-1}\,s^{-1})$	$(2.97 \pm 0.17) \times 10^{-5}$	$(8.25 \pm 0.80) \times 10^{-6}$	$(1.19 \pm 0.12) \times 10^{-5}$	
estimated density ($g\,cm^{-3}$)	$1.18^{+0.04}_{-0.04}$	$0.76^{+0.05}_{-0.05}$	$0.23^{+0.02}_{-0.02}$	
ECC detector: $S = 27\,cm^2$, $T = 1.45 \times 10^7$ s				
inclination range: θ	domain (a)	domain (b)	domain (c)	efficiency (%): ϵ
0–0.200	–	15	2	>
0.200–0.317	27	2	–	98.4 ±
0.317–0.416	75	–	–	94.4 ±
total statistics	102	17	2	
flux: $F^{ECC}(cm^{-2}\,sr^{-1}\,s^{-1})$	$(8.23 \pm 0.81) \times 10^{-6}$	$(1.15 \pm 0.28) \times 10^{-6}$	too low statistics	
estimated density ($g\,cm^{-3}$)	$2.33^{+0.12}_{-0.10}$	$2.00^{+0.23}_{-0.17}$	too low statistics	

... TOMUVOL-MURAY 2013 campaign on Puy de Dôme

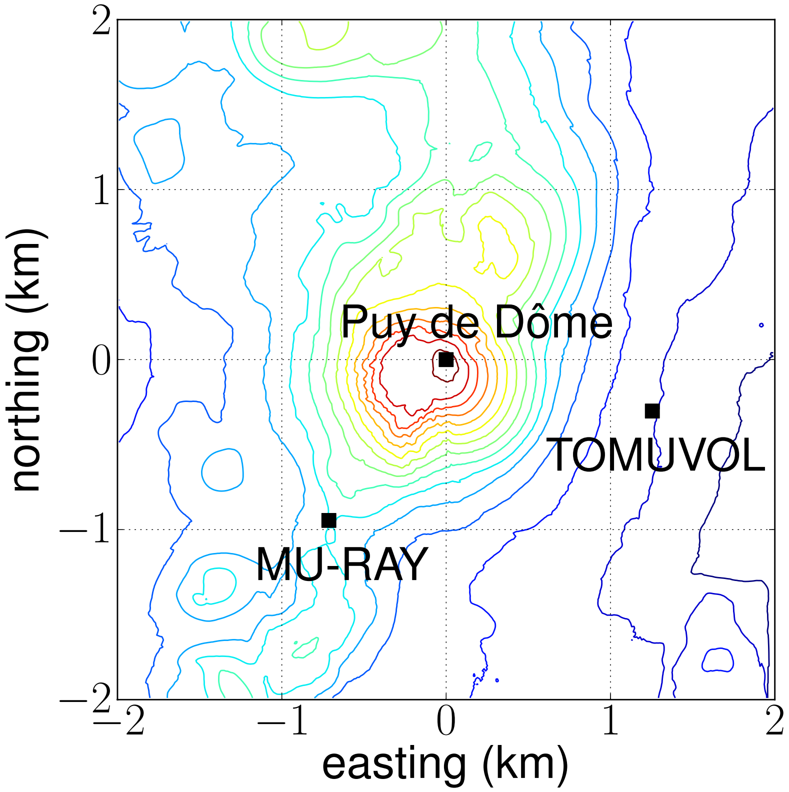

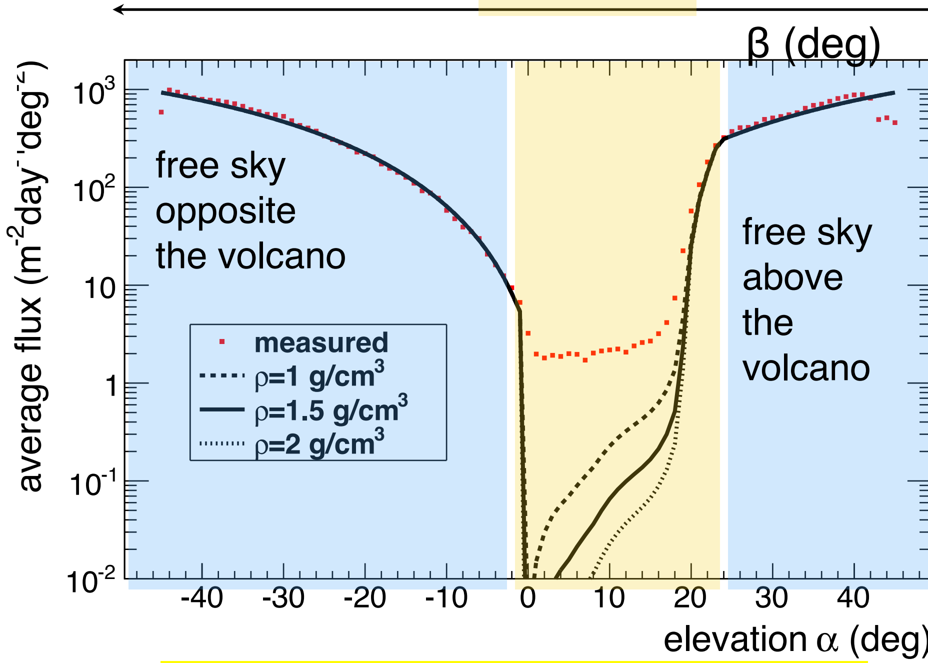

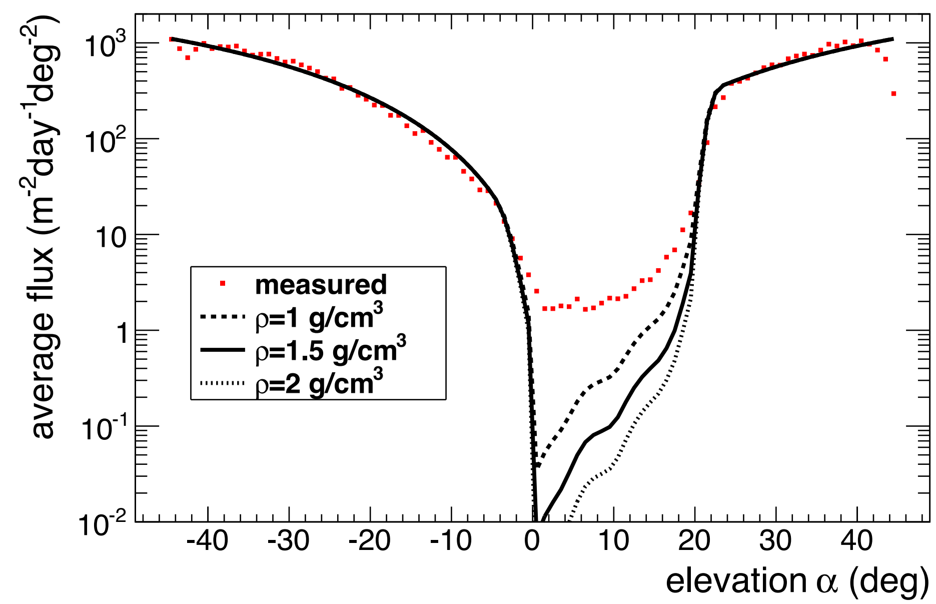

J. Geophys. Res. Solid Earth, 120, doi:10.1002/2015JB011969

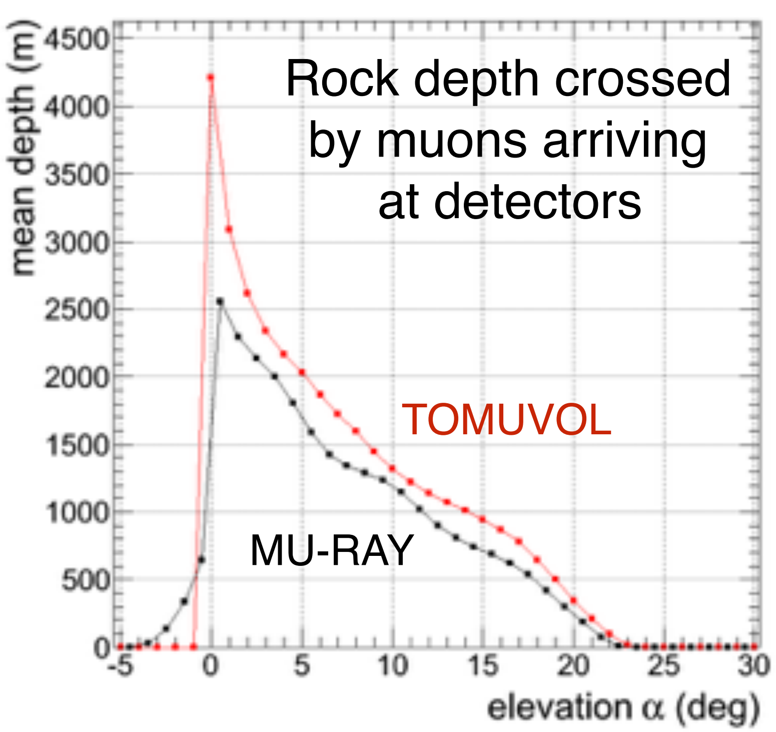

Data/flux model agreement:
~5% for free sky

TOMUVOL 2015 campaign on Puy de Dôme

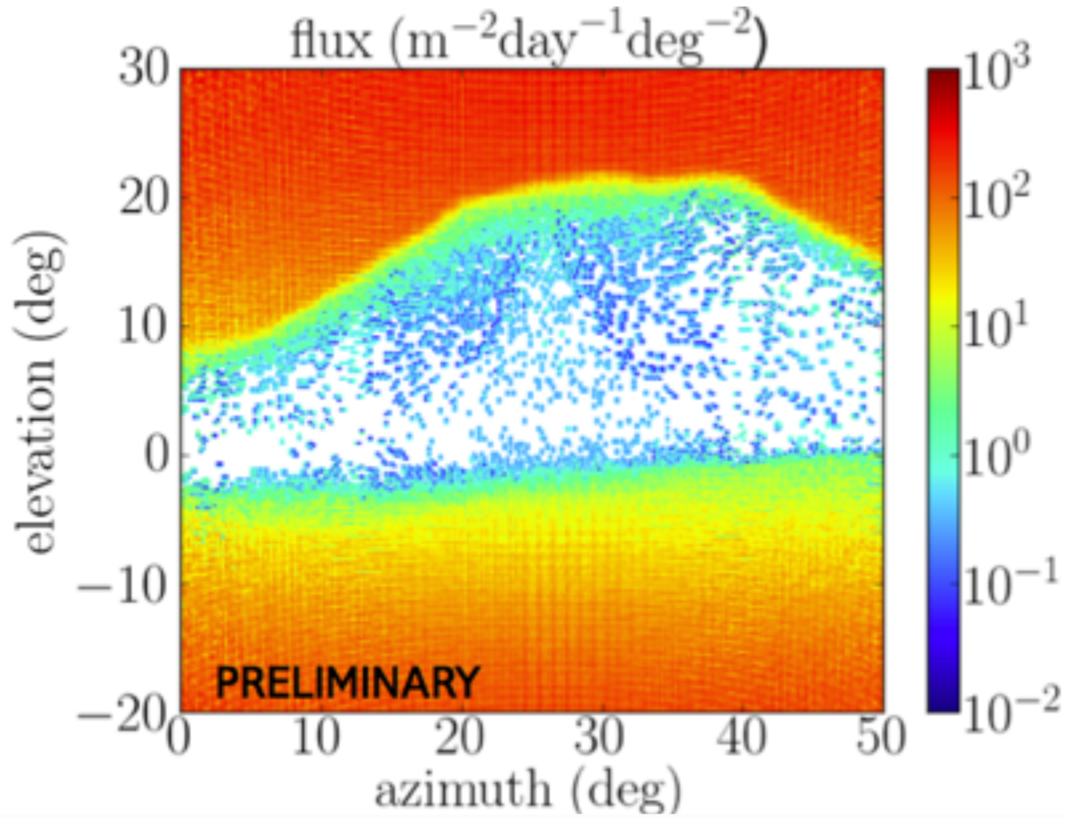

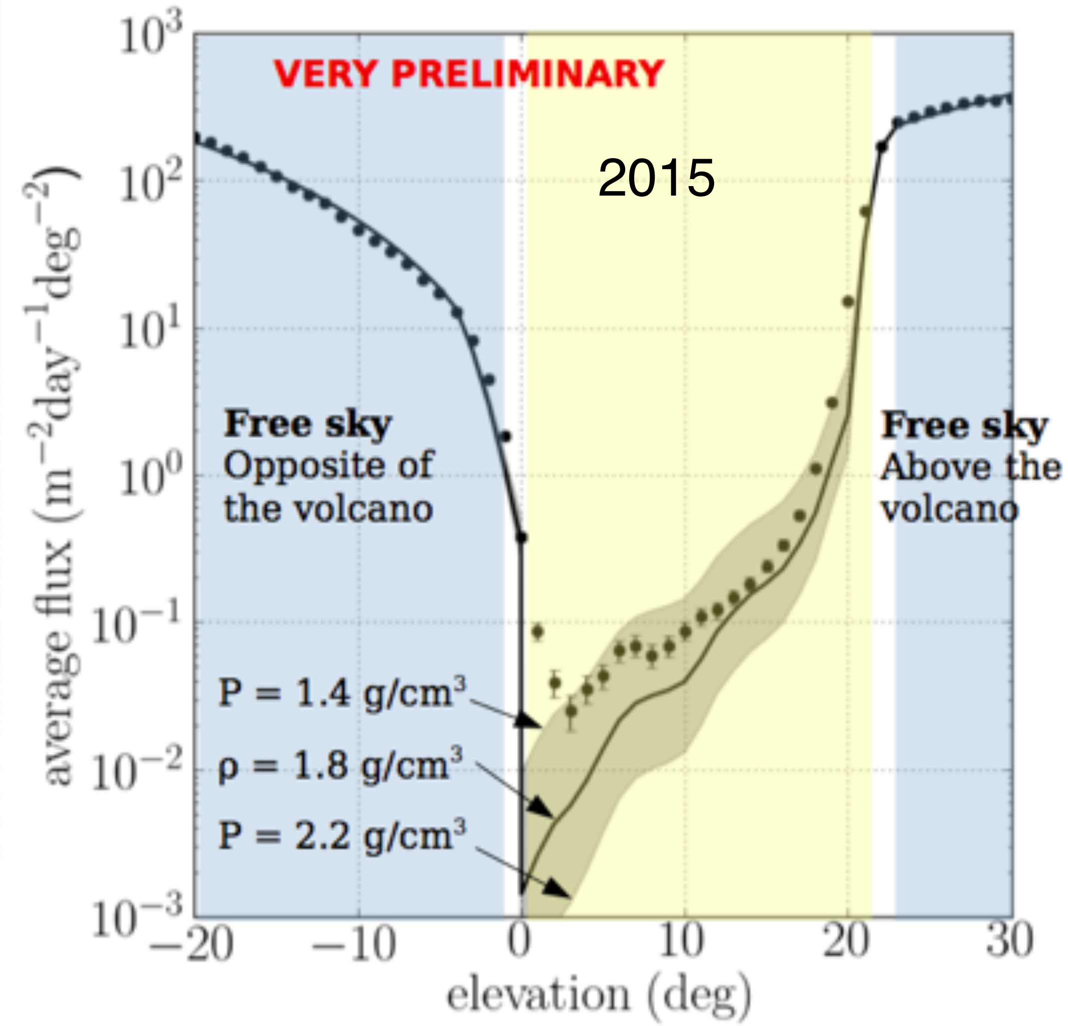

For the moment, systematic uncertainty estimated from comparison between data and model in the free sky

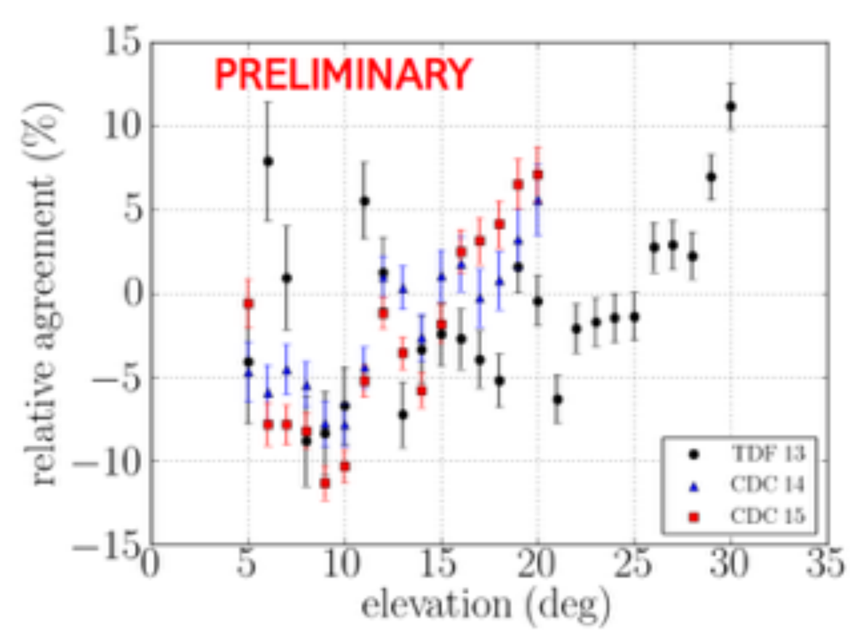

$$rel.\ agreement = 100 \times \left(\frac{data}{pred} - 1\right)$$

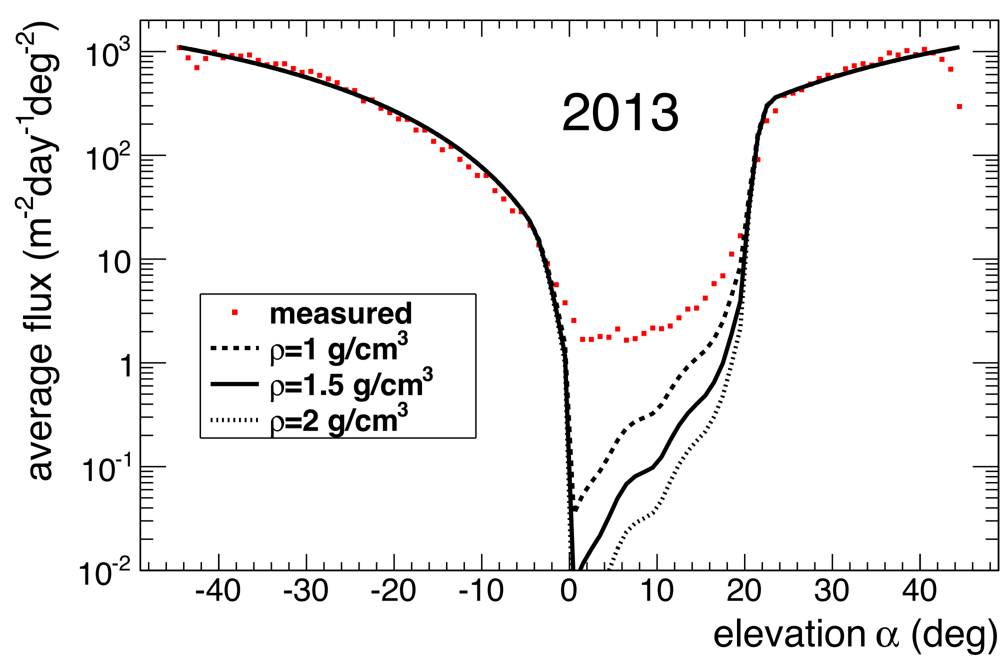

How do we compare detectors

- effective surface
- position & angular resolution
- energy(momentum) threshold
- time resolution
- dead time

- weight
- robustness
- power consumption
- price

- calibration
- background rejection
- ….


CUSTOMS

Early muographic attempts: George, 1955

Cosmic Rays Measure Overburden of Tunnel

• Fig. 1—Geiger counter "telescope" in operation in the Guthega-Munyang tunnel. From left are Dr. George and his assistants, Mr. Lehane and Mr. O'Neill.

Geiger counter telescope used for mass determination at Guthega project of Snowy Scheme . . . Equipment described

By Dr. E. P. George*
University of Sydney, N.S.W.

Early muographic attempts: Alvarez 1970

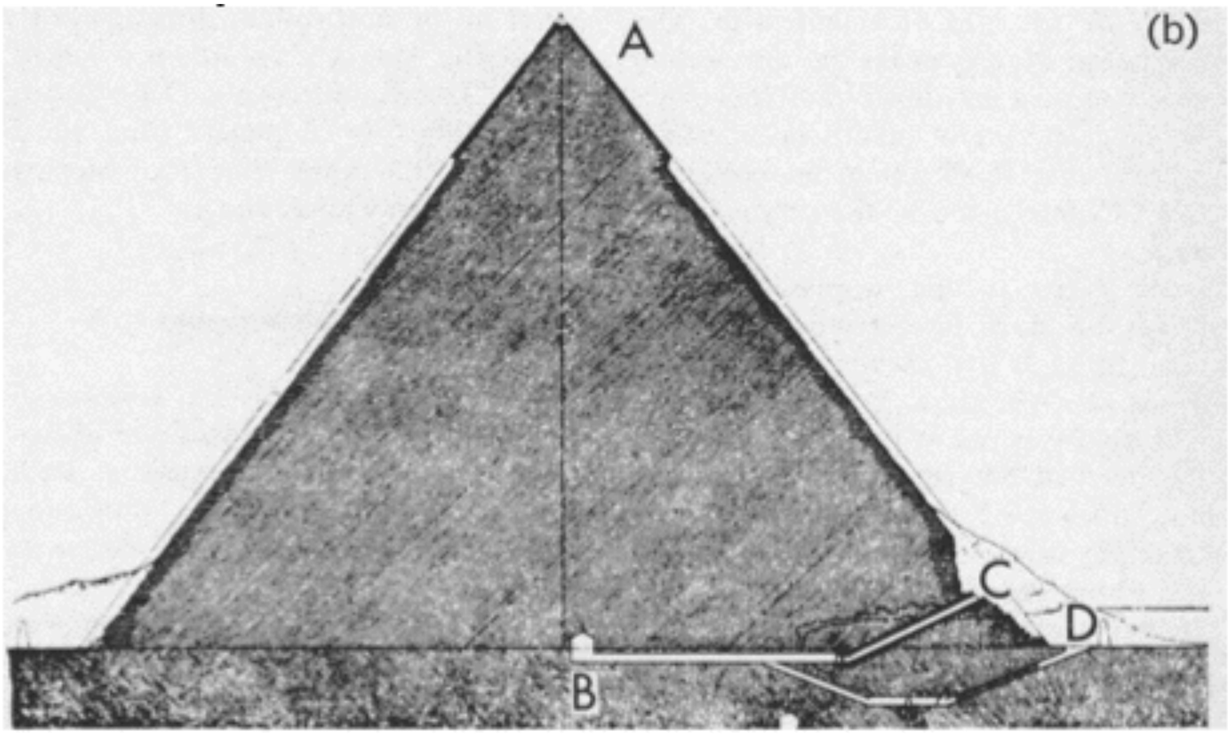

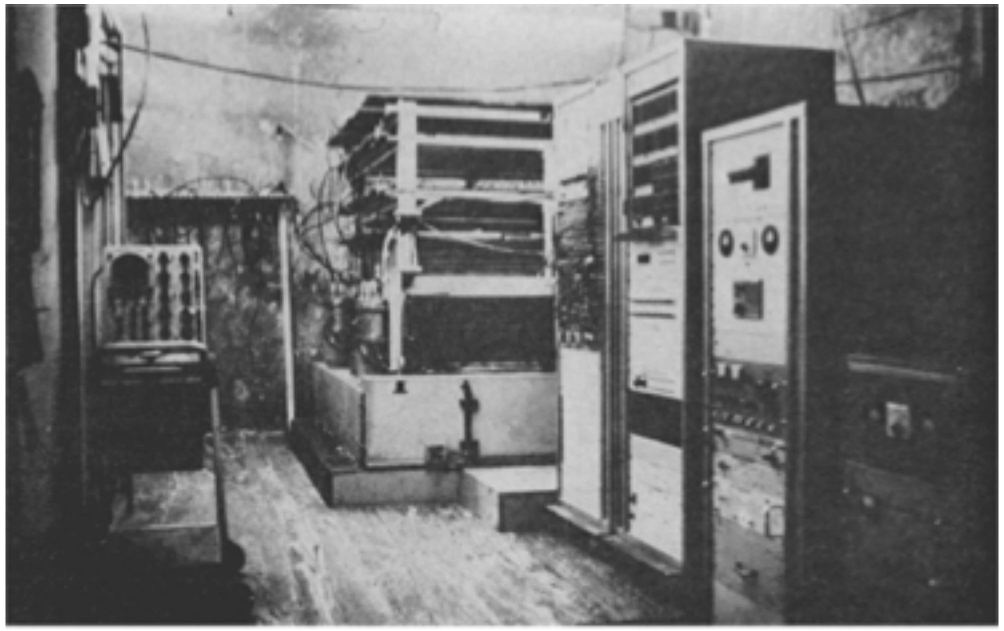

Fig. 6 (left). The equipment in place in the Belzoni Chamber under the pyramid.
Fig. 7 (right). The detection apparatus containing the spark chambers.

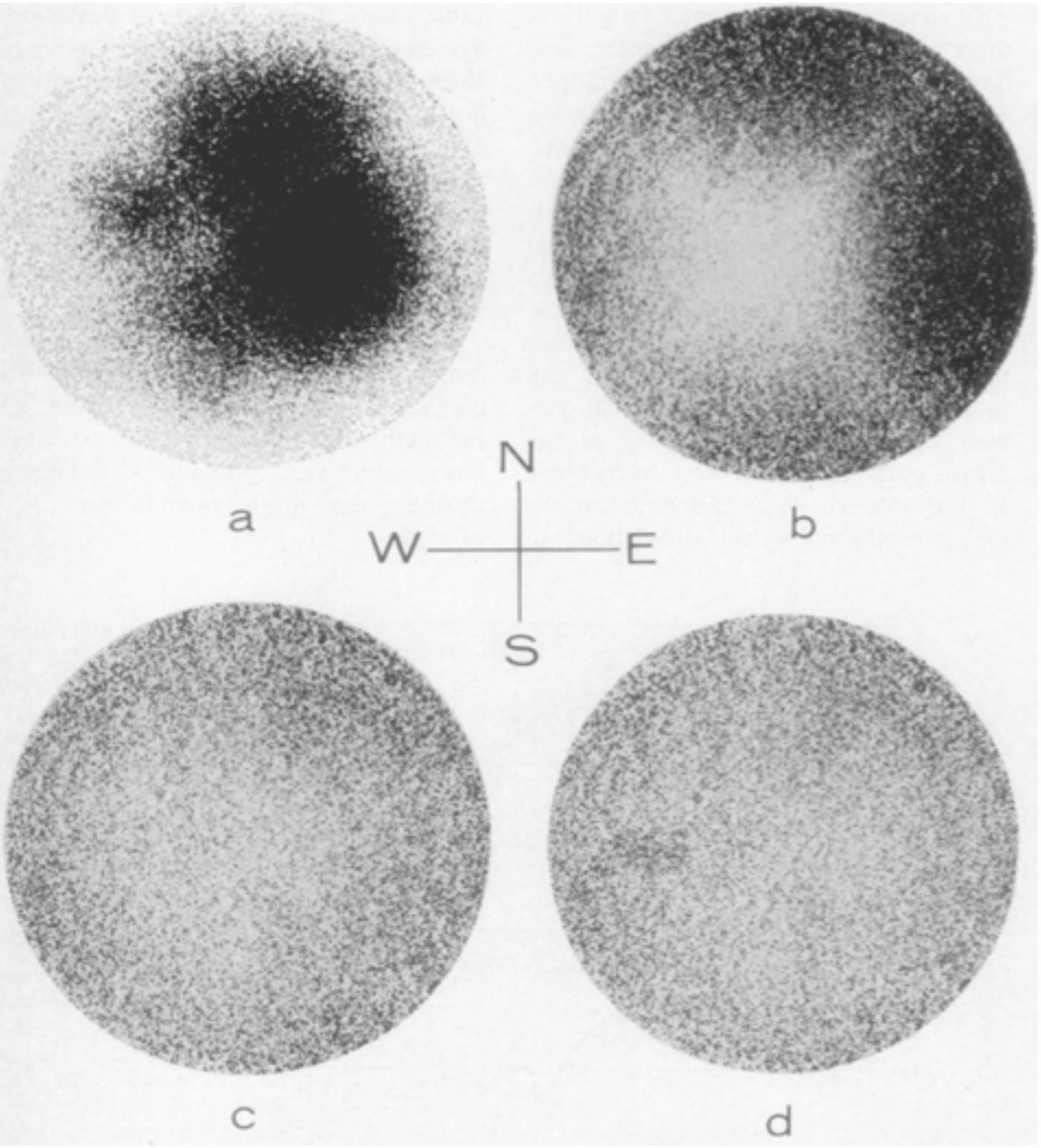

Fig. 13. Scatter plots showing the three stages in the combined analytic and visual analysis of the data and a plot with a simulated chamber. (a) Simulated "x-ray photograph" of uncorrected data. (b) Data corrected for the geometrical acceptance of the apparatus. (c) Data corrected for pyramid structure as well as geometrical acceptance. (d) Same as (c) but with simulated chamber, as in Fig. 12.

Transmission muography:: inside or outside?

Universidad Nacional Autonoma de México

When a tunnel / borehole / cavity available use it to host your detector and look above your heads

- for metal deposits (@ Triumph, scintillators)
- for water infiltration or rock structure alterations

➥little/no background (shielded by the target)
➥can use lower energy muons
➥ generally little space
➥ sometimes demanding environment

Monitoring subsurface CO² emplacent and security of storage using muons

V.A. Kudryavtsev et al, Int. J. of Greenhouse Gas Control 11(2012) 21-24

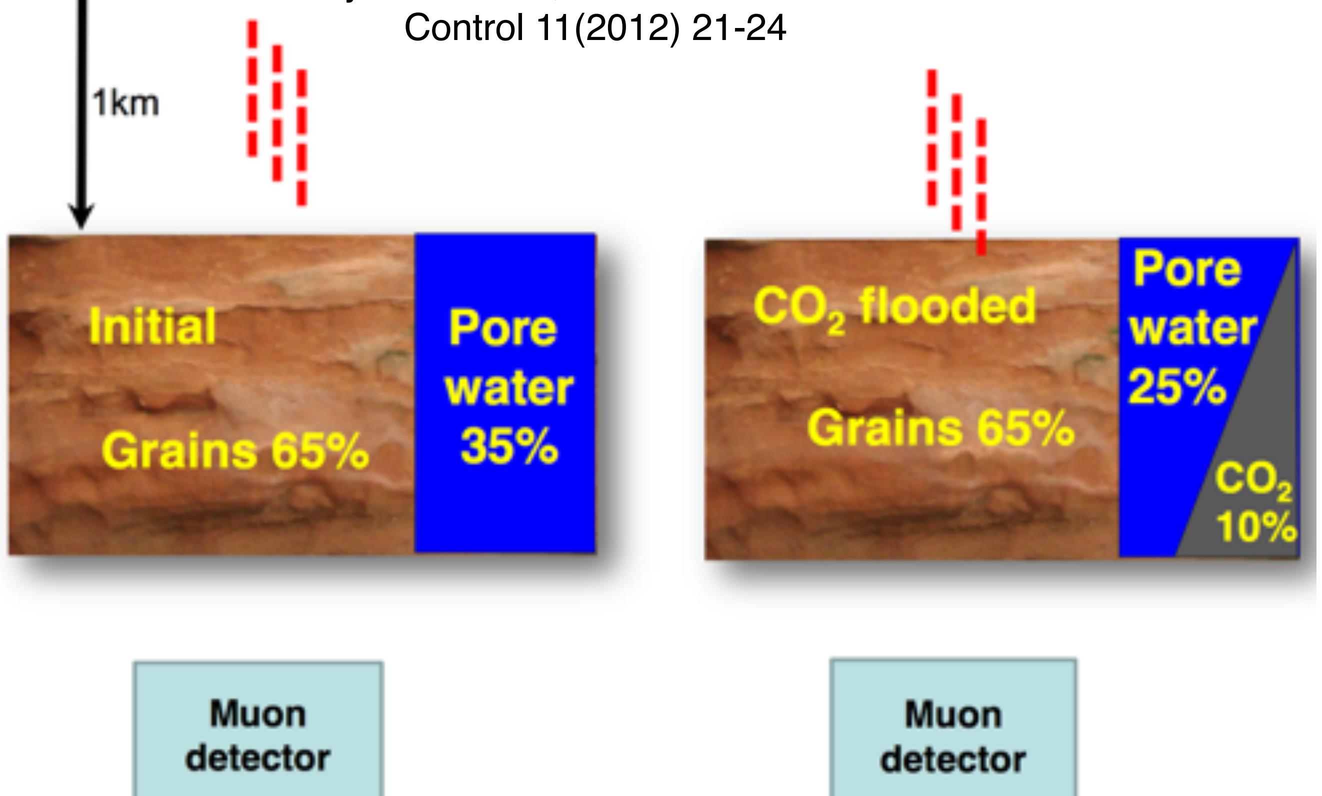

Durham University

CeREES
Centre for Research into Earth Energy Systems

Cosmic Ray Muon Tomography; A New Method for Monitoring Sweep in Oilfield Waterfloods?

Jon Gluyas[1], Vitaly Kudryavtsev[2], Lee Thompson[2], Dave Allan[1], Chris Benton[3], Paula Chadwick[1], Sam Clark[1], Max Coleman[4], Joel Klinger[2], Cathryn Mitchell[3], Sam Nolan[1], Sumanta Pal[2], Sean Paling[5], Neil Spooner[2], Sam Telfer[2], David Woodward[2]

[1]Department of Earth Sciences, Centre, Durham University,
[2]Department of Physics and Astronomy, University of Sheffield,
[3]JEngineering School, University of Bath,
[4]Jet Propulsion Laboratory, California Institute of Technology, Pasadena, USA
[5]Science & Technology Facilities Council, Rutherford Appleton Lab, Didcot

PESGB DEVEX, Aberdeen, May 2015

1.5 M pounds from DECC & Premier Oil

CO_2 storage monitoring

- Successful capture and storage isn't the end of the problem
- EU legislation is likely to require less than 1% leakage per 1000 years

- Monitoring will be required
- Costs of monitoring will need to factored in

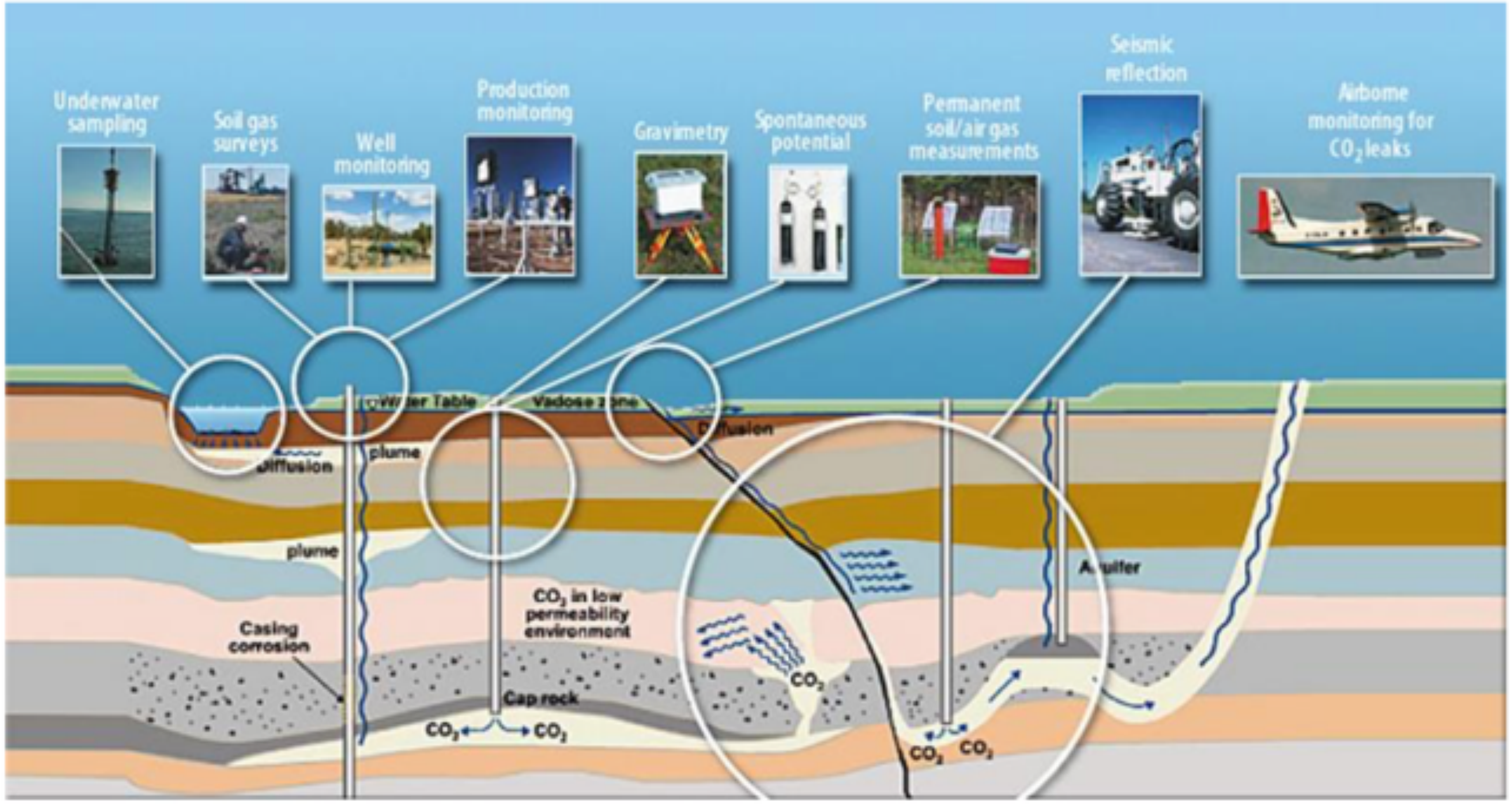

http://www.co2captureproject.org/operation.html

Borehole Detector Prototype

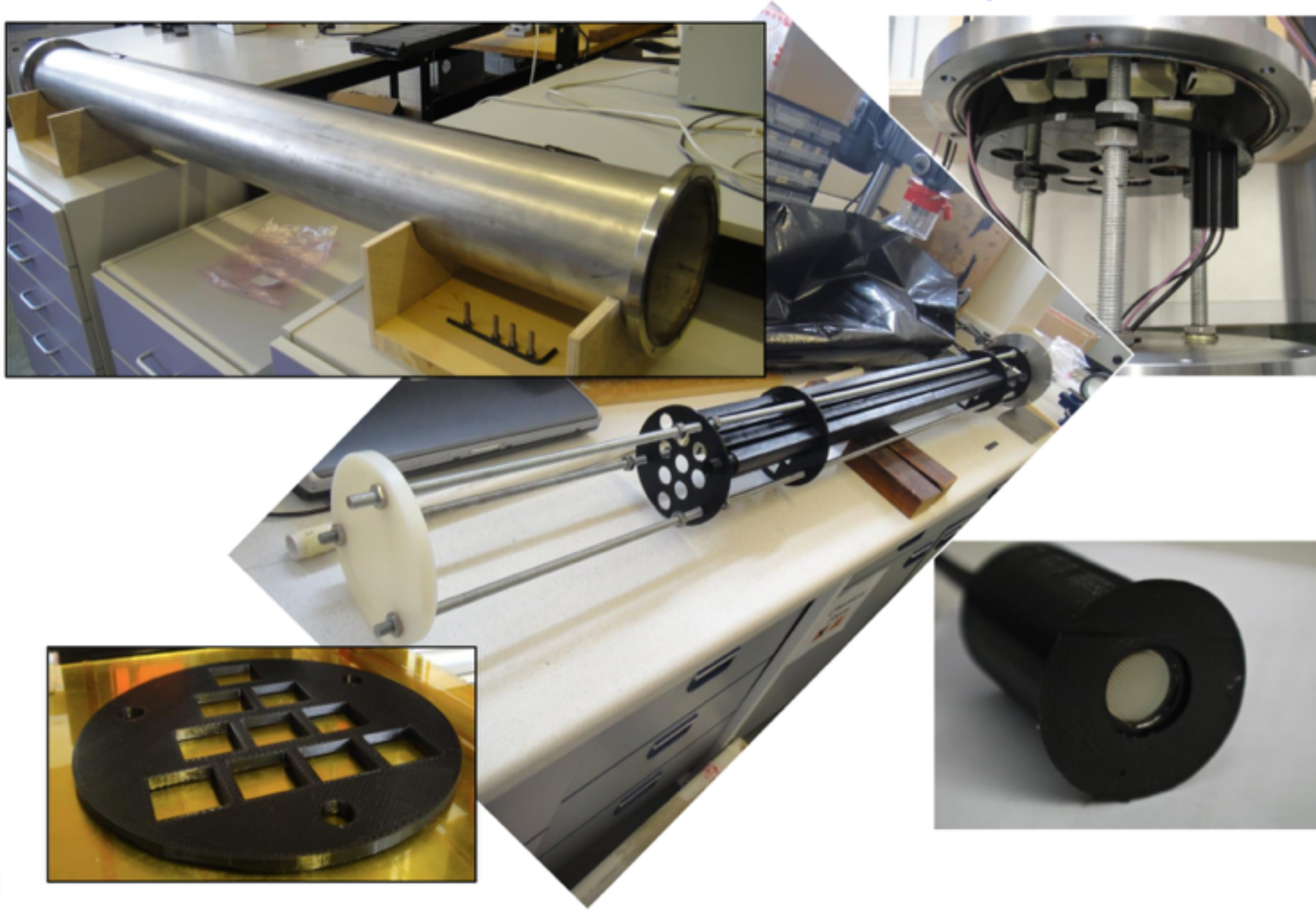

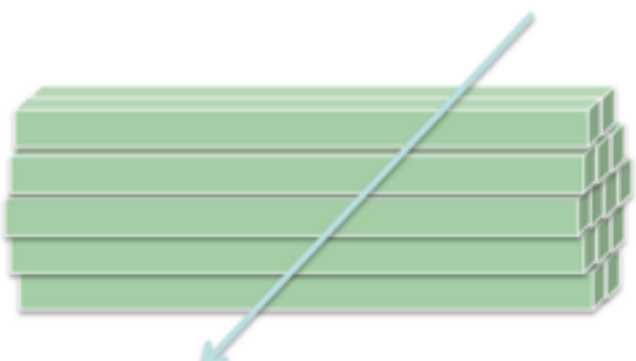

Search for cavities in the Teotihuacan Pyramid of the Sun using cosmic muons: preliminary results.

S. AGUILAR1, R. ALFARO1, E. BELMONT1, V. GRABSKI1, T. IBARRA1, V. LEMUS1, L. MANZANILLA2 A. MARTINEZ1, A. MENCHACA-ROCHA1, M. MORENO1 AND A. SANDOVAL1,
1 *Instituto de Fısica, Universidad Nacional Autonoma de Me´xico, Me´xico.* 2 *Instituto de Investigaciones Antropolo´gicas, Universidad Nacional Autonoma de Mexico Me´xico.*
33RD INTERNATIONAL COSMIC RAY CONFERENCE, RIO DE JANEIRO 2013 THE ASTROPARTICLE PHYSICS CONFERENCE

$2x1m^2$ Scintillators for trigger

$6x1m^2$ MWPCs for tracking

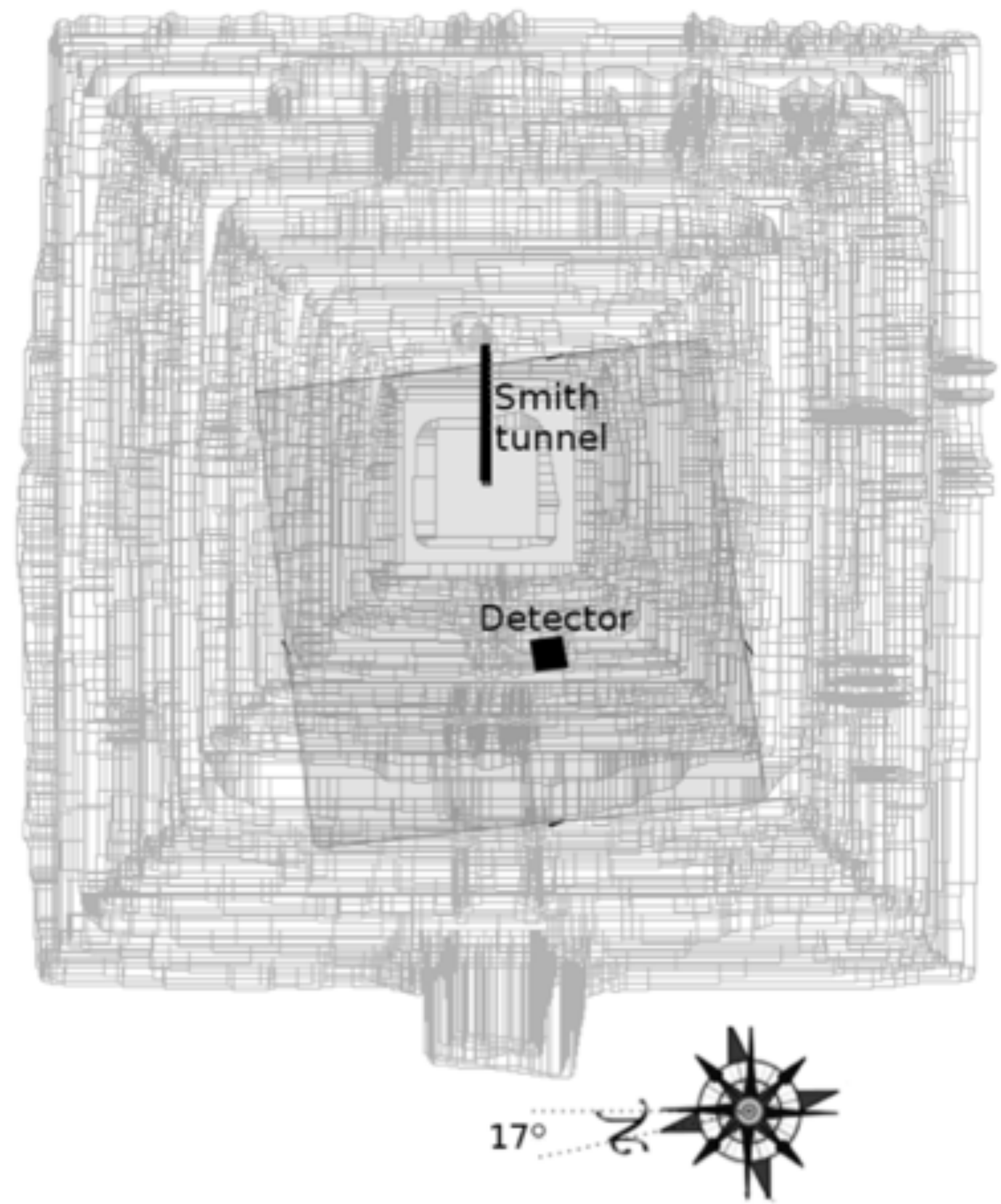

top view of the pyramid

Eiger Muon Tomography: Mapping the subglacial bedrock topography of an active mountain glacier

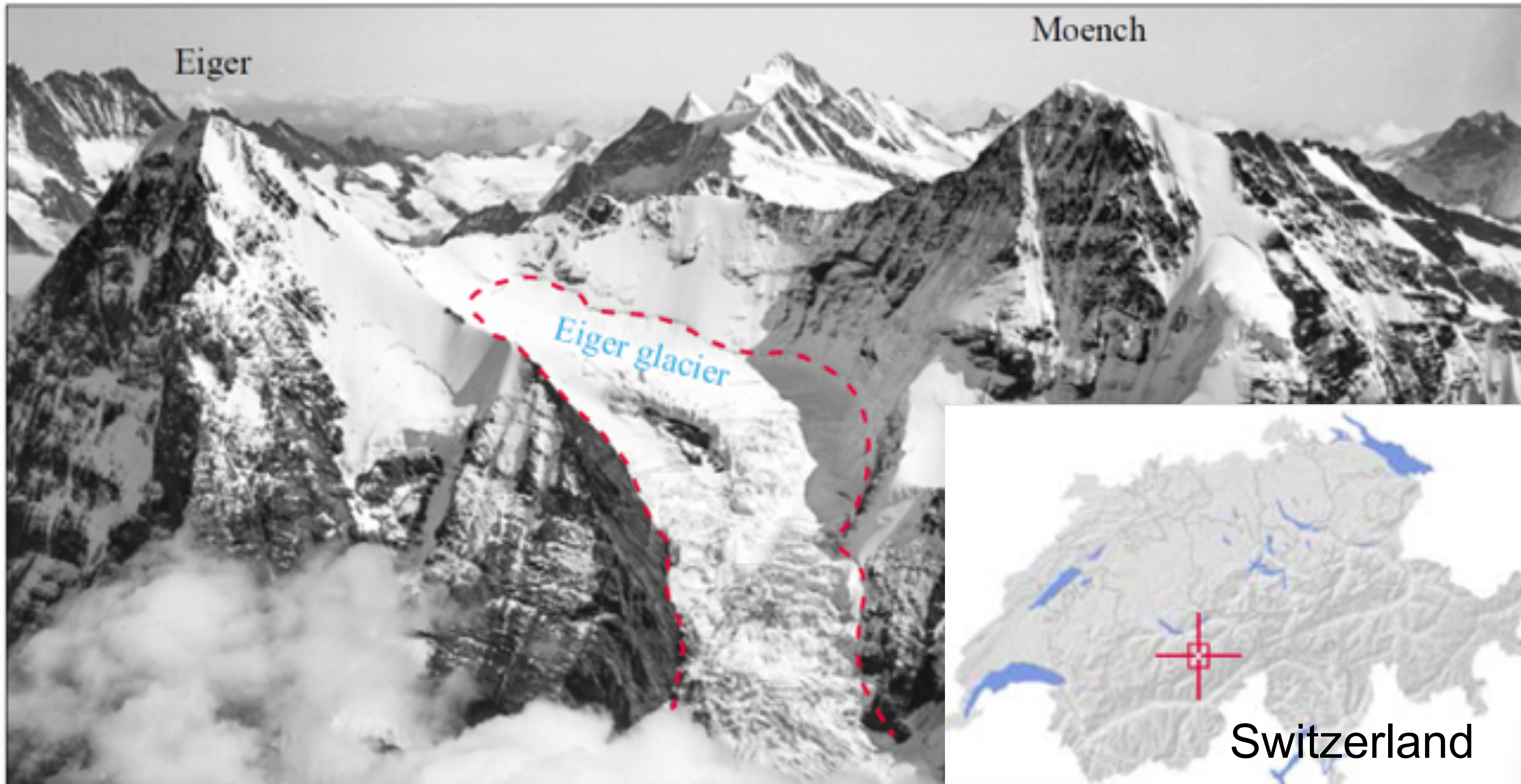

- Using the density contrast to map the ice/rock boundary
- Aiming for 3D inversion of results with different detector sites in a railway tunnel

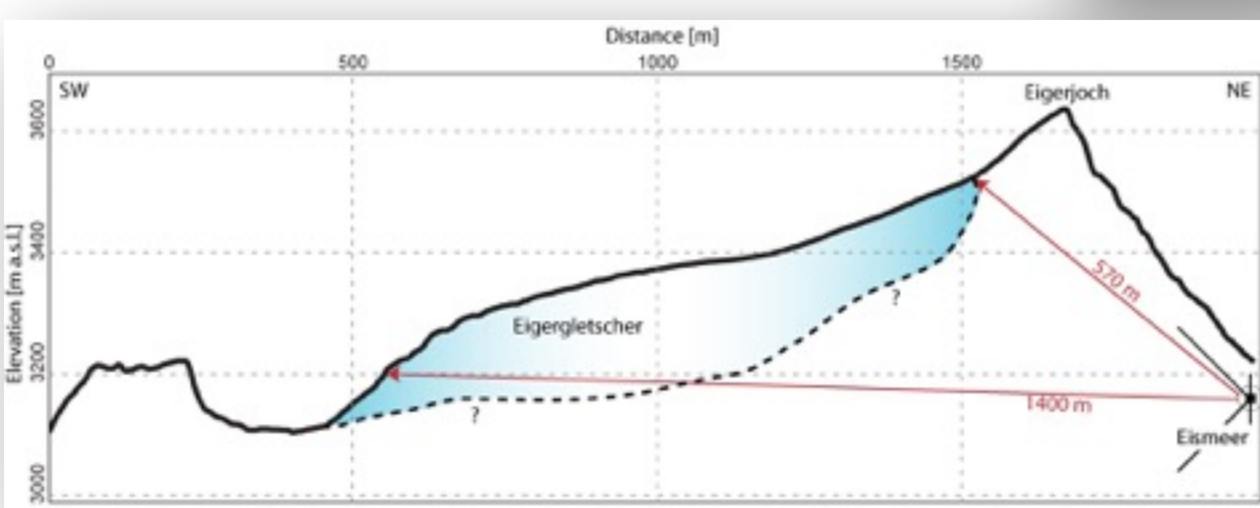

Method: Nuclear Emulsion Films

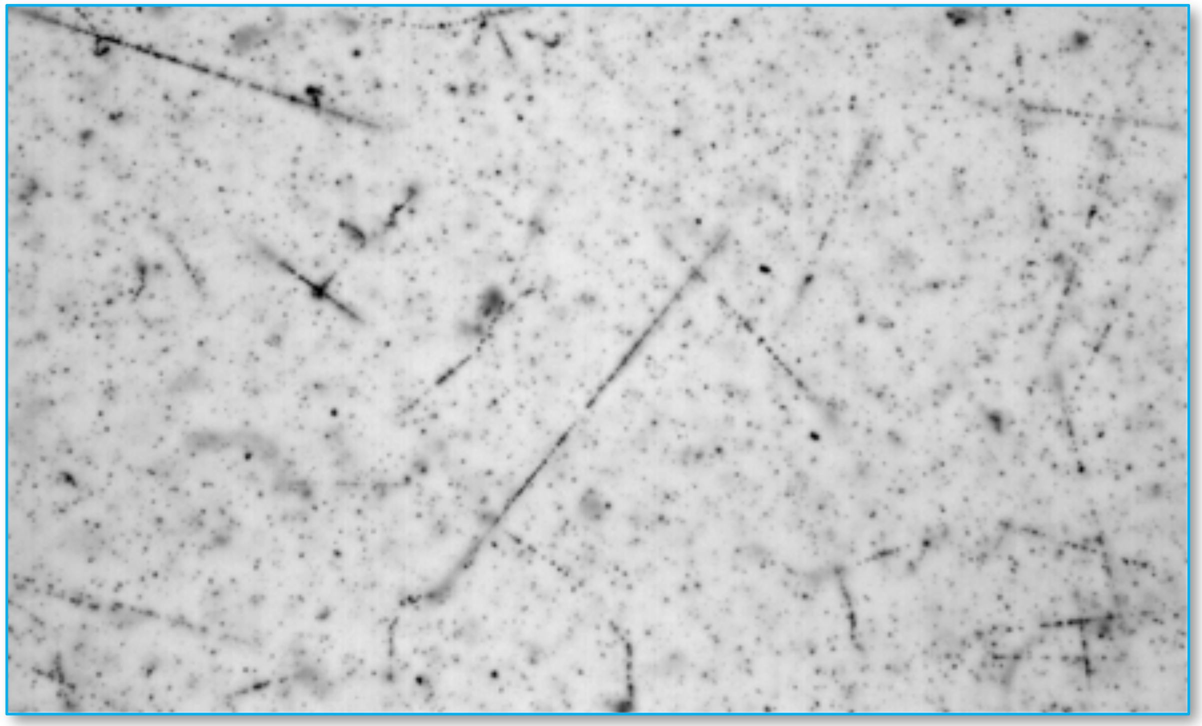

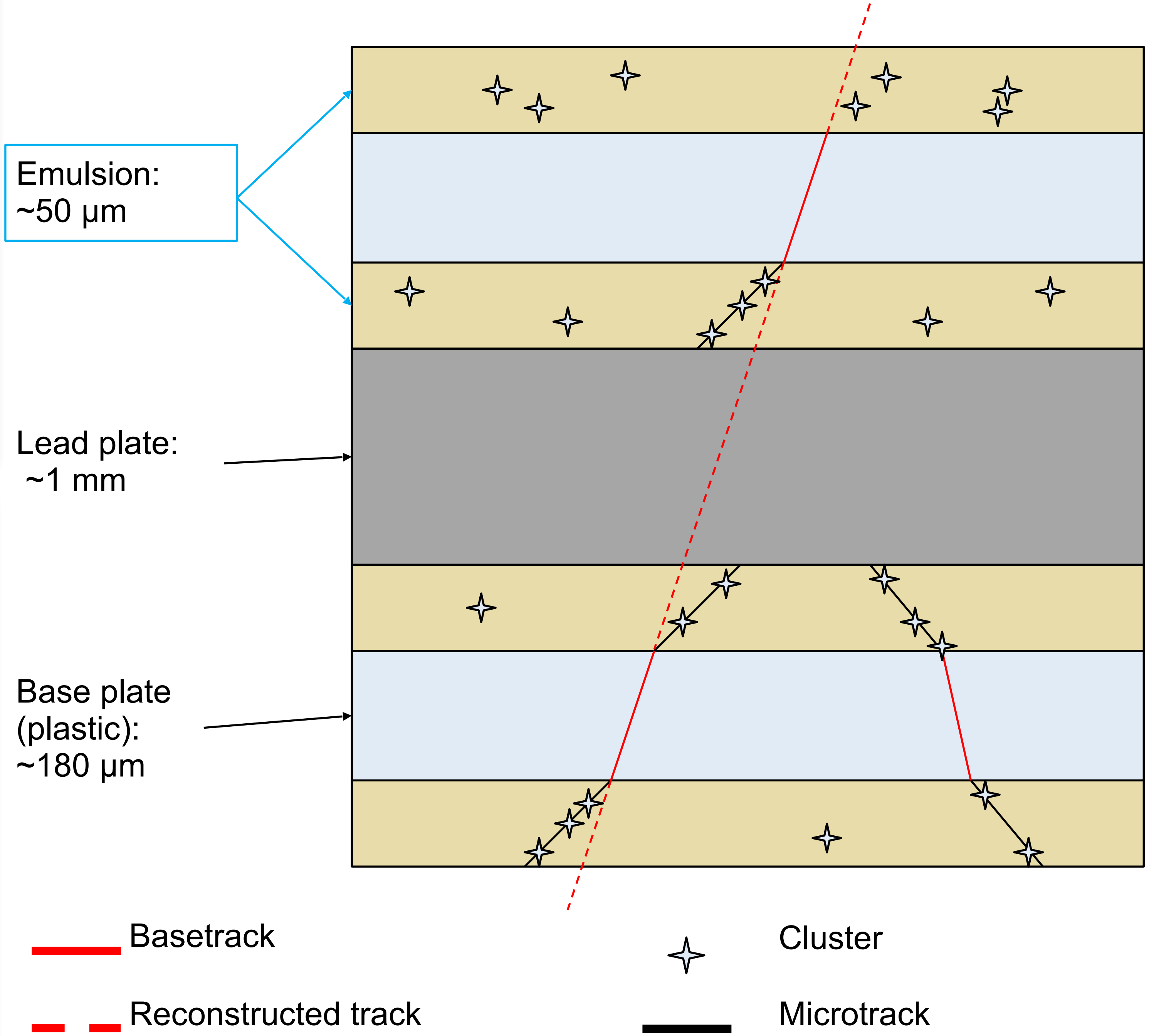

First Simulation: Prototype detector

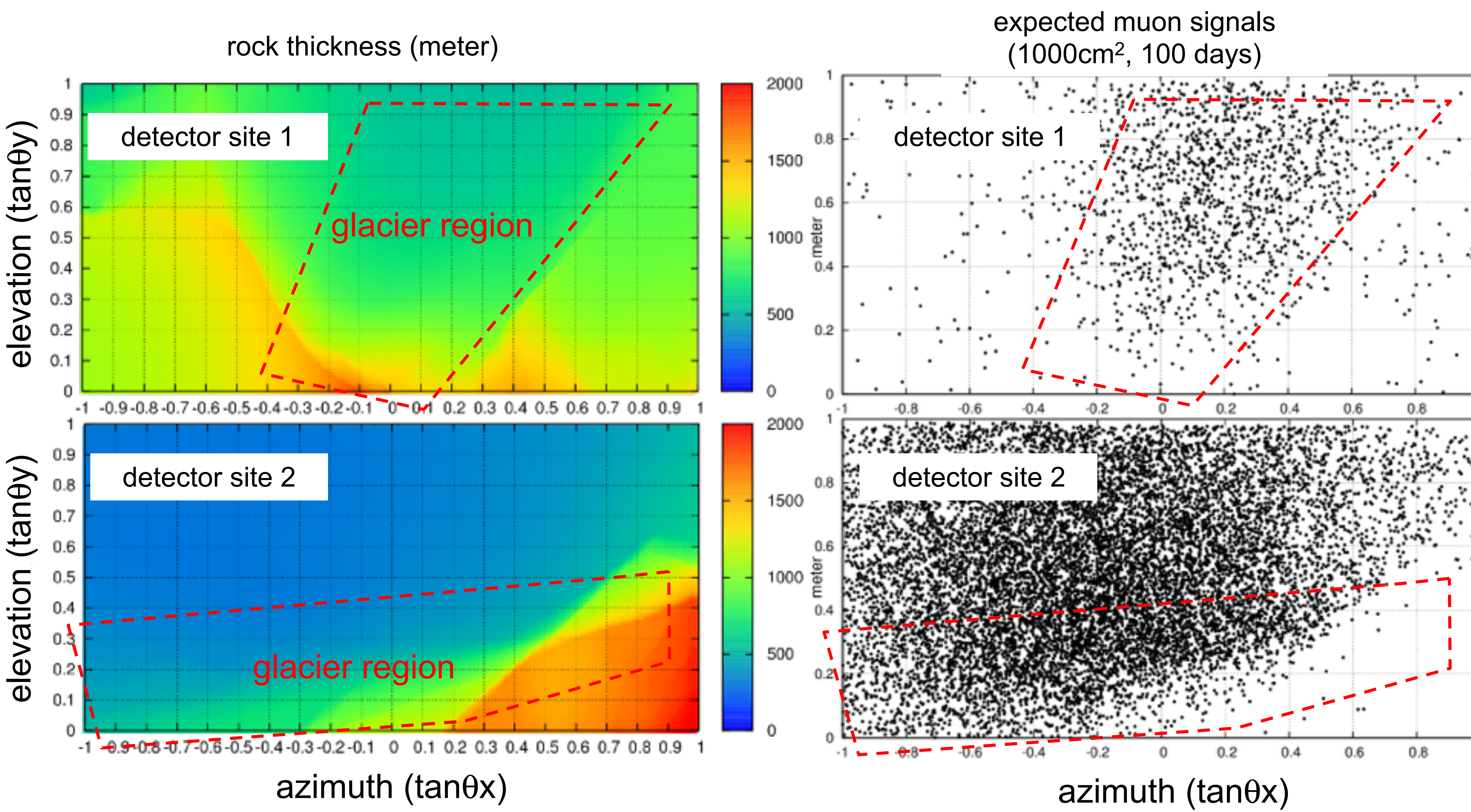

Napoli underground (Toledo station)

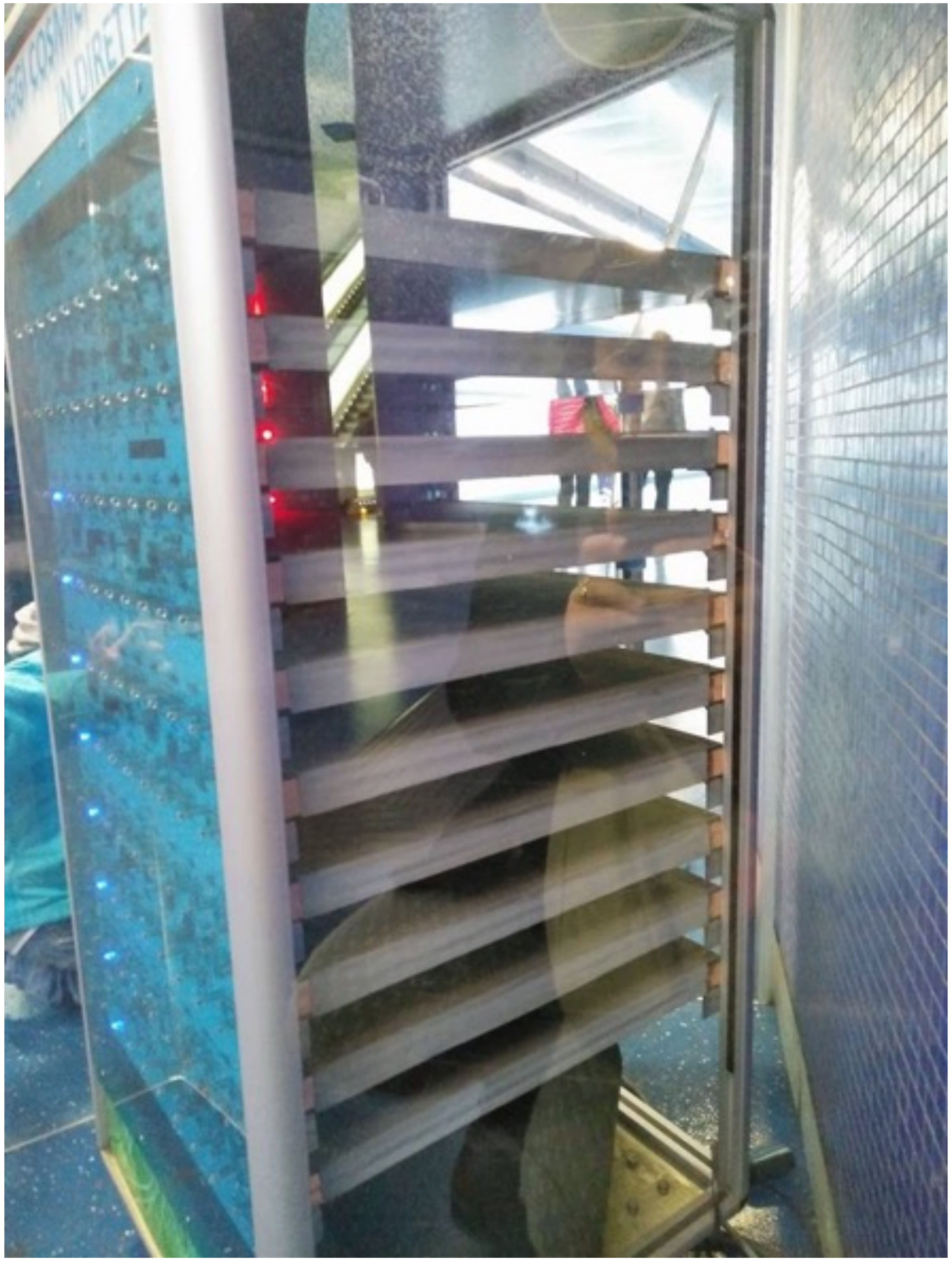

Contents lists available at SciVerse ScienceDirect

Nuclear Instruments and Methods in Physics Research A

journal homepage: www.elsevier.com/locate/nima

Portable cosmic muon telescope for environmental applications

Gergely Gábor Barnaföldi [a], Gergő Hamar [a,b], Hunor Gergely Melegh [c], László Oláh [b], Gergely Surányi [d], Dezső Varga [b,*]

[a] Institute for Particle and Nuclear Physics, Wigner Research Centre for Physics, Hungarian Academy of Sciences, 29-33 Konkoly-Thege Miklós Str., H-1121 Budapest, Hungary
[b] Department of Physics of Complex Systems, Eötvös University, 1/A Pázmány P. sétány, H-1117 Budapest, Hungary
[c] Budapest University of Technology and Economics, 3-9 Műegyetem rkp., H-1111 Budapest, Hungary
[d] Geological, Geophysical and Space Science Research Group of the HAS, Eötvös University, 1/C Pázmány P. sétány, H-1117 Budapest, Hungary

Fig. 2. Photo of the Muontomograph deployed in the Ajándék Cave in Pilis Mountains, Hungary.

1,5 mm resolution
10 MeV threshold
32x32 cm2 surface

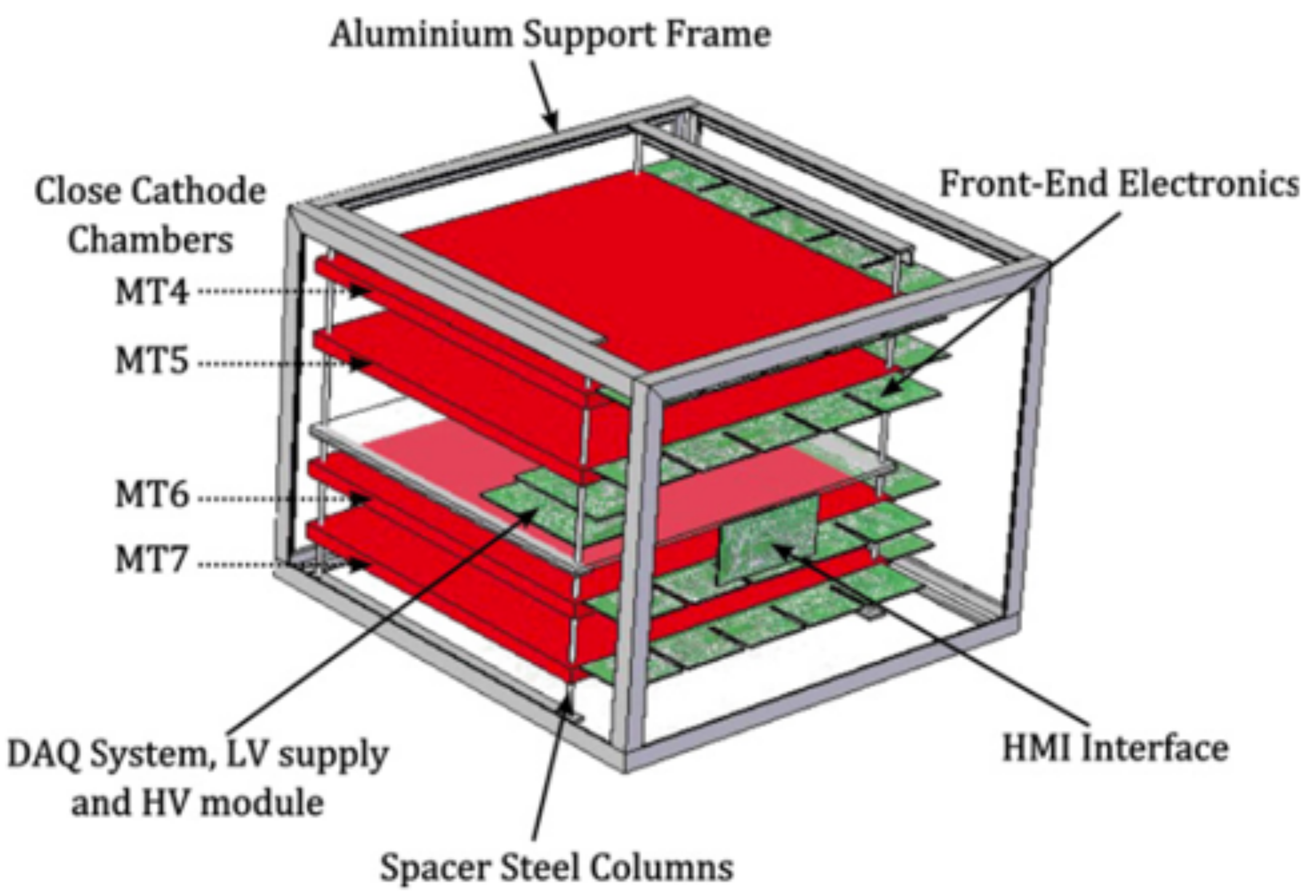

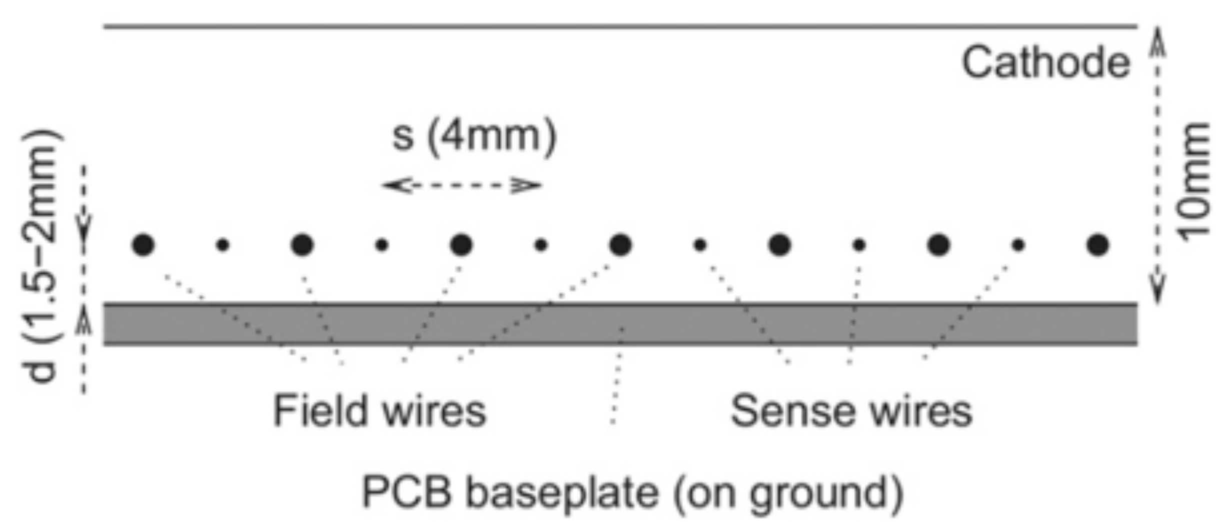

Fig. 3. The inner structure of a Close Cathode Chamber [10].

Long range muography of volcanoes

➥ close to the target
- statistics optimised
- can generally isolate the target from neighboring relief
- no need for extraordinary resolution
- deployment difficulties
- tropicalisation / safety issues

➥ safely away from the target (~ kilometers)
- deployment/safety issues minimised
- larger detectors needed
- very good resolution required, helps with background rejection

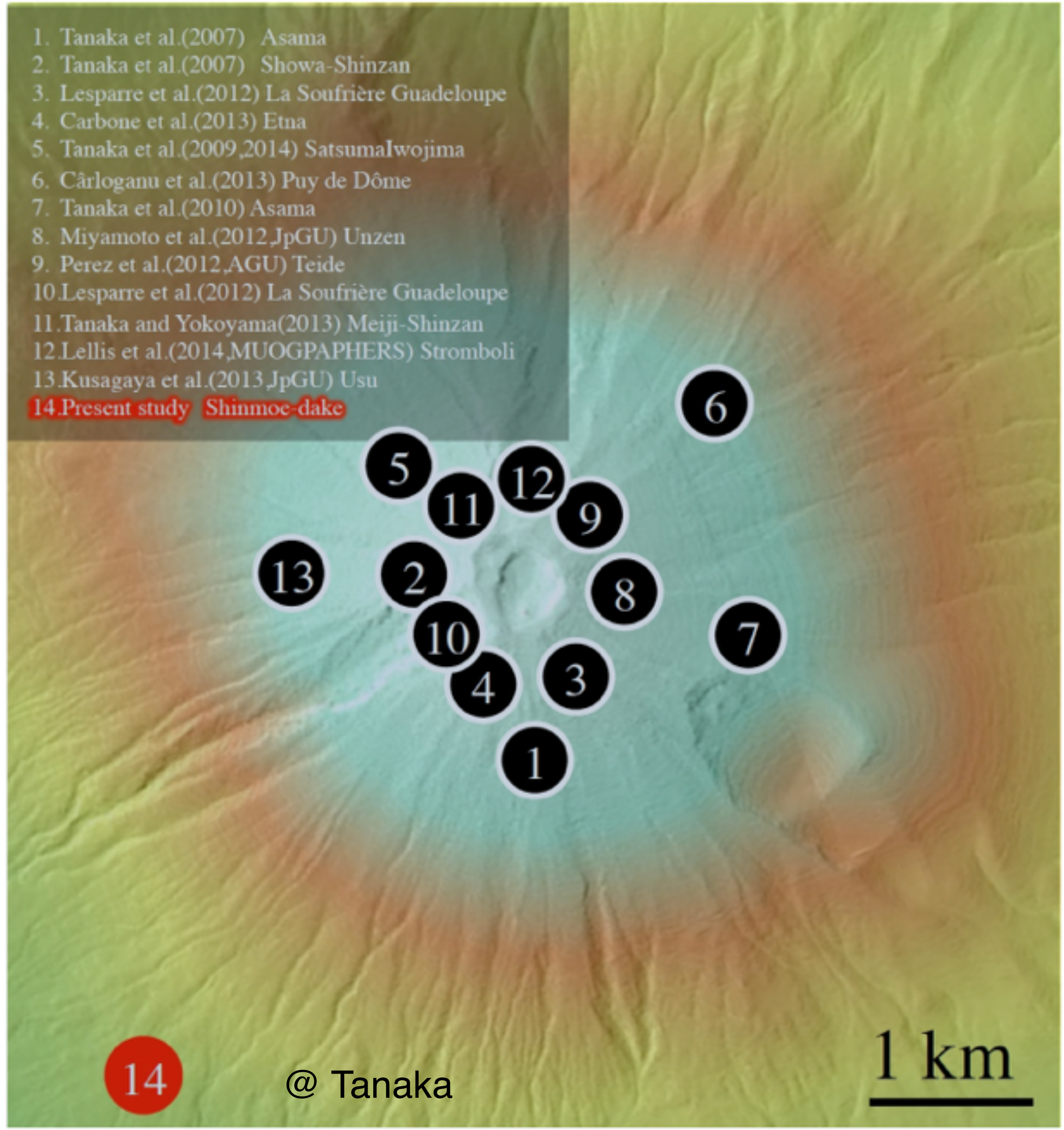

Muography Projects

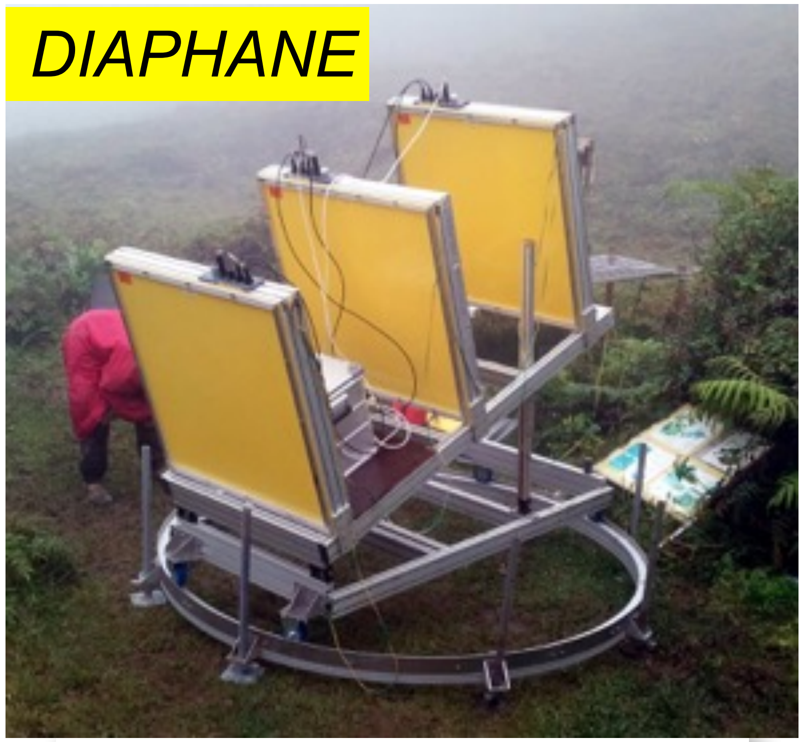

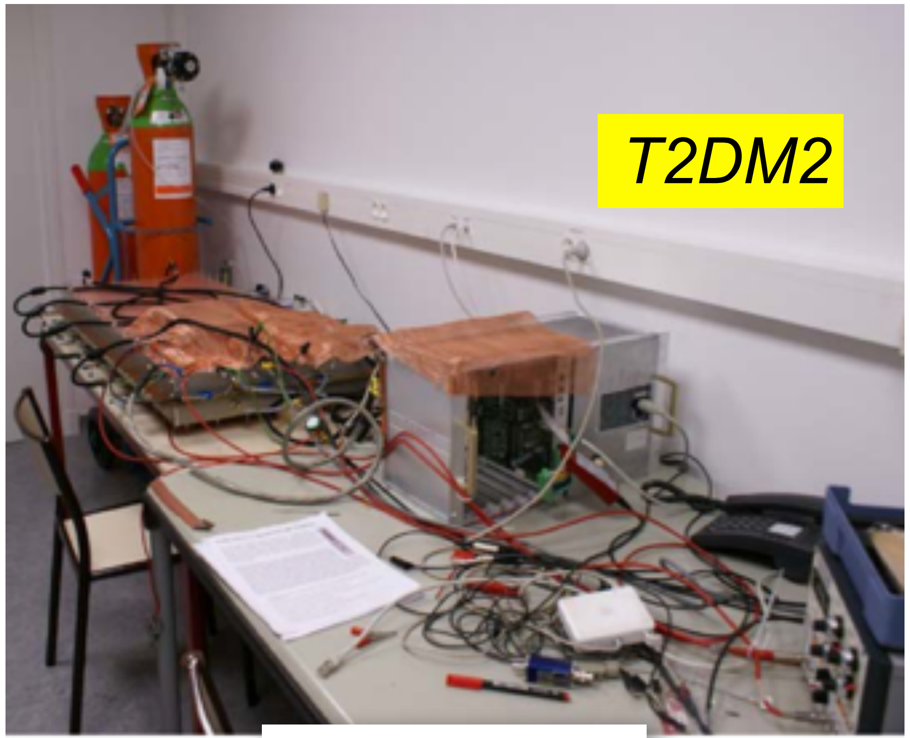

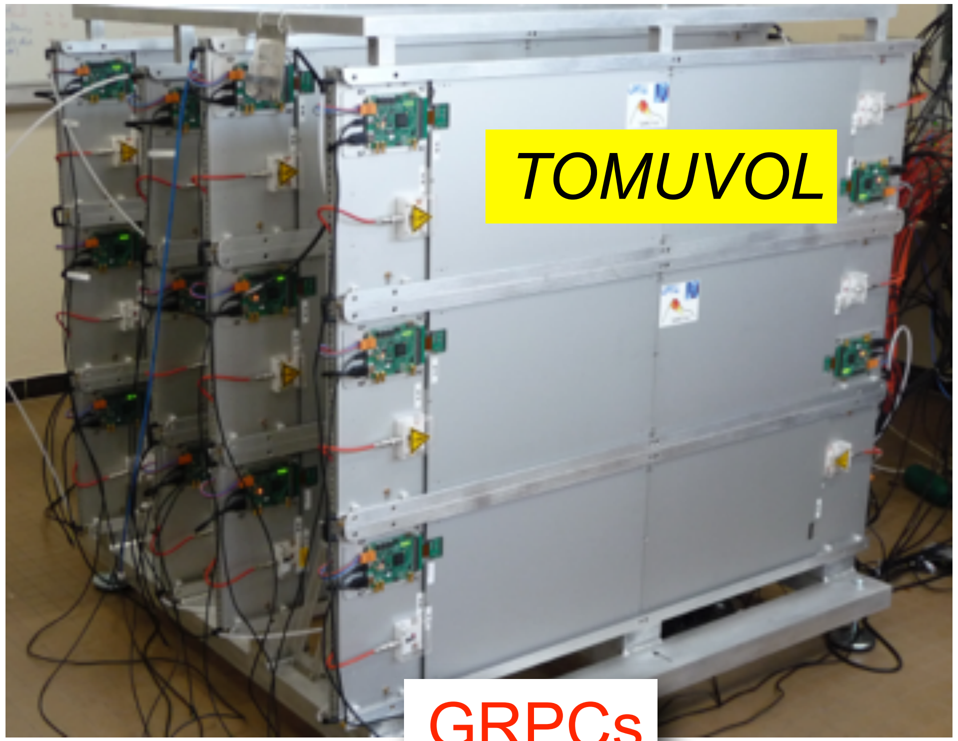

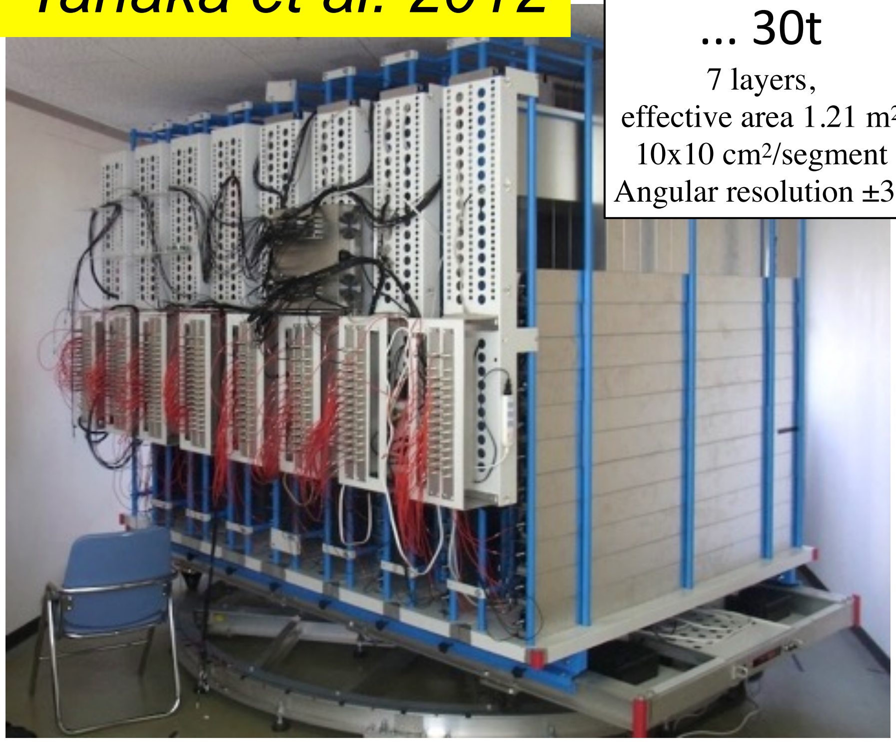

Muography emulsion projects with contribution of Italian laboratories

- Unzen – contributed to data scanning and analysis (2011)
- Stromboli – Design, installation and data analysis (2012)
- Teide – exposure is completed, scanning is started (2013)
- La Palma – modules design, installation, analysis started (2014)

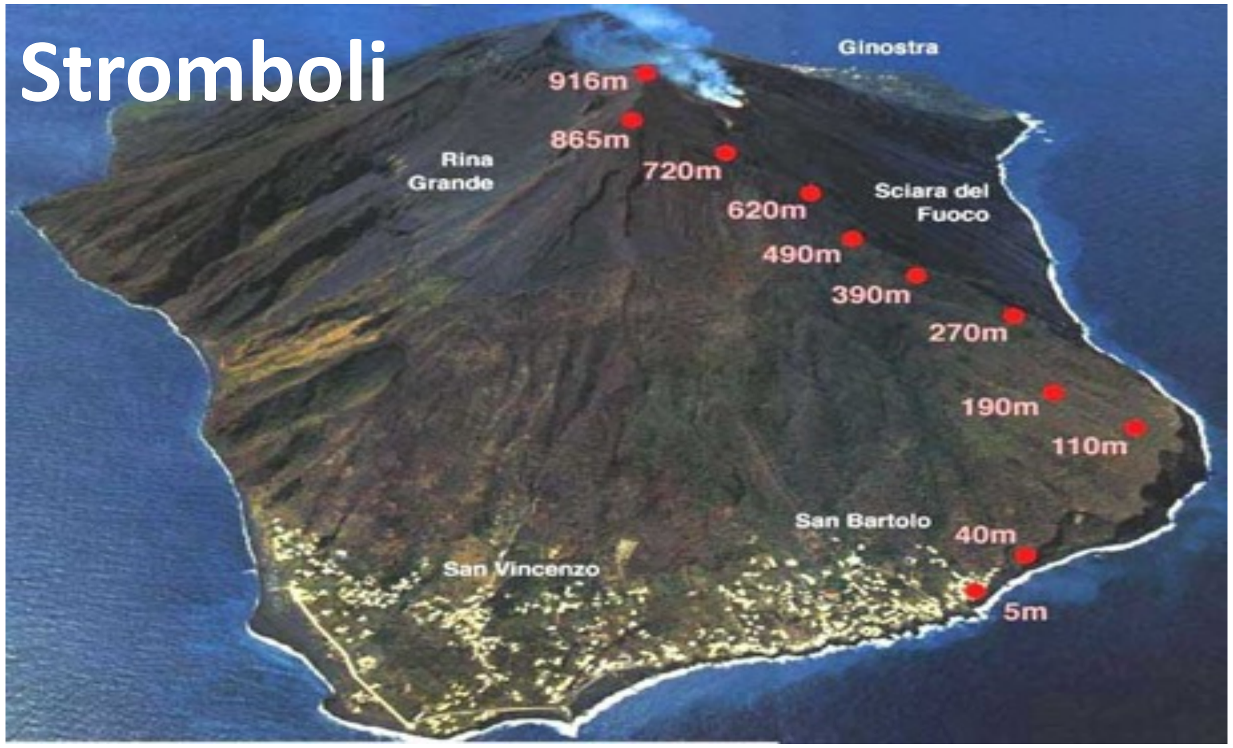

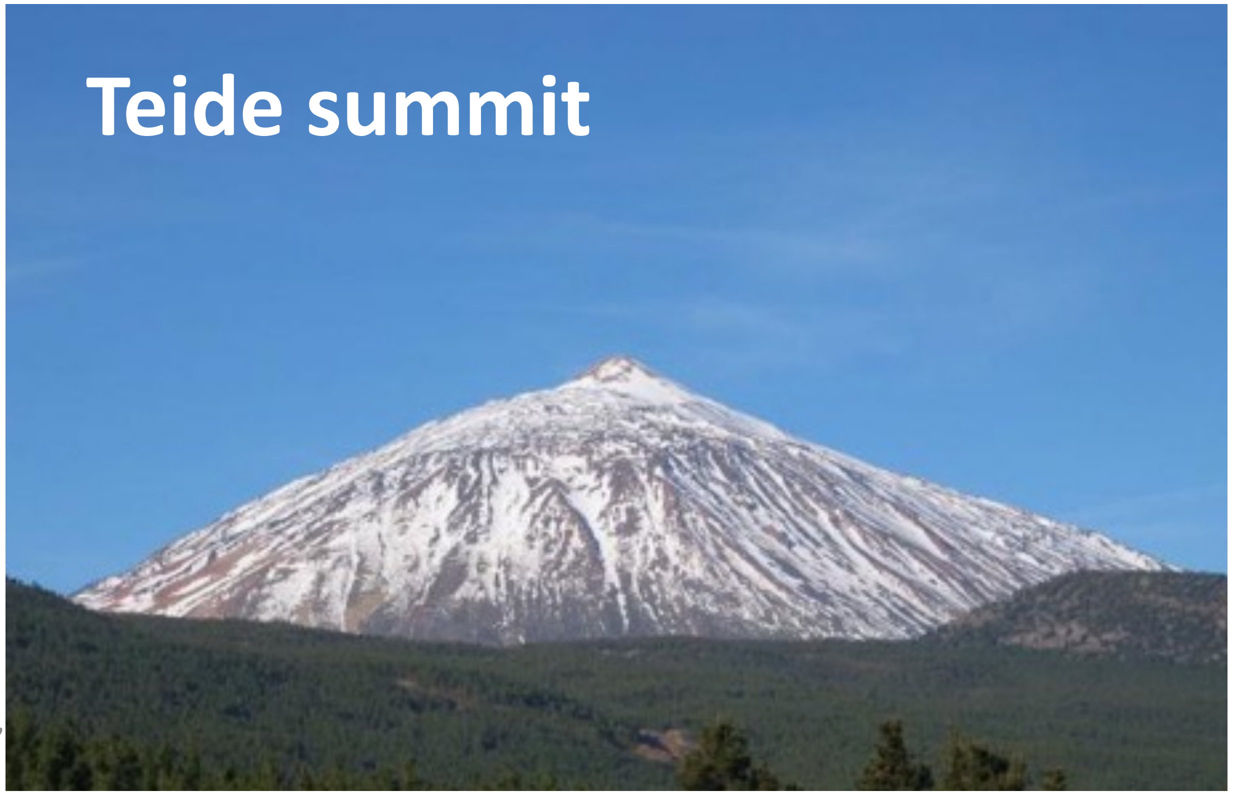

Nuclear Emulsions as Muons detector

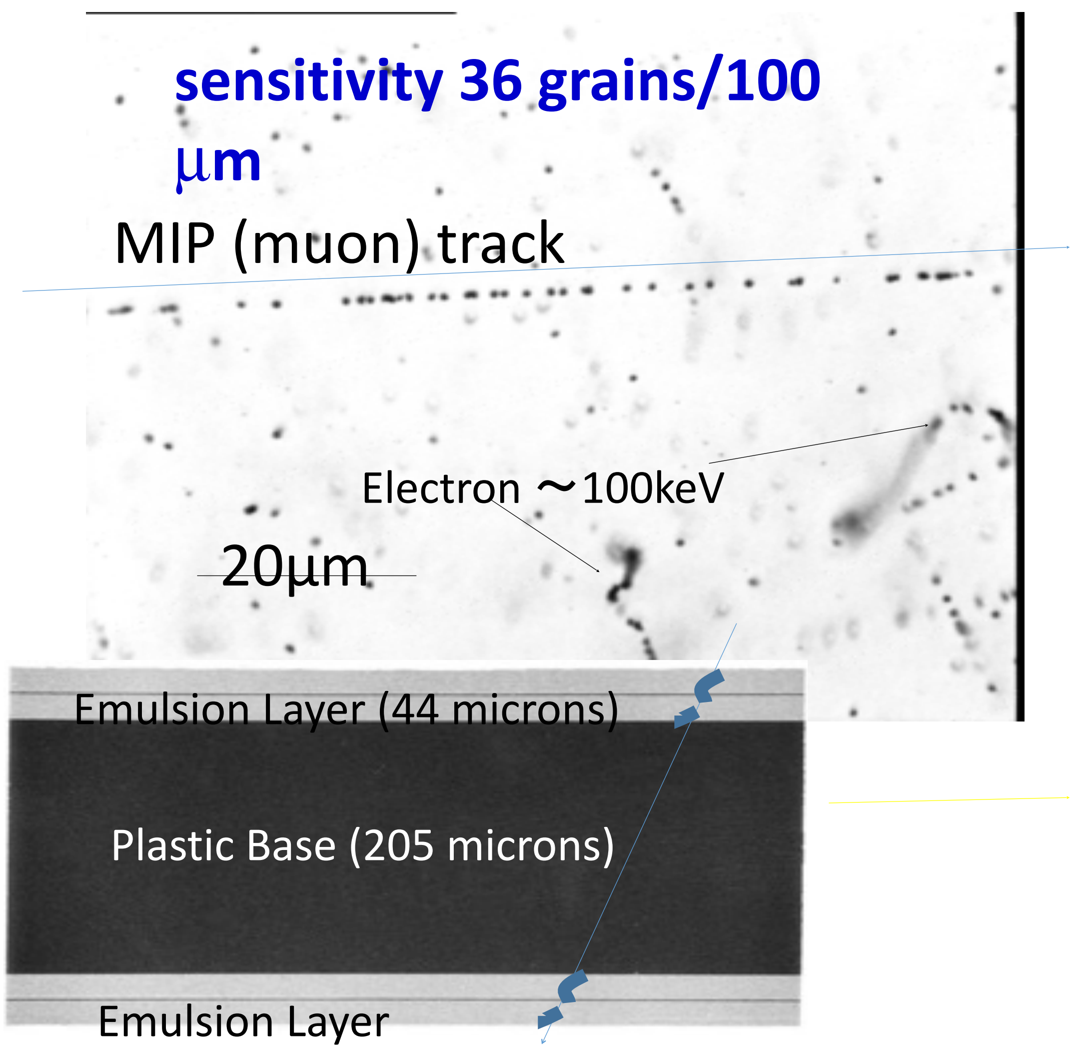

- Very high angular resolution (better then 2 mrad) in thin (300 microns) plates
- Compact and easy to transport

But:

- Complex and time consuming data processing (emulsion scanning)

- **Good news: Fast Scannig is already developed for Neutrino physics (OPERA experiment)**

The OPERA detector: 8.9 mln films with the total emulsion sensitive surface of 200000 m^2

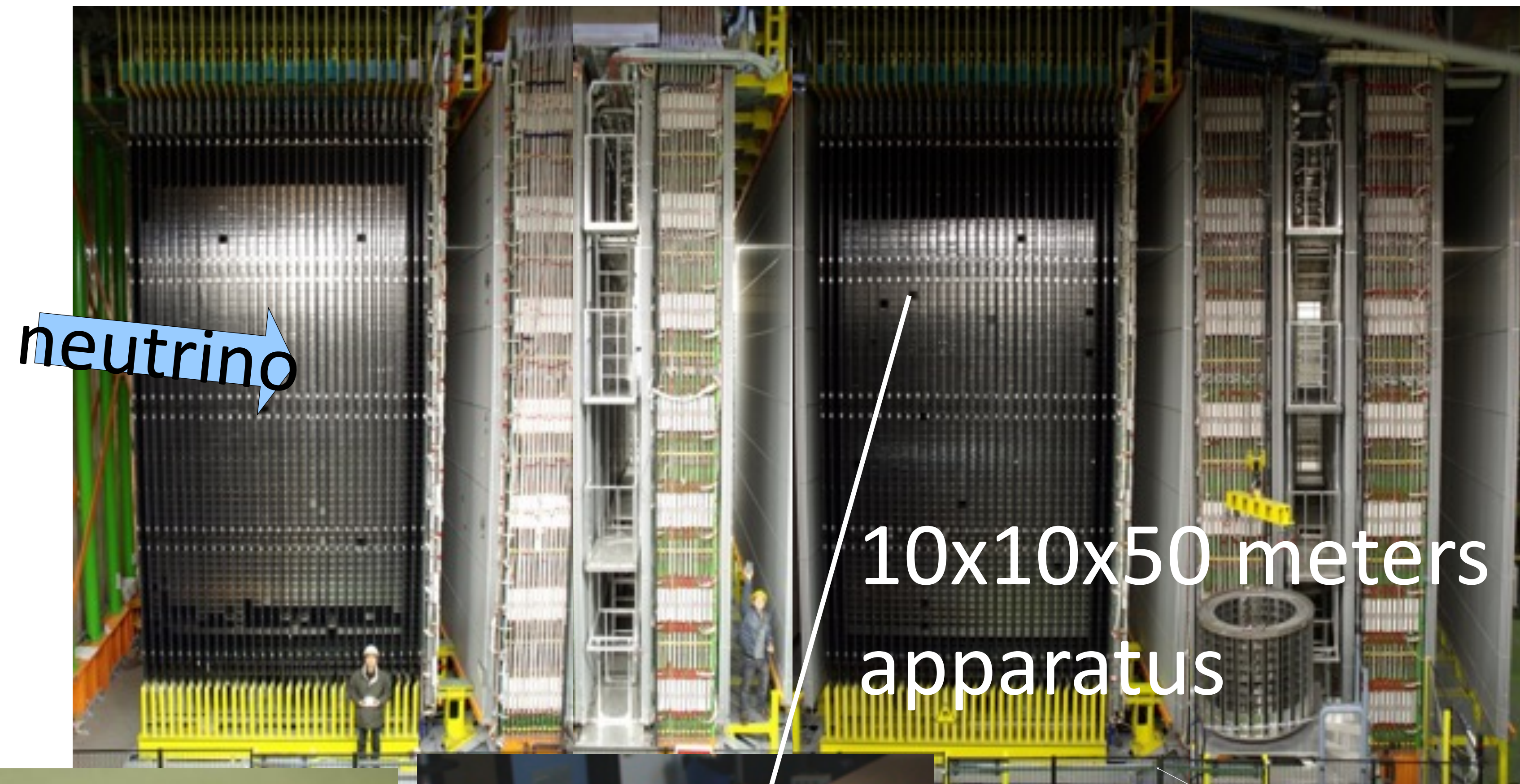

Tomography images taken with 2.5 microns step

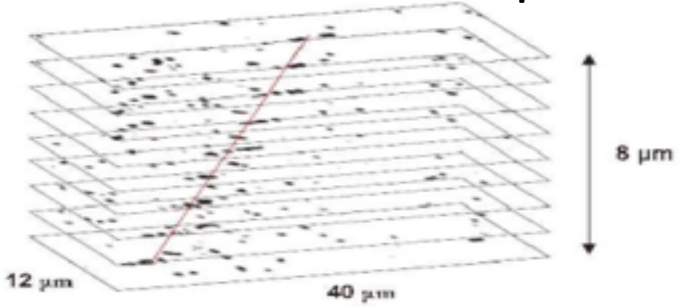

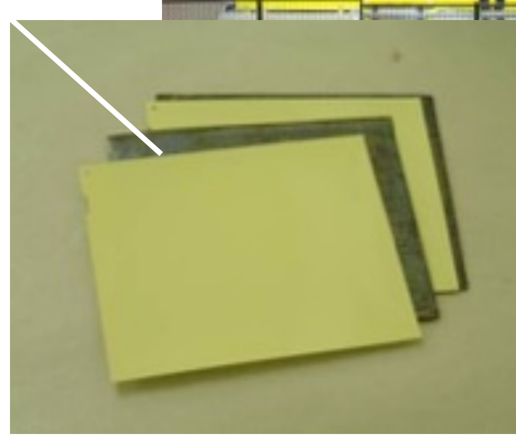

ECC "brick"
57 emulsion plates
56 lead plates
10x12x7 cm, 8 kg

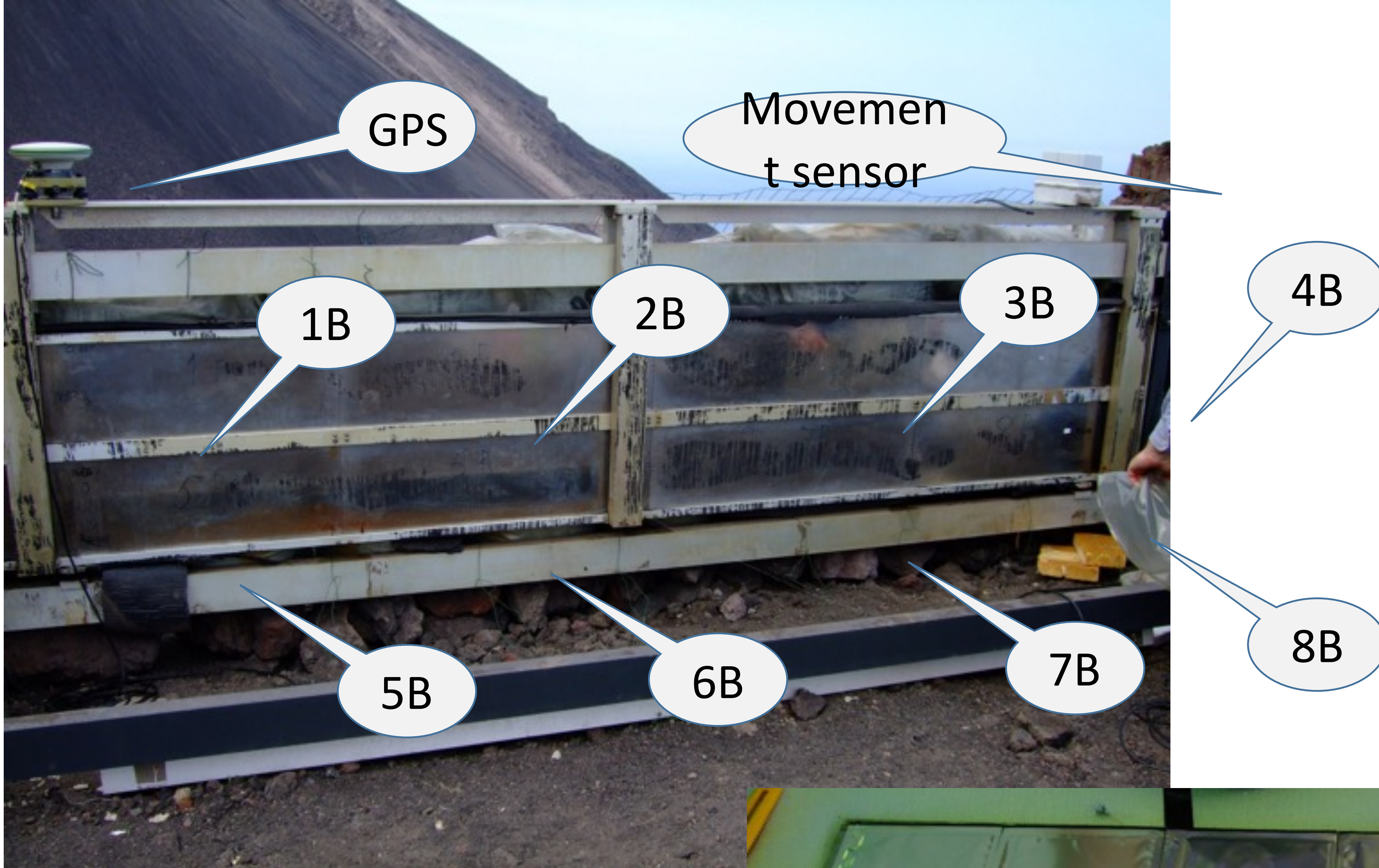

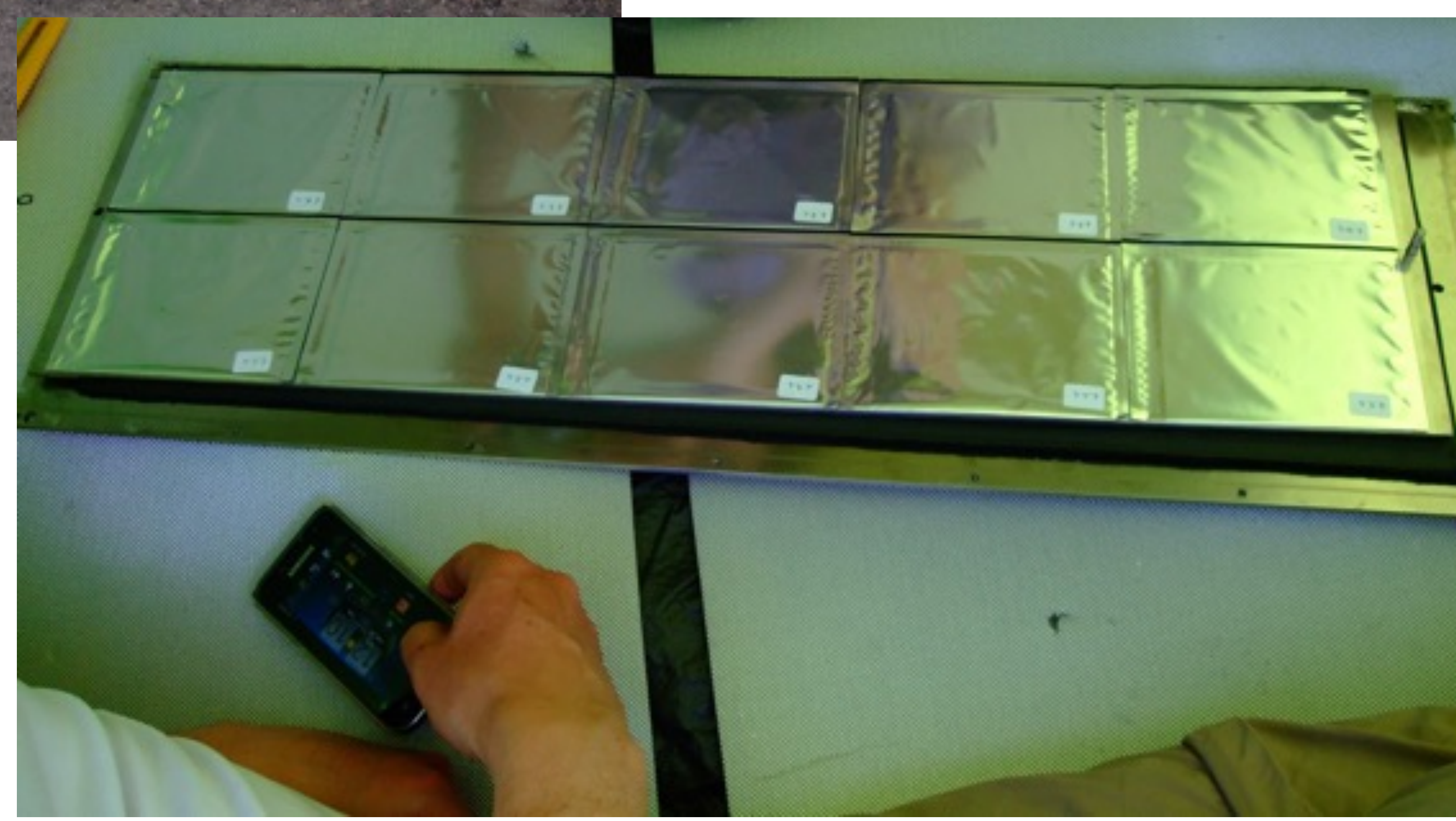

Emulsions extraction after 5 months exposure. The envelopes are in a good shape

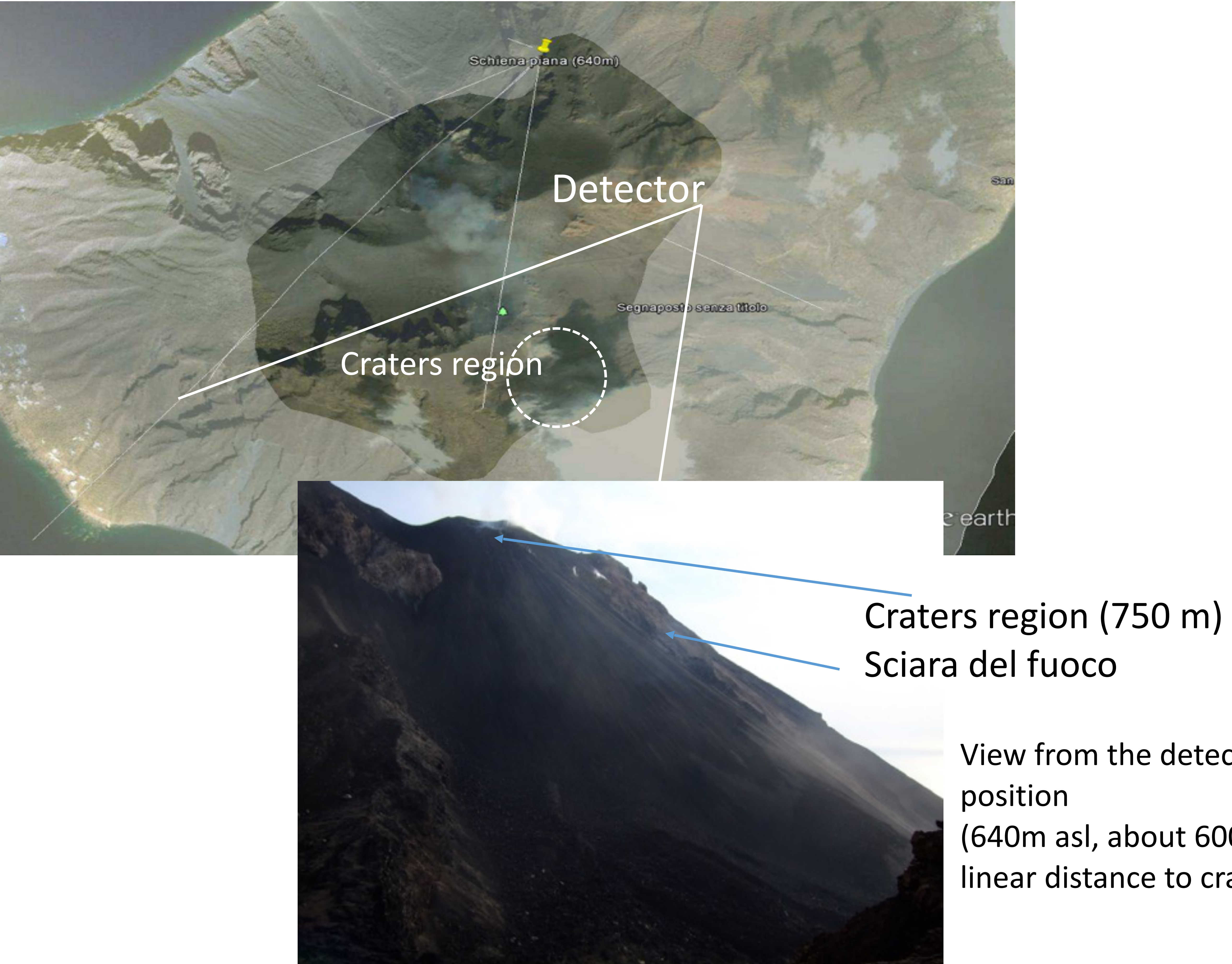

View from the detector position (640m asl, about 600 m linear distance to craters)

To keep memory about the module orientation 3 fixed vertices were installed and the distances measured with the laser distanziometer (+-2 mm accuracy) GPS data were recorded on 2 detector and on 2 vertex points

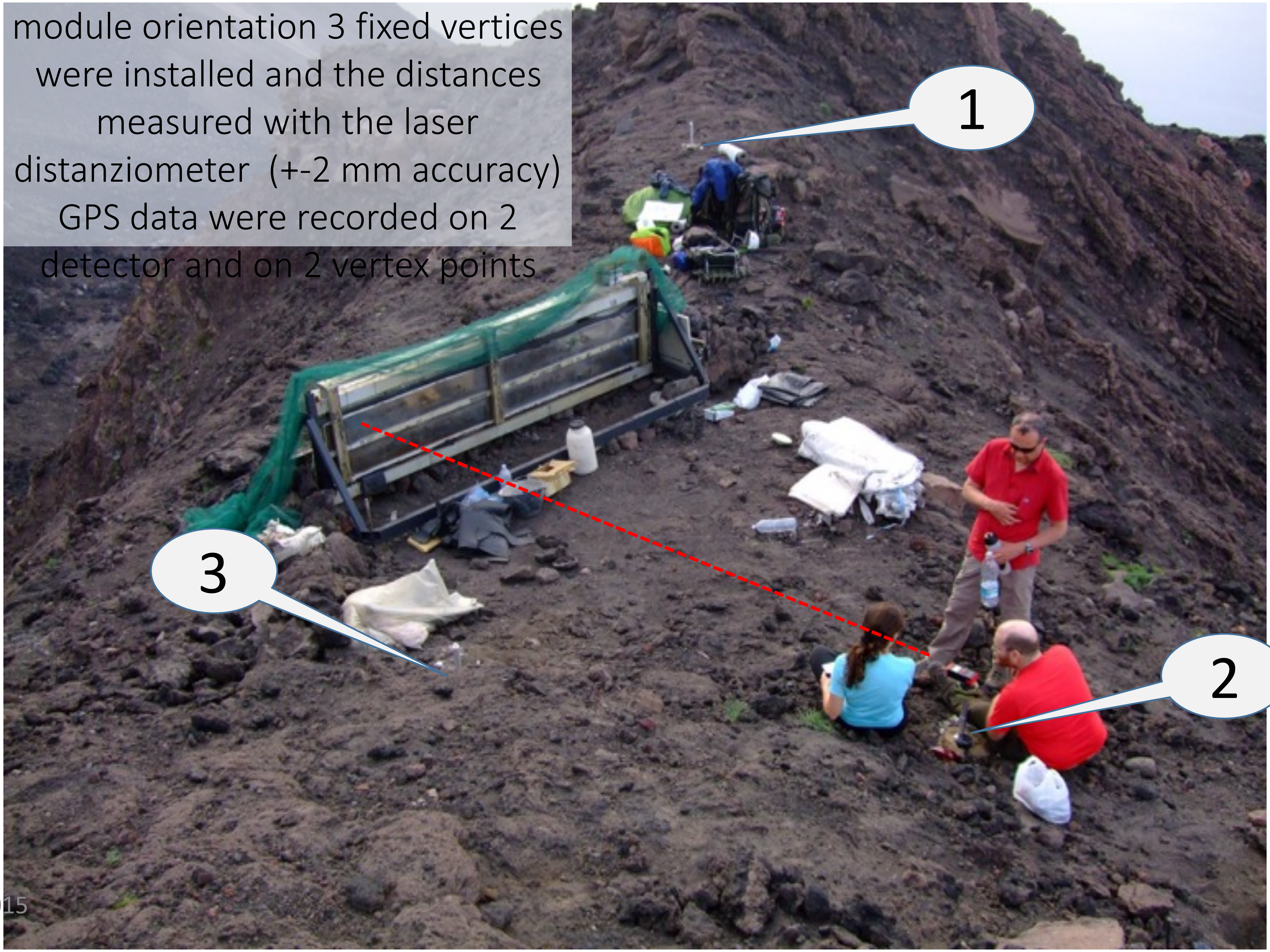

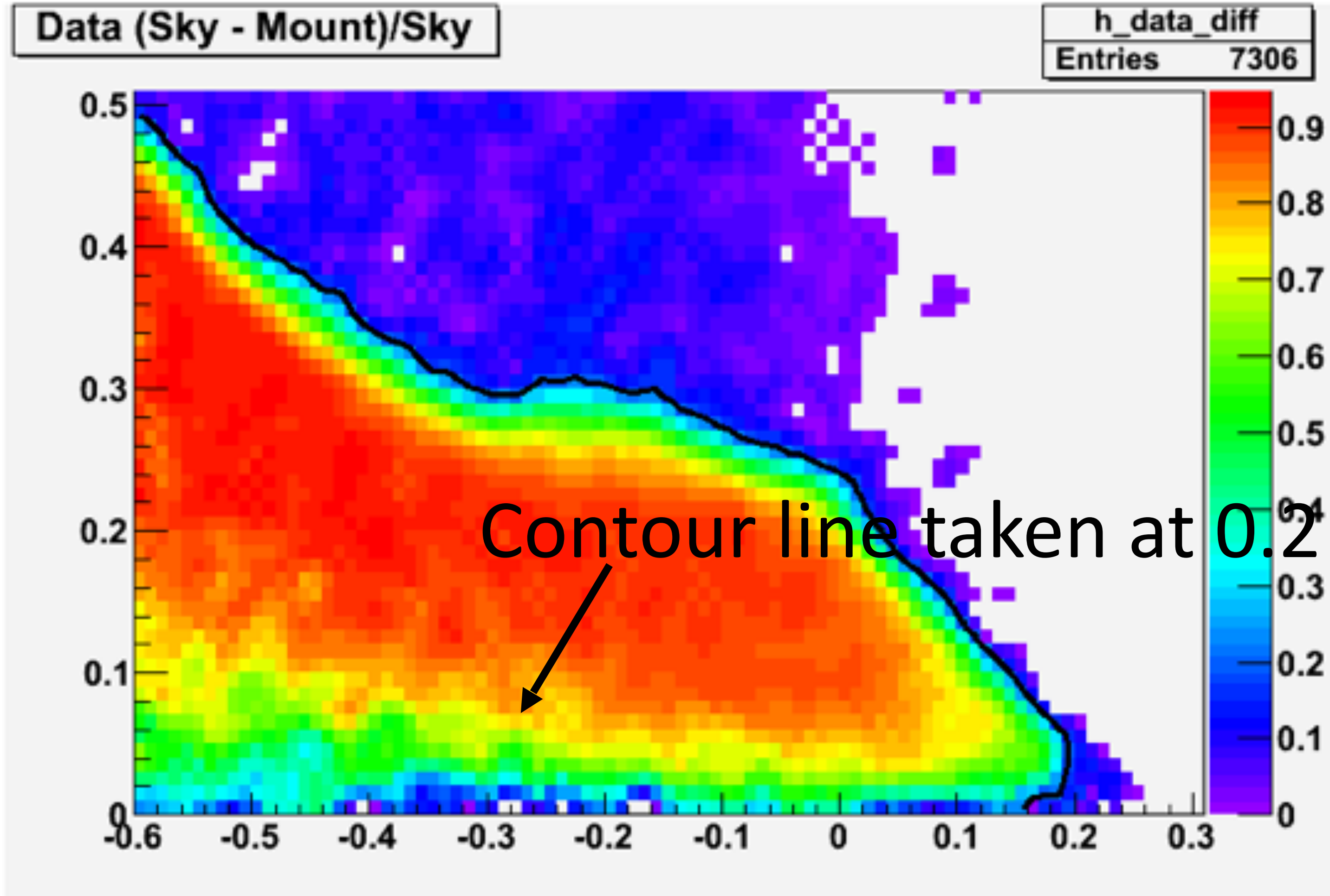

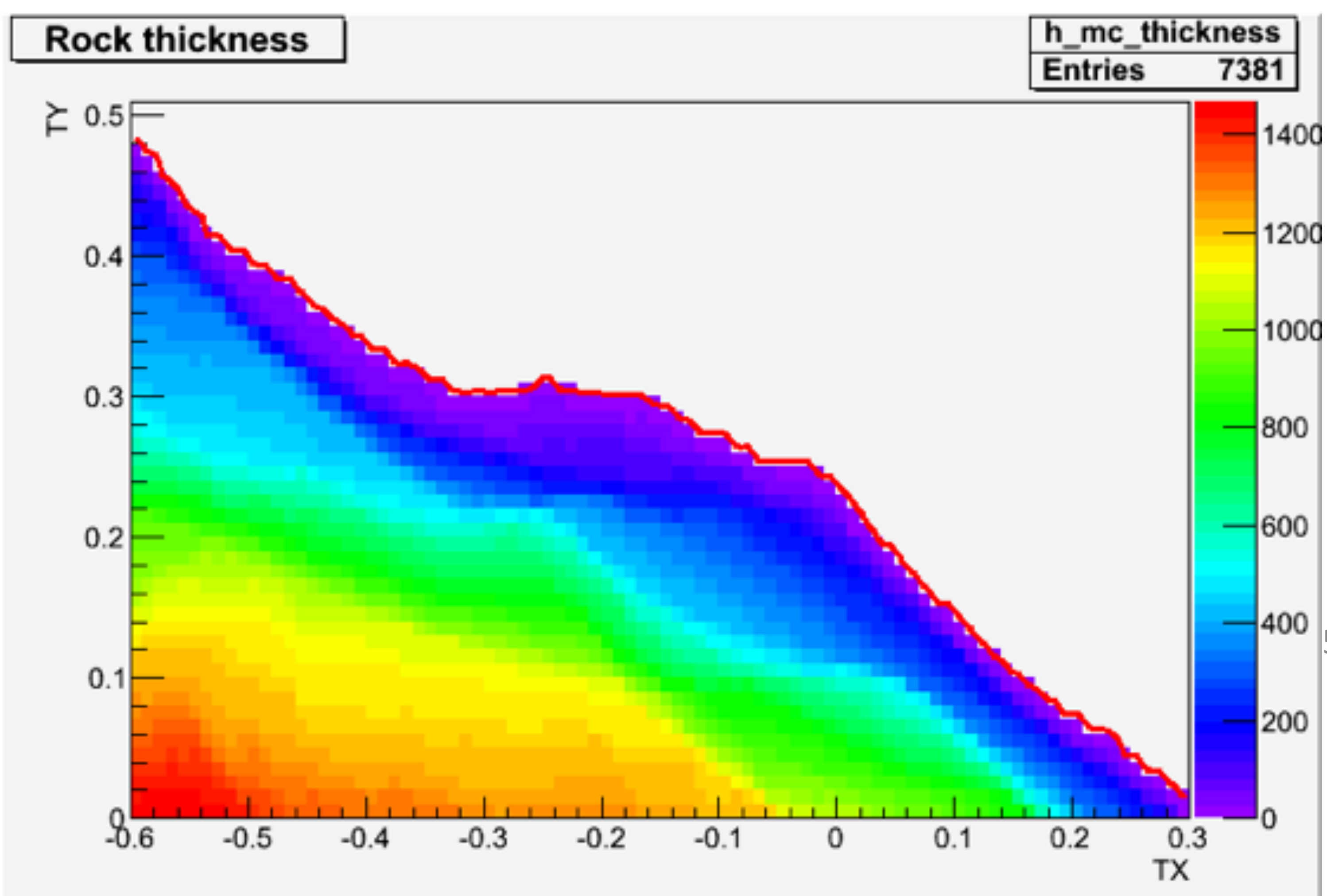

For precise definition of the mount shape by muons data the Mount (positive ty) was subtracted from the free Sky (negative ty) and normalized to Sky

Cherenkov telescopes : CTA (10.1016/j.nima.2015.10.065

matrix of Silicon Photomultiplier (SiPM)

secondary optics is a monolithic 1.8 m diameter mirror

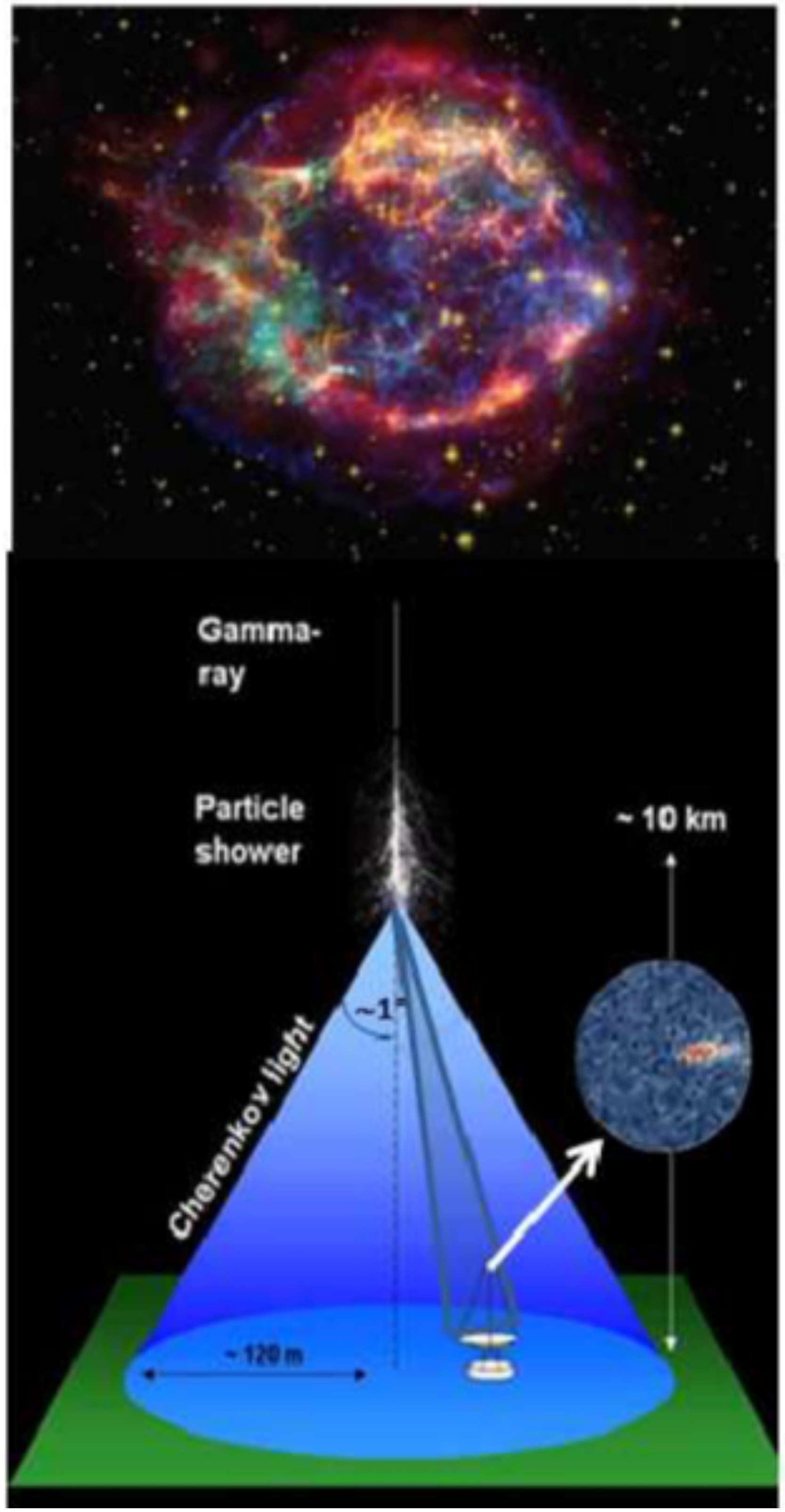

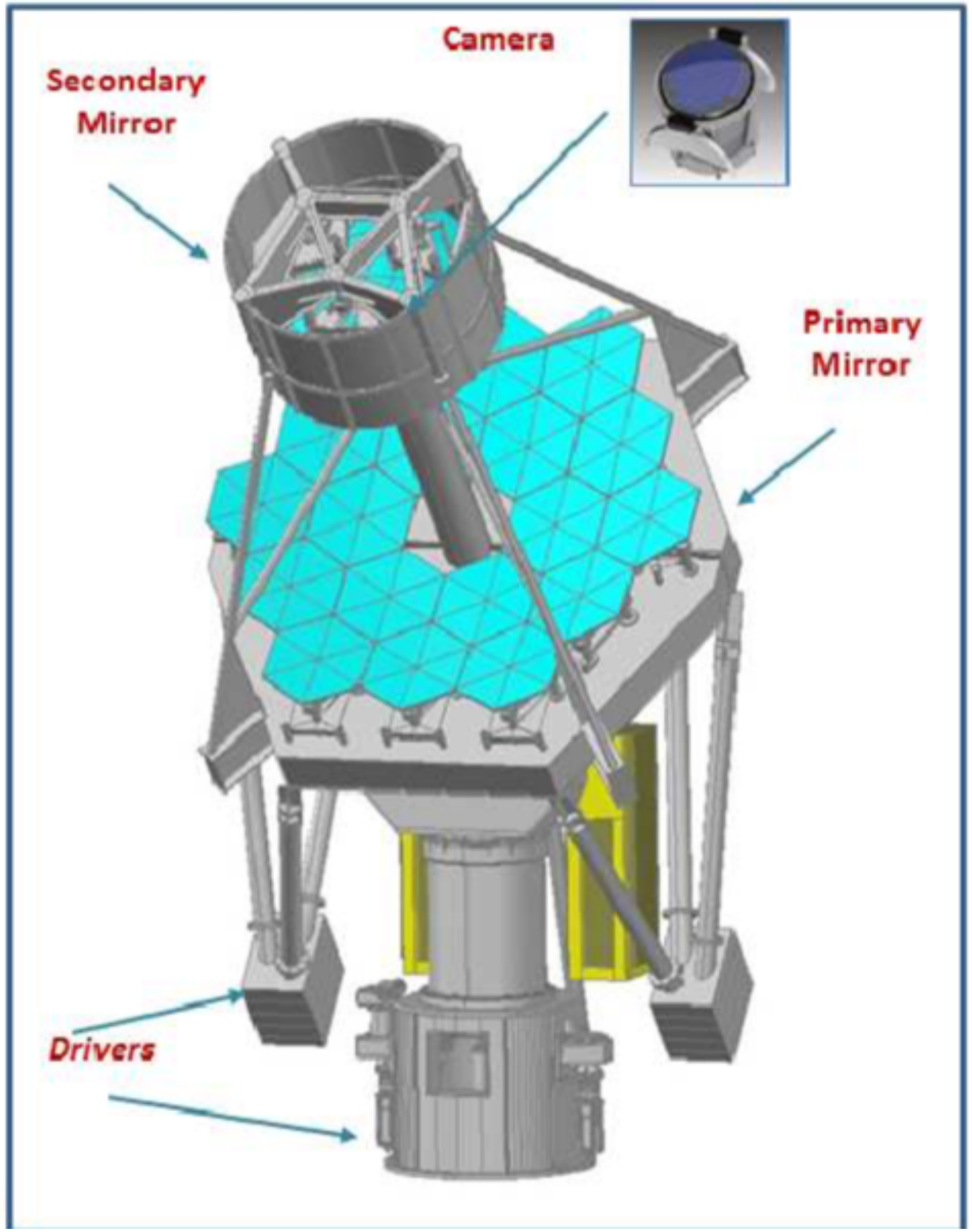

The primary mirror of the telescope has a 4.2 m diameter

Cherenkov telescopes : CTA (10.1016/j.nima.2015.10.065

$$E_\mu = \frac{0.105}{\sqrt{1-(n\ \cos\ \Theta)^{-2}}}\ (\text{GeV}).$$

Saturates towards
50 GeV @ 1800m

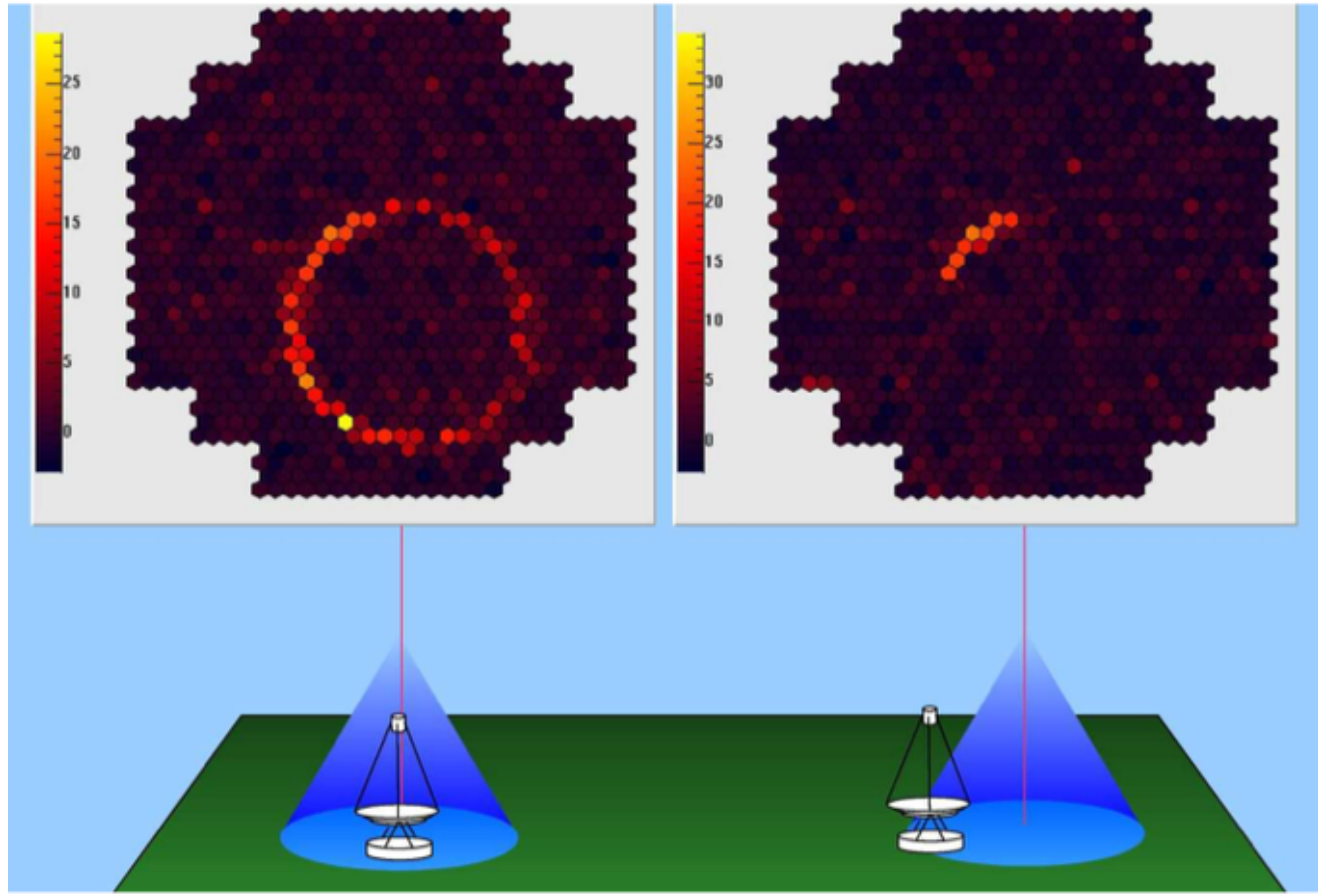

Ring centre = muon arrival direction with respect to the telescope optics axis. precision ~ 0.14°

detect muons by collecting in a single ring the light emitted along the last ~100 m of its path towards the primary mirror

energy threshold ~20 GeV and the muon hits the primary mirror up to an off-axis angle of 3.6°

MURAVES

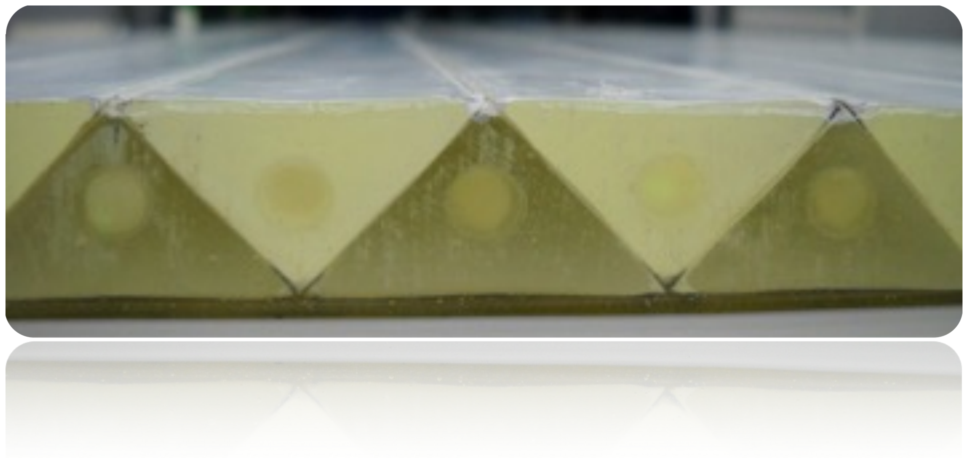

Proof of Principle for Muographic Imaging of Volcanoes

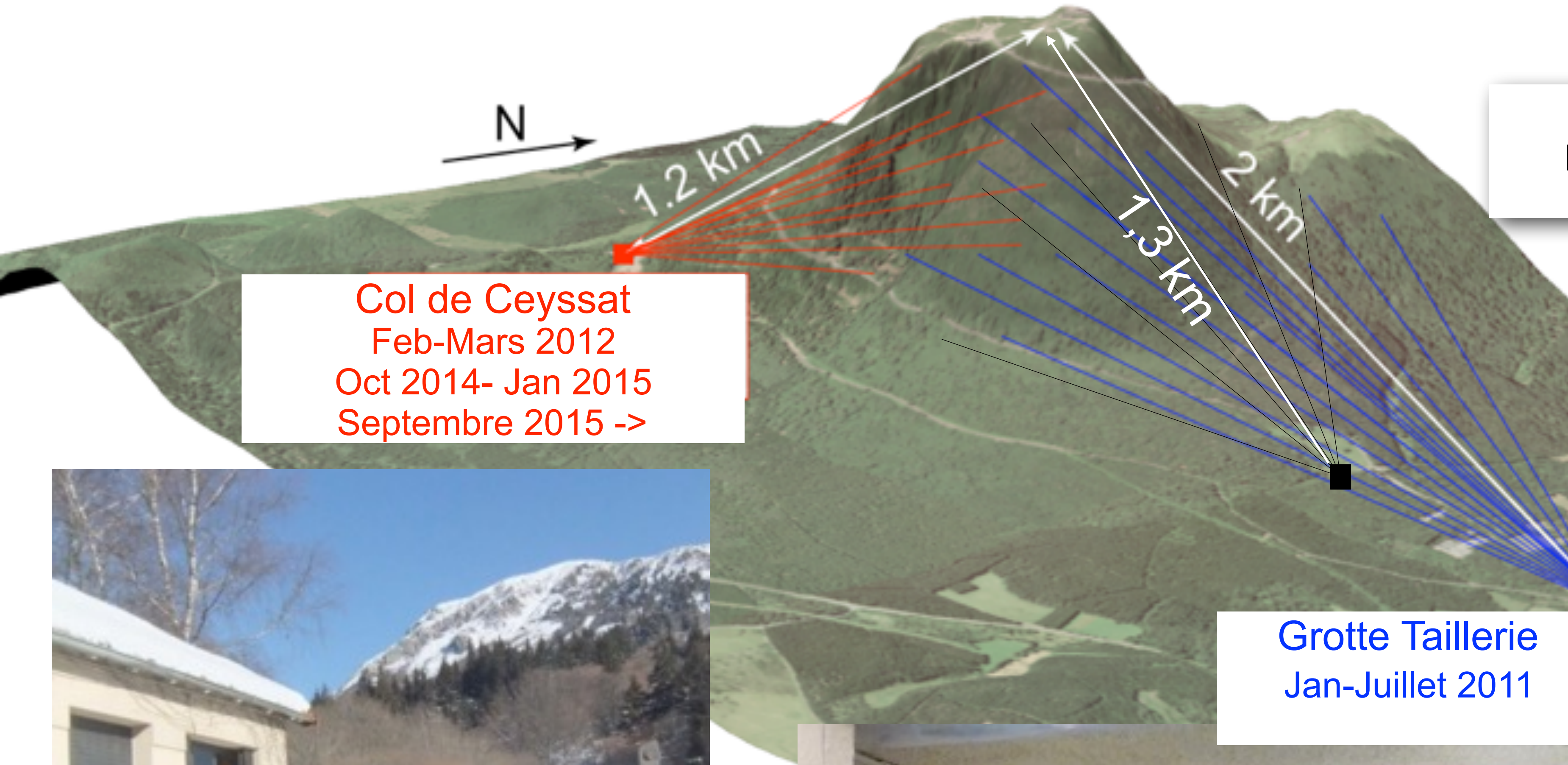

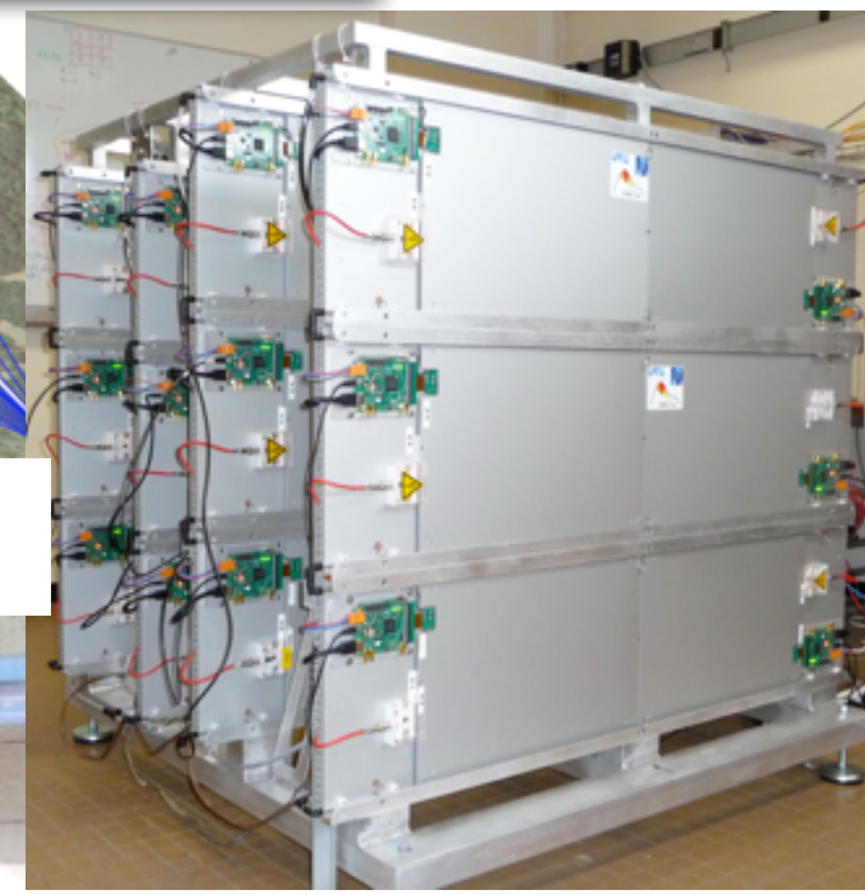

CALICE GRPC's

Avalanche mode: total mean MIP charge 2.6pC, RMS: 1.6pC

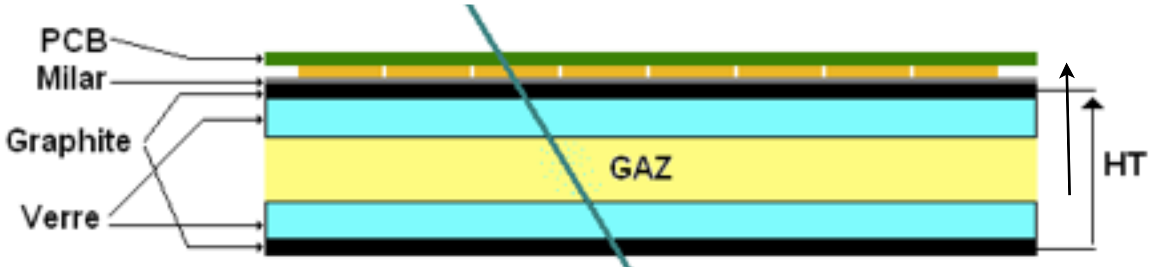

Gas: 93% TFE, 5% Isobutane (CO2), 2% SF_6

M. Bedjidian et al, "Performance of Glass Resistive Plate Chambers for a high granularity semi-digital calorimeter", JINST 6:P02001,2011

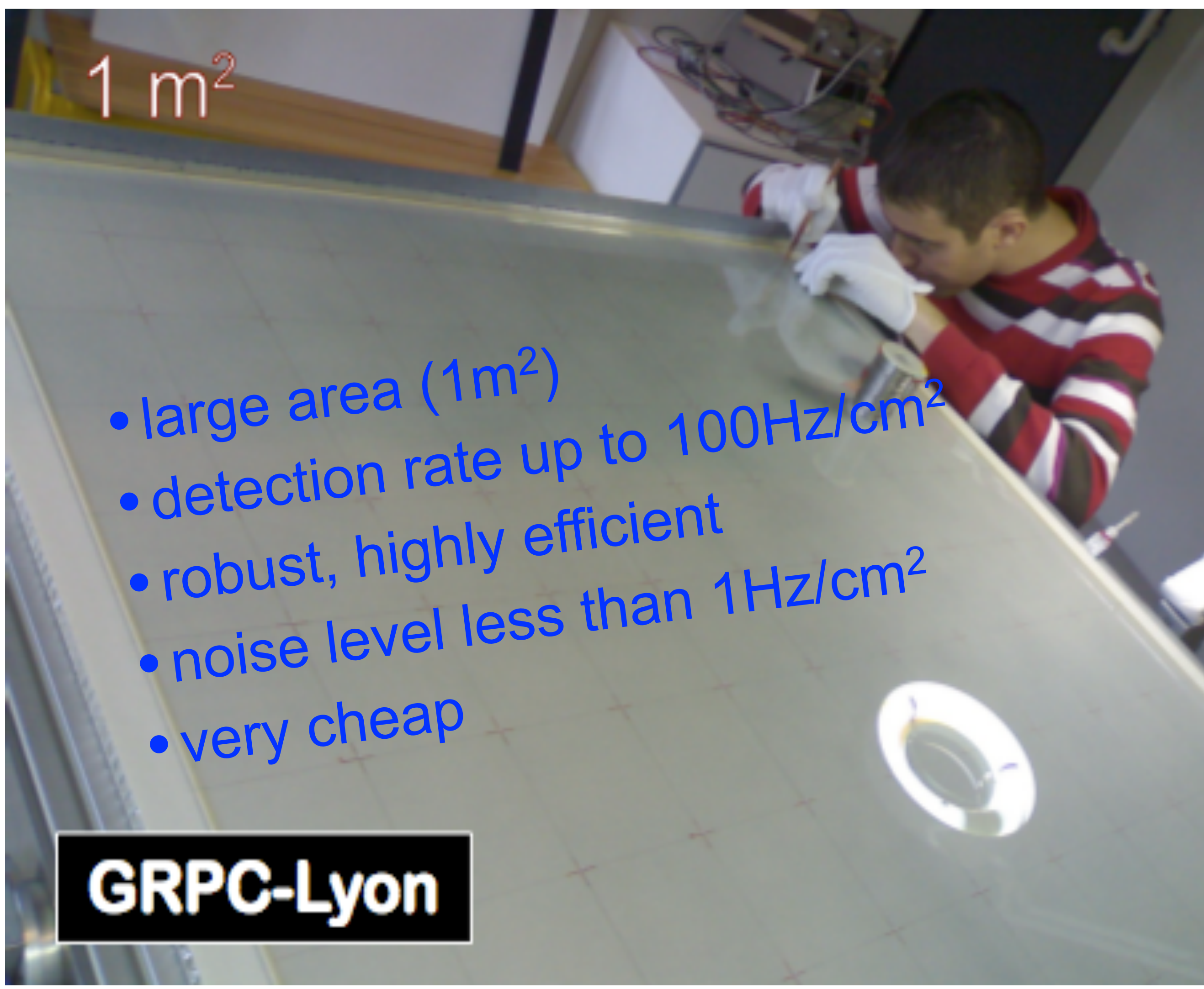

Efficiency vs. HV & track incident angle

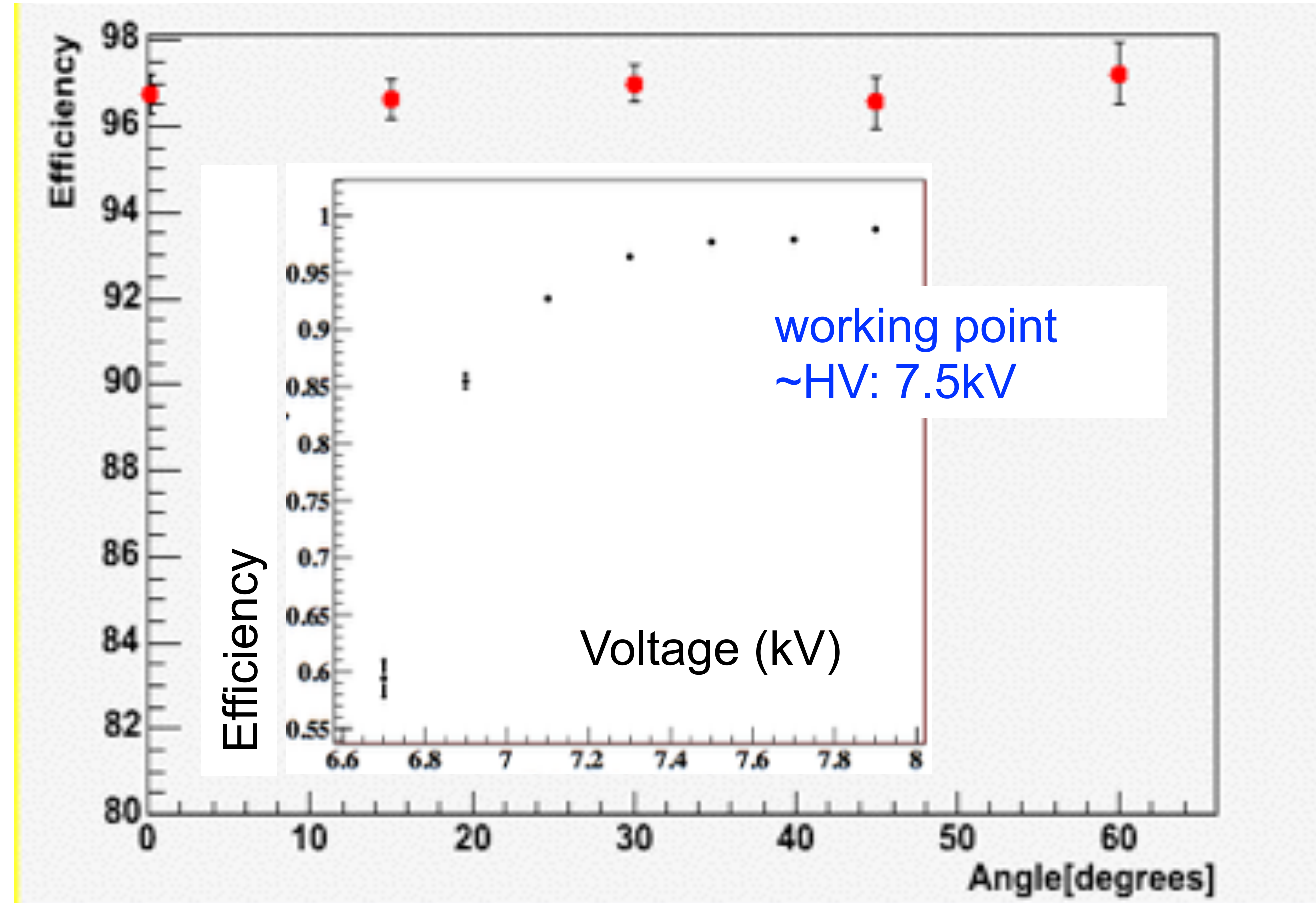

Noise rate (Hz)

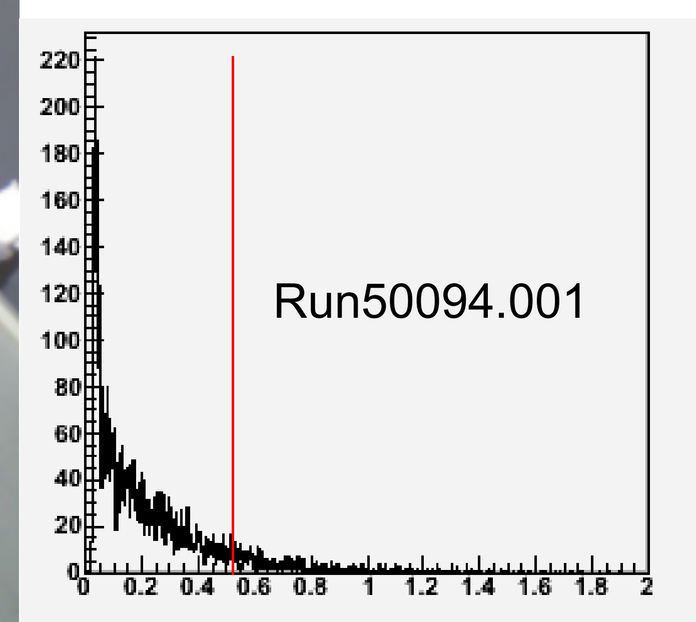

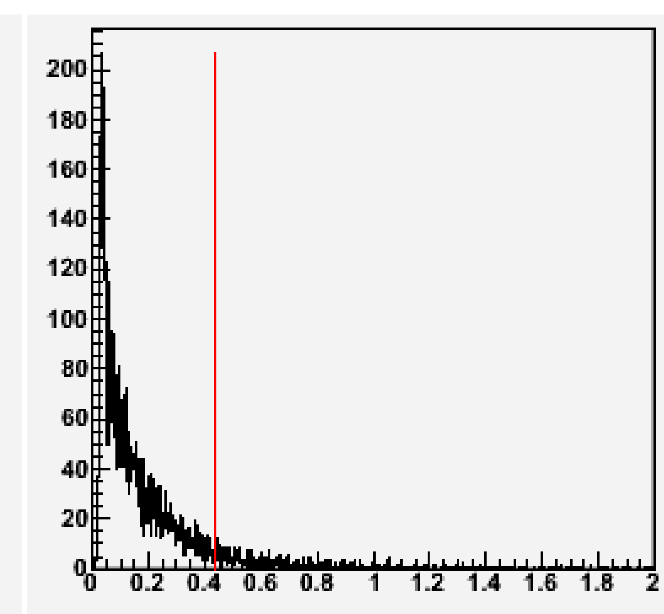

Muon Tracker : CALICE Electronics

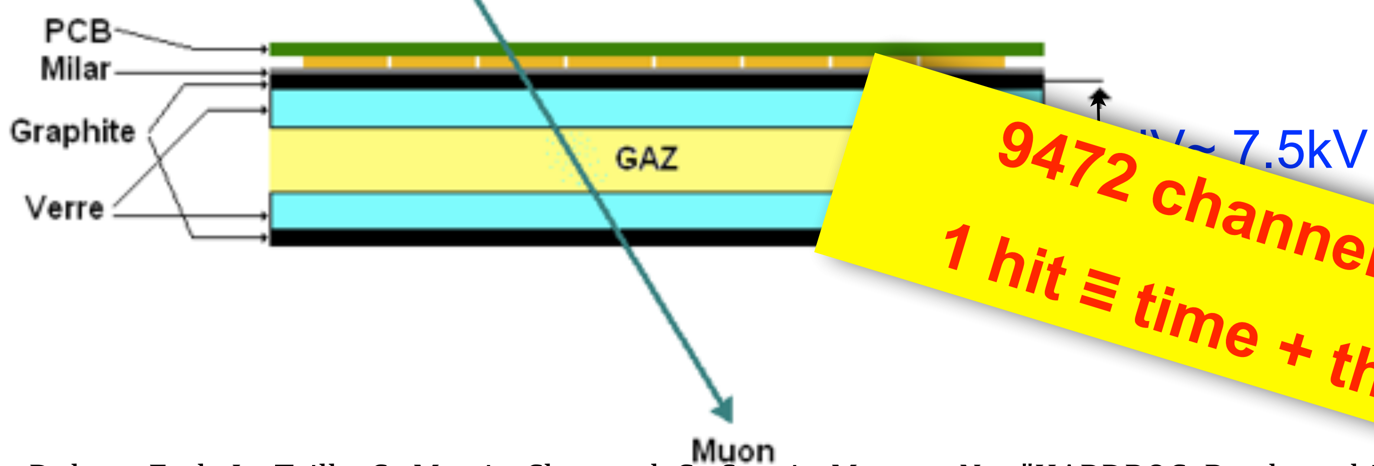

9472 channels/m2
1 hit ≡ time + thresh

Dulucq, F.; de La Taille, C.; Martin-Chassard, G.; Seguin-Moreau, N.; , "HARDROC: Readout chip for CALICE/EUDET Digital Hadronic Calorimeter," *Nuclear Science Symposium Conference Record (NSS/MIC), 2010 IEEE*

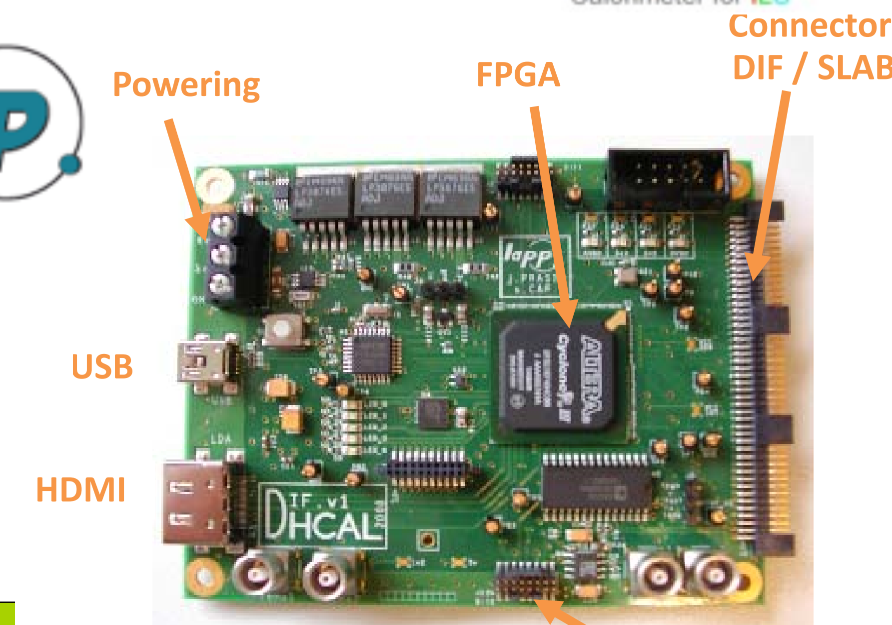

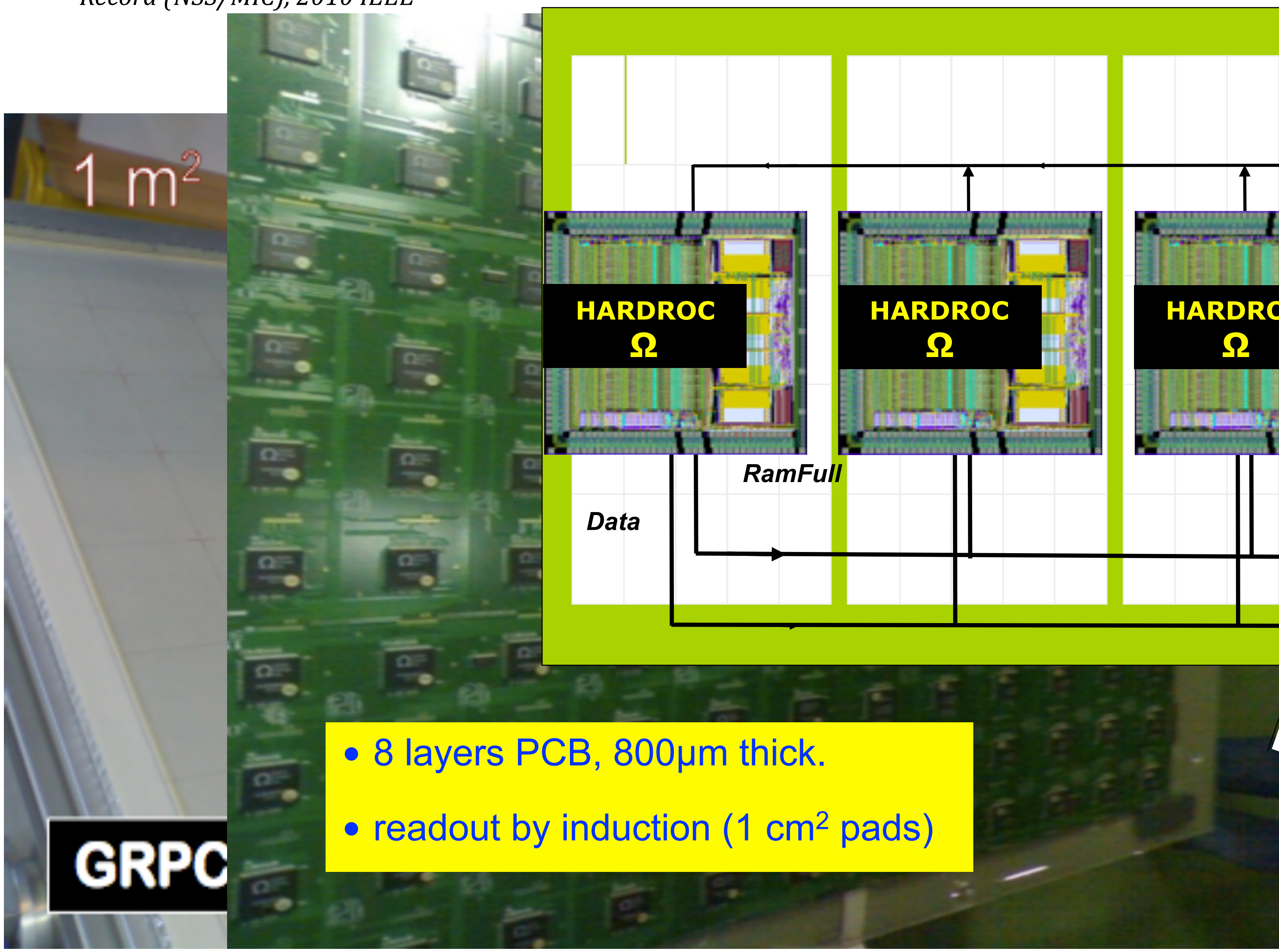

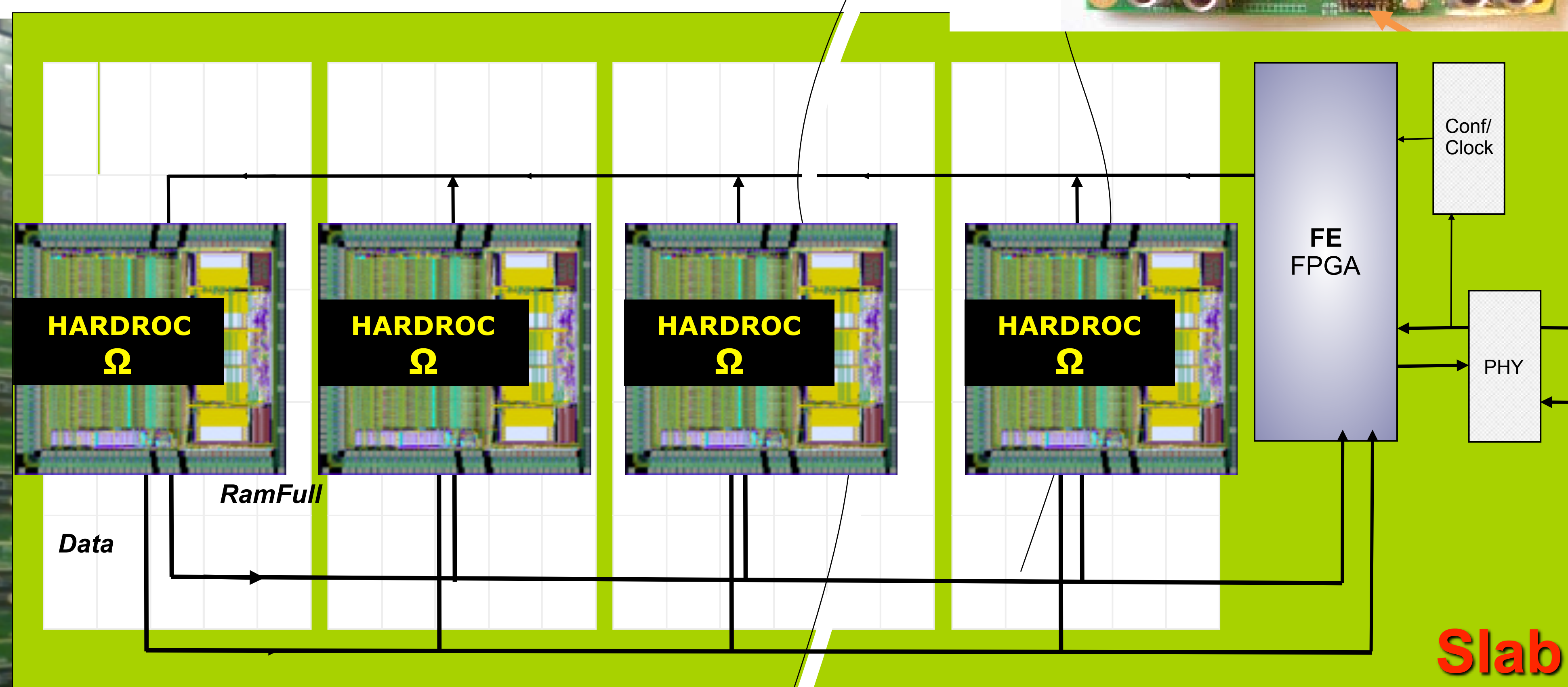

- 8 layers PCB, 800µm thick.
- readout by induction (1 cm^2 pads)

- 64 channels, 16 mm^2
- digital output (3 adjustable thrs)
- low power consumption (1.5 mW/ch)
- large gain range
- xtalk <2%
- ajustable gain for each channel

Tomuvol: a typical data taking campaign

Network :

- La Taillerie : using wifi antenna, relayed by the Puy-de-Dôme.
- Col de Ceyssat : “regular” Internet Service Provider.

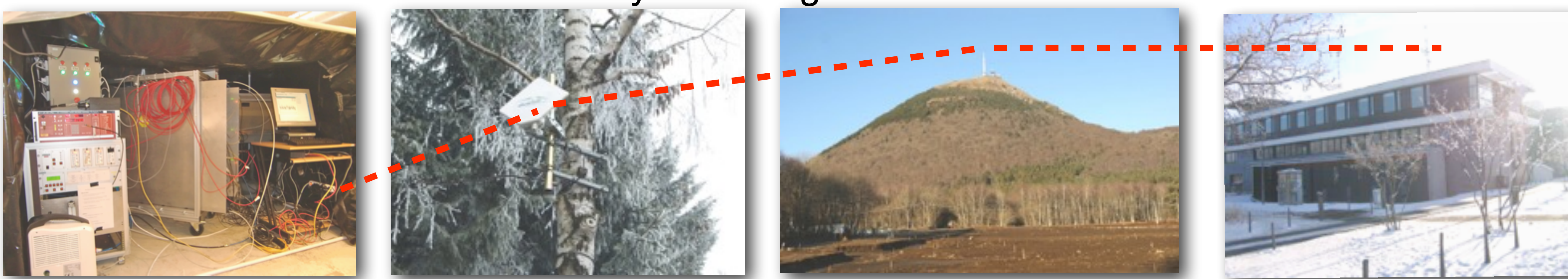

Integrated number of selected tracks (Millions)

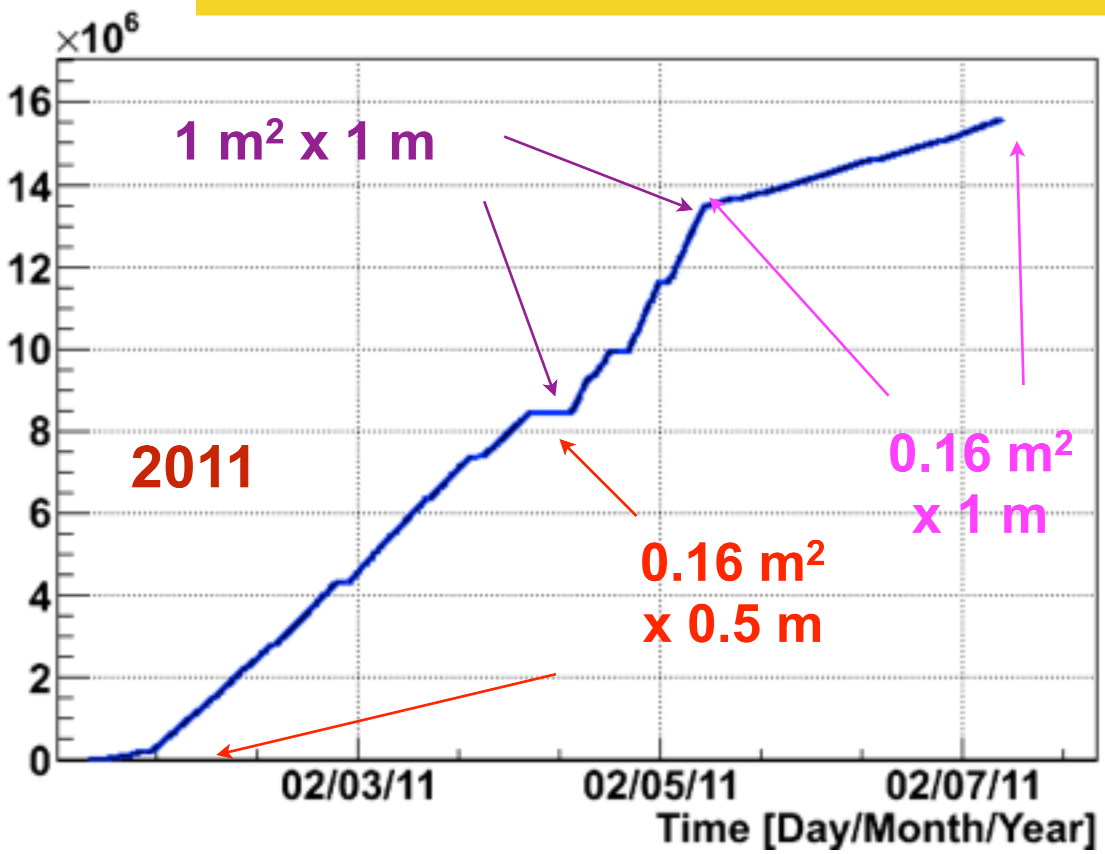

Integrated number of selected tracks

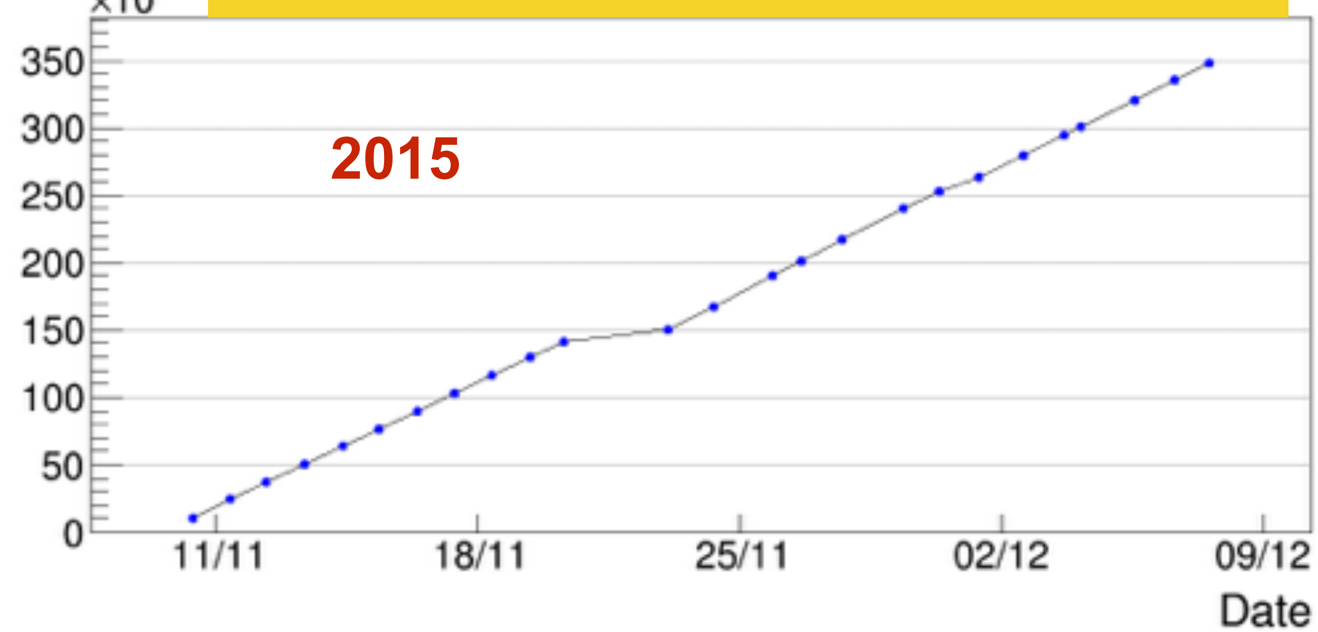

4 layers of 1 m^2 each with modular transportable design and improved timing.

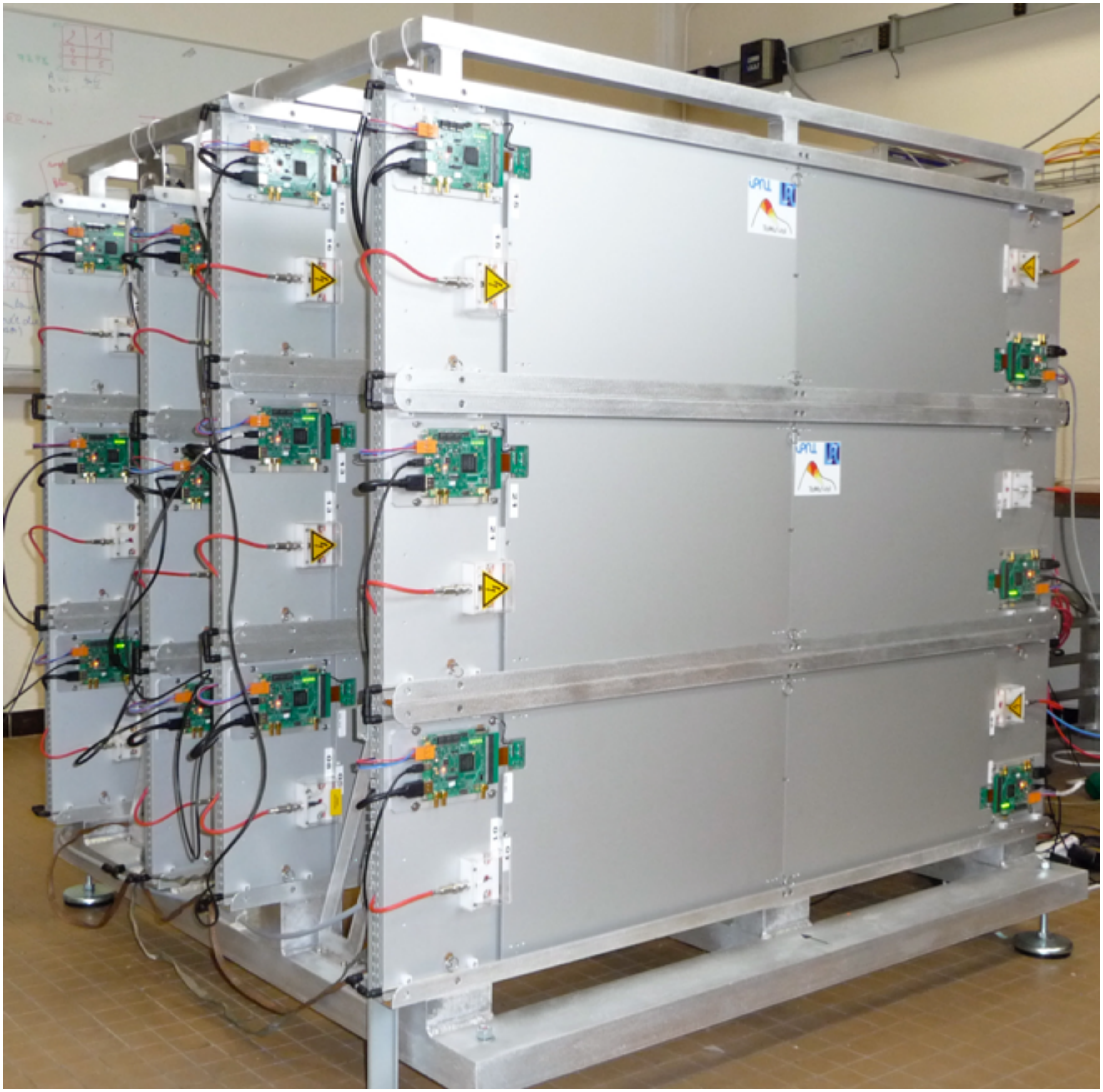

TOMUVOL 2015 campaign on Puy de Dôme

- Very preliminary results on the CDC 2015-2016 campaign
- 99.6 effective days of data taking
- 1 m^2 detector

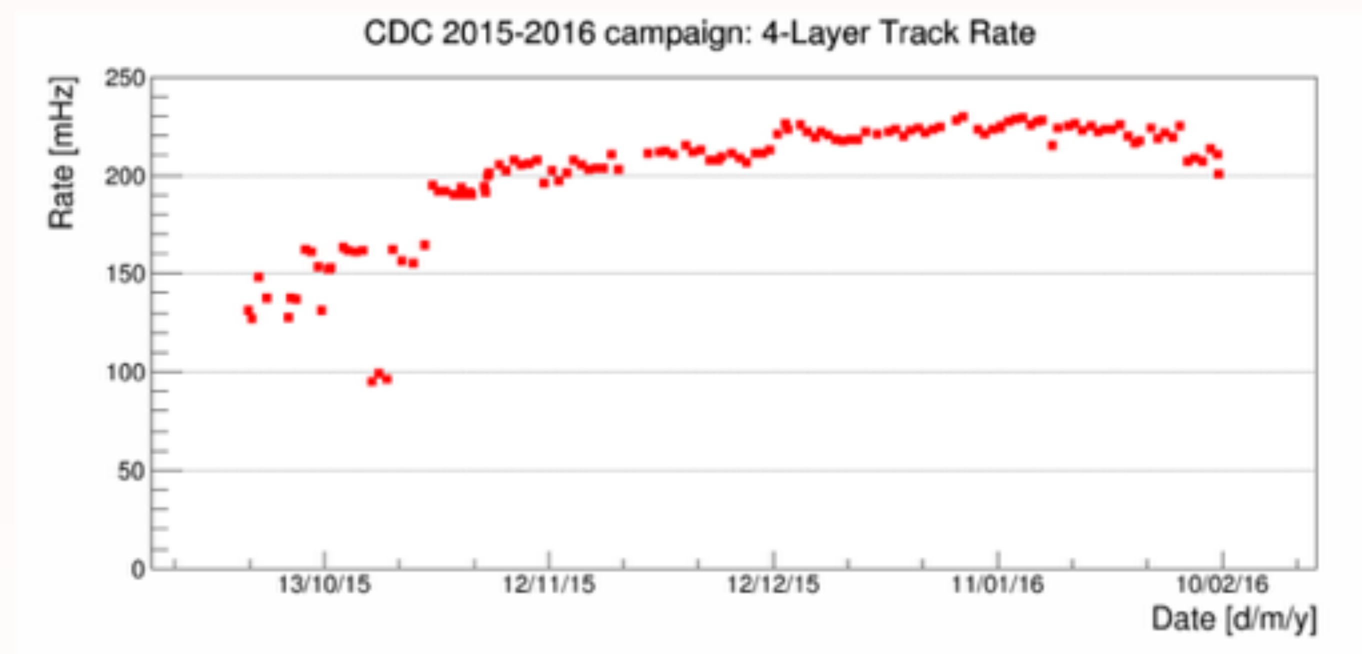

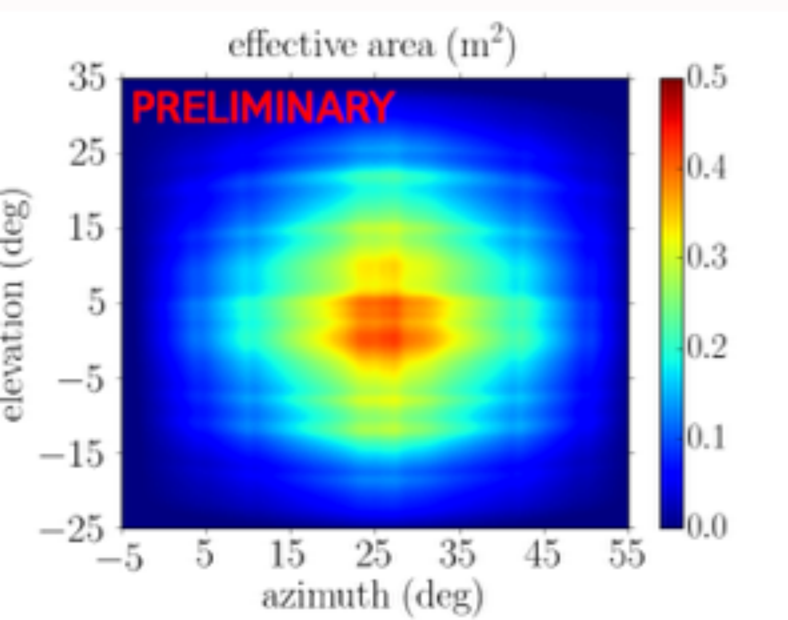

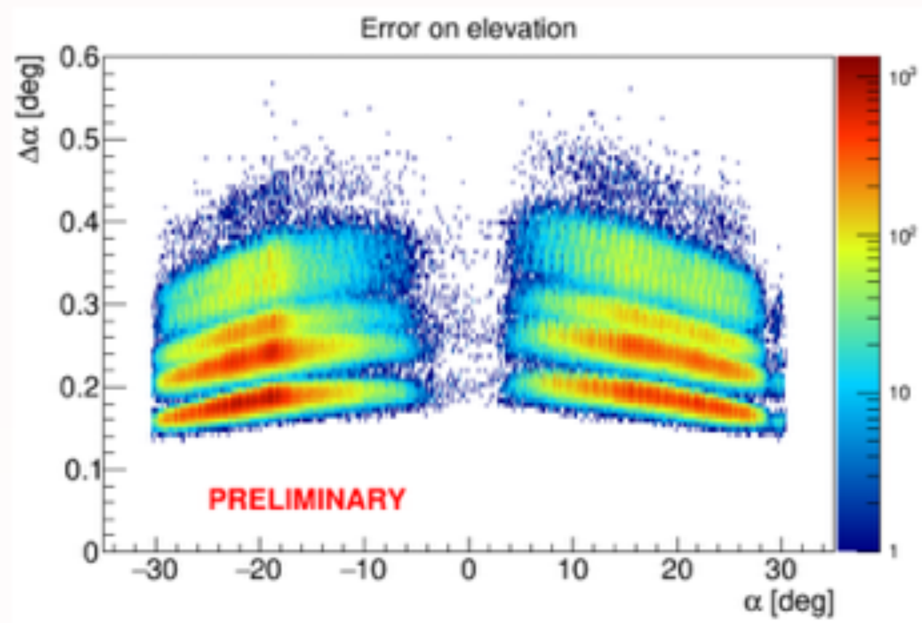

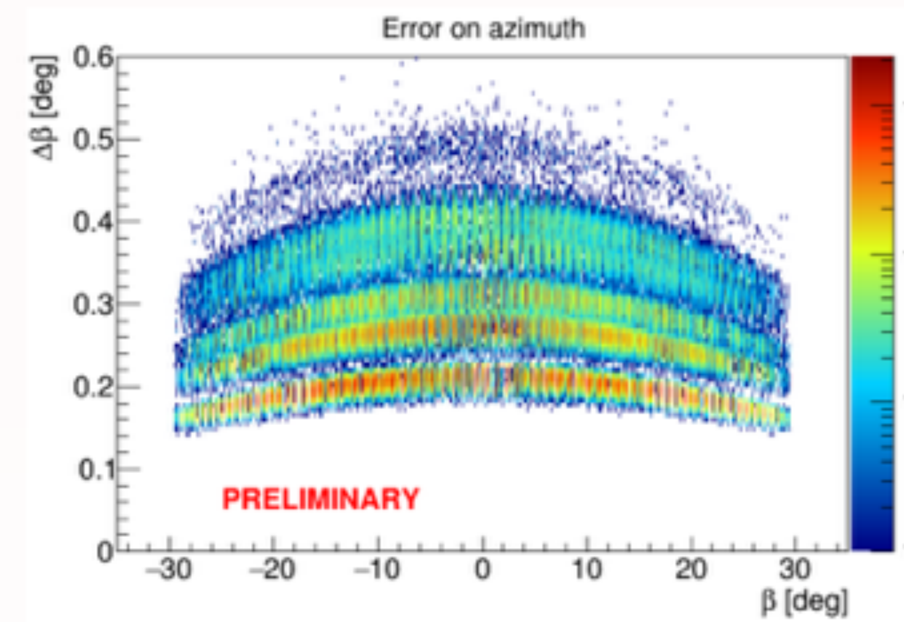

Puy de Dôme : gravimetry vs muography data

Gravimetric model

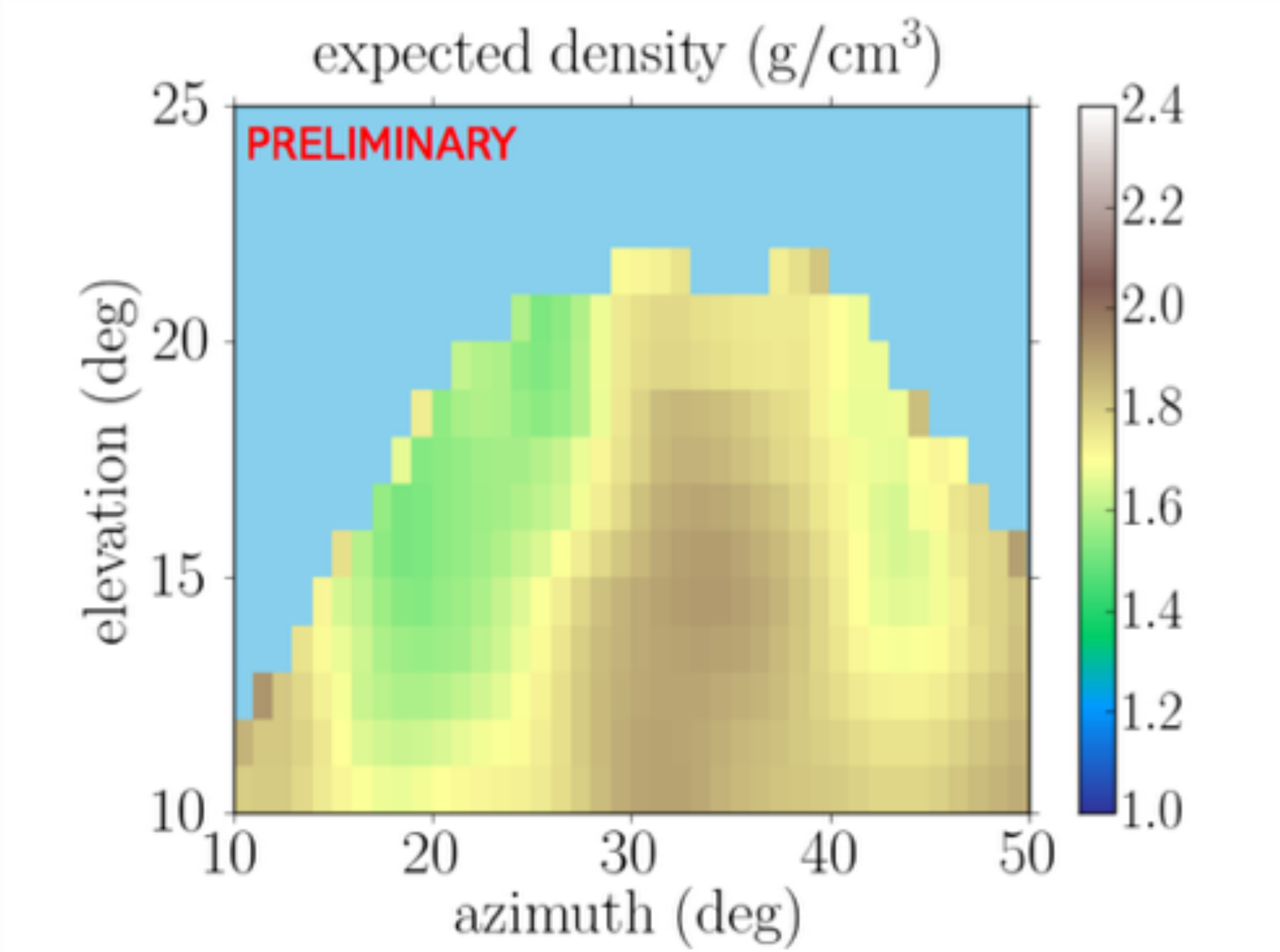

Muon data

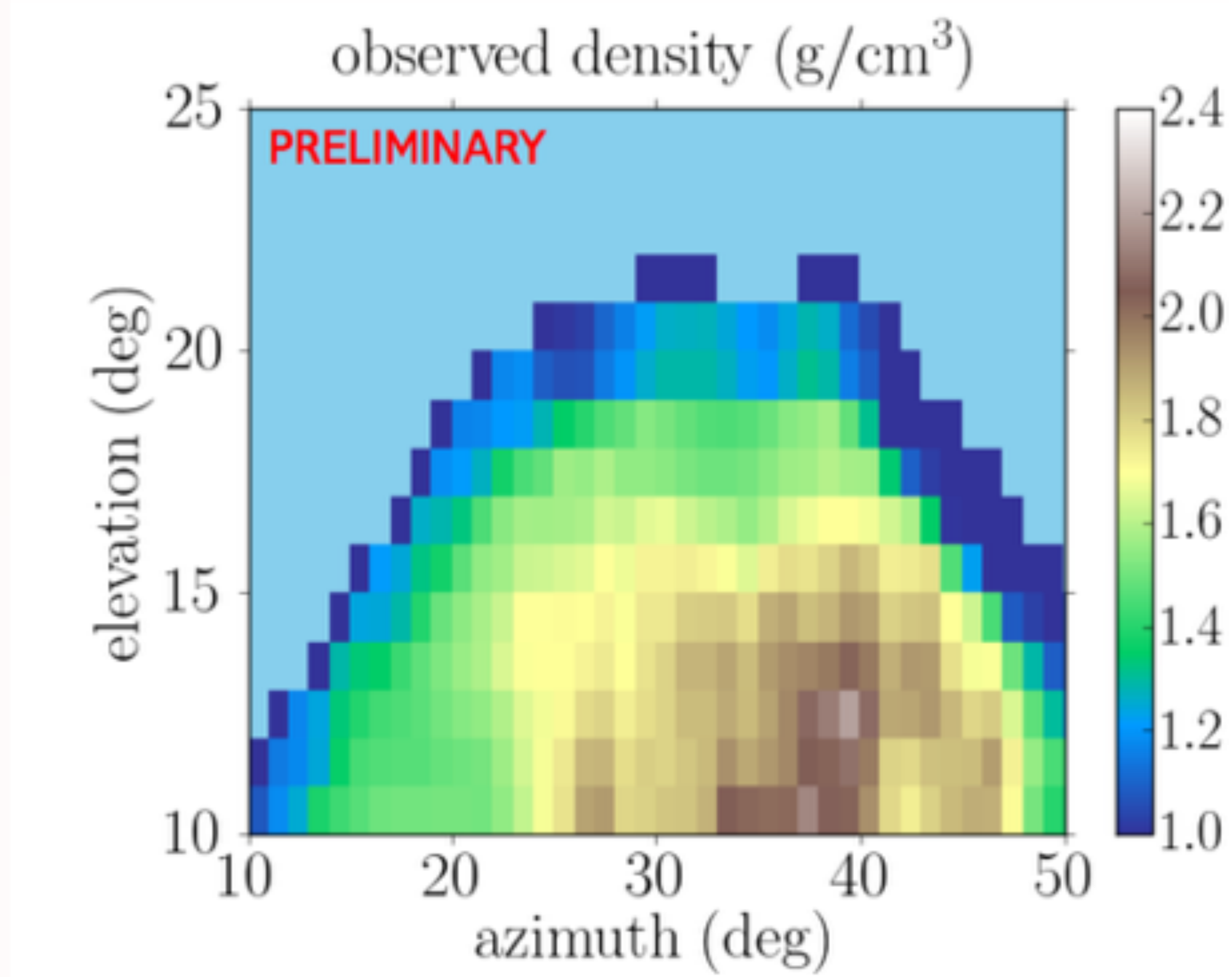

- The muon data are obviously contaminated close to the border, e.g. uncertainties on the muon direction, background leakage flux of low energy particles.
- There is a qualitative agreement on a denser core below 15° of elevation, but not for the somital area.

Puy de Dôme : gravimetry vs muography data

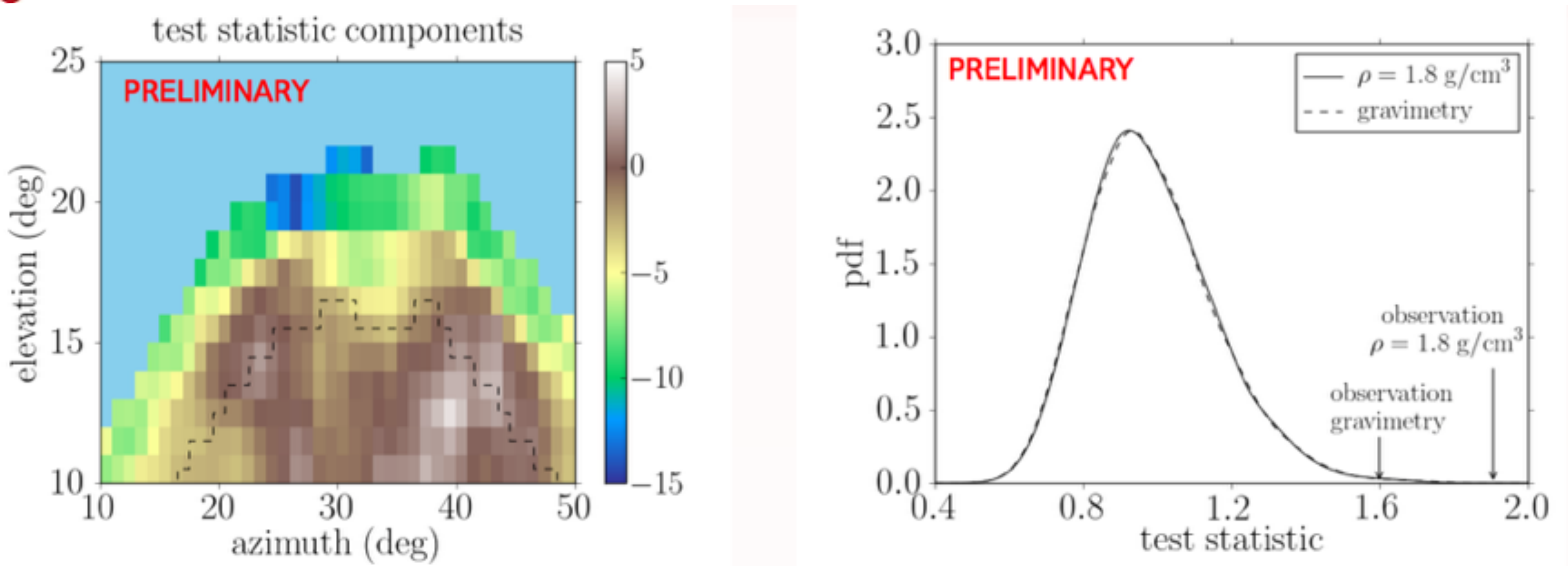

- Build a residual like test statistic as $\sum_i \frac{(o_i - m_i - b_i)^2}{\sigma_i^2}$ between the observation (o_i) and the expectation ($m_i - b_i$) normalised to the statistical uncertainties (σ_i), with i the bin.
- The distribution has a χ^2 like shape.
  - No uncertainties in the gravimetric model
  - No systematic uncertainties on muography
  - Below 6° from the border
    - Muon vs gravimetric data disagree at 2.9 σ (p-value = 3.6^{-4})
    - Muon data vs uniform model disagree at 3.9 σ (p-value = 1.10^{-4})
- To be improved with better uncertainties treatment and joint inversion.

Frequentist measurement vs bayesian hypothesis testing

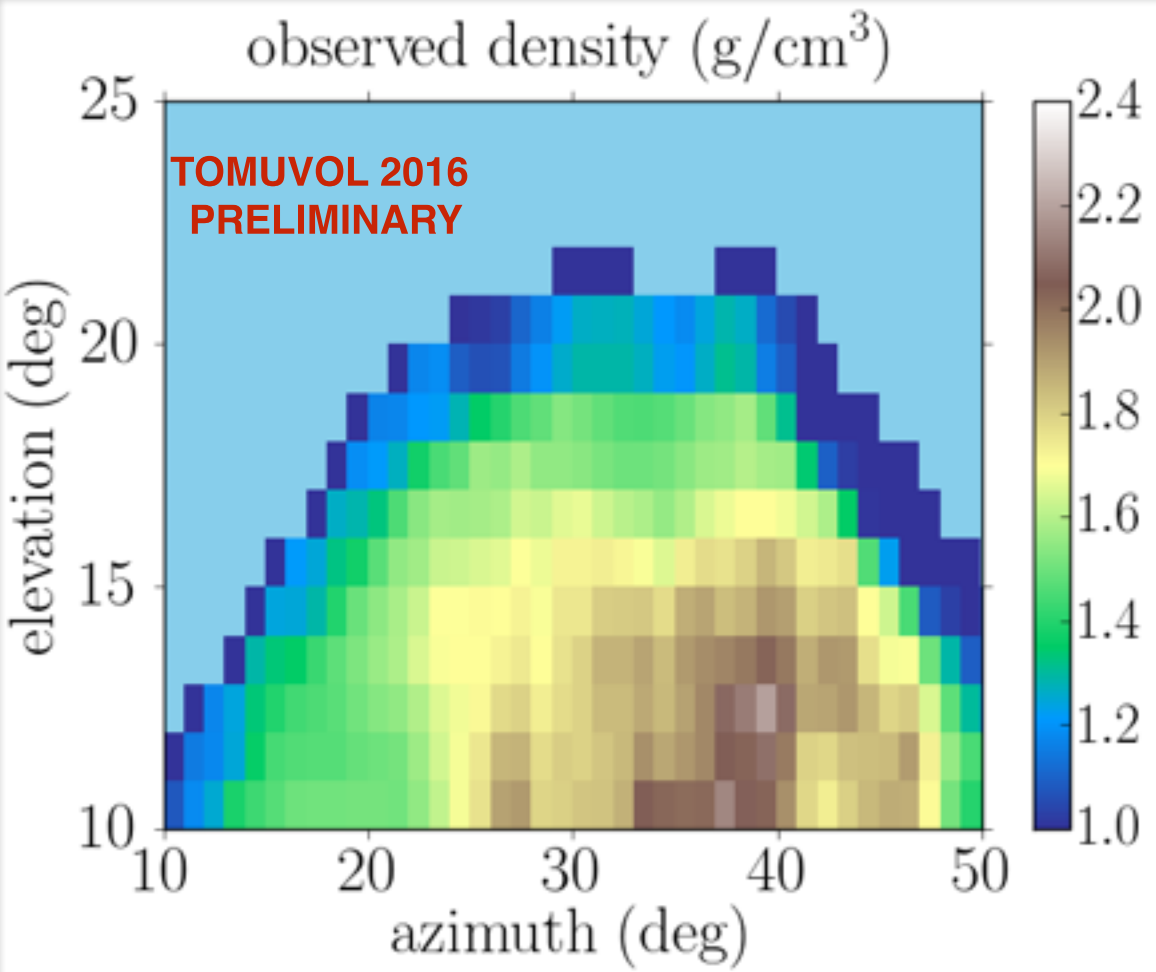

Measurement (the image binning follows strictly the uncertainties, no filtering, smoothing, etc)

If additional image treatment & geophysical hypothesis considered the image greatly improved, but uncertainty information lost ☞

Puy de Dôme as seen from the muon telescope site

Internal structure observed through muography

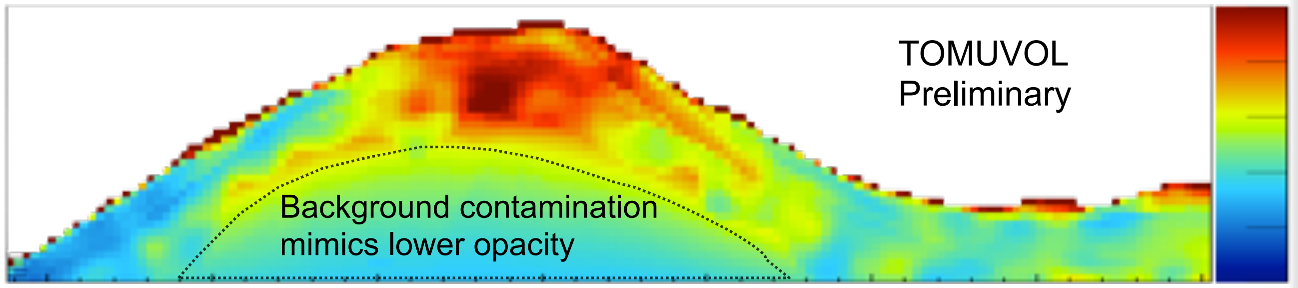

Linear opacity to atmospheric muons

65.8 days of data taking, 0.16 m^2 x 0.5 m

Physics Today, December 2012

Muography: present & future

1896
First X-Ray : Anna Bertha Röntgen’s hand

nowadays
common X-ray

2012
proton radiography
H. Sadrozinski, IEEE